



# HHS Public Access

Author manuscript

*Chem Rev.* Author manuscript; available in PMC 2023 January 26.

Published in final edited form as:

*Chem Rev.* 2022 January 26; 122(2): 2695–2751. doi:10.1021/acs.chemrev.1c00388.

## Aryl Transfer Strategies Mediated by Photoinduced Electron Transfer

Anthony R. Allen<sup>†</sup>, Efrey A. Noten<sup>†</sup>, Corey R. J. Stephenson<sup>†,\*</sup>

<sup>†</sup> Department of Chemistry, Willard Henry Dow Laboratory, University of Michigan, 930 North University Avenue, Ann Arbor, Michigan 48109, United States.

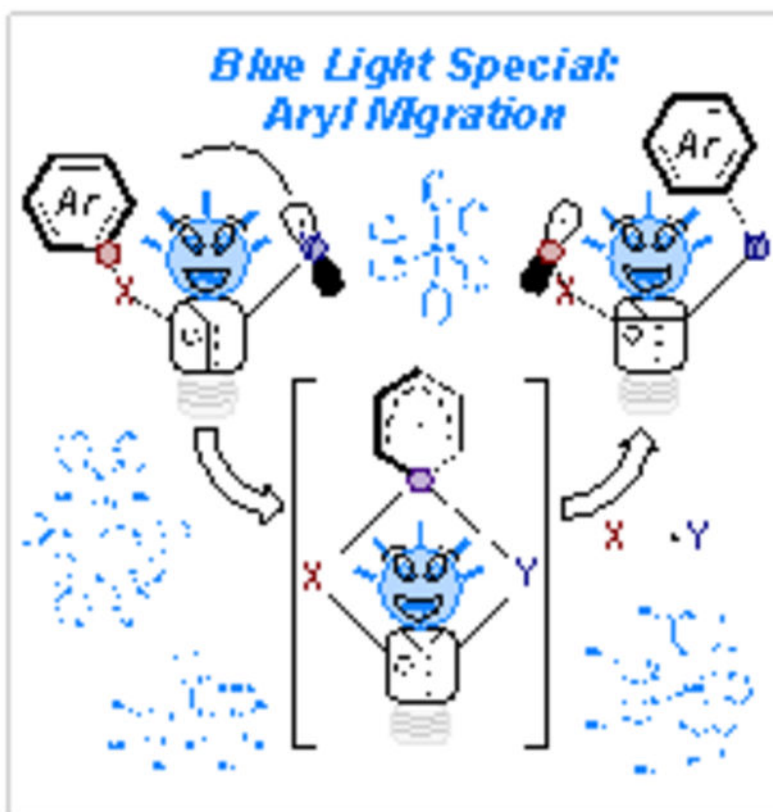
### Abstract

Radical aryl migrations are powerful techniques to forge new bonds in aromatic compounds. The growing popularity of photoredox catalysis has led to an influx of novel strategies to initiate and control aryl migration starting from widely available radical precursors. This review encapsulates progress in radical aryl migration enabled by photochemical methods—particularly photoredox catalysis—since 2015. Special attention is paid to descriptions of scope, mechanism, and synthetic applications of each method.

### Graphical Abstract

---

\* crjsteph@umich.edu.



## 1. Introduction

The ubiquity of aromatic functionality in pharmaceuticals, natural products, agrochemicals, polymers/materials, electronics, and other classes of compounds that are central to modern society is self-evident. Fascination with the unique physical, chemical, and biological properties of aromatic systems has only grown since the initial investigations and hypotheses of Kekulé and Erlenmeyer in the 1860s.<sup>1, 2</sup> In fact, lively debate surrounding the definition of “aromatic” persists even to the present date.<sup>3–6</sup>

The primary concern of synthetic chemists, however, is the selective introduction and manipulation of these groups, most often within complex molecular frameworks. Aromaticity poses significant thermodynamic challenges to developing selective, facile, and generalizable methods for arene reactivity because of the energetic penalties associated with dearomatized intermediates. In light of these considerations, radical aryl migration reactions, a class of intramolecular aromatic substitutions, comprise some of the most successful and well-studied aromatic transformations.

In this Review, these migrations will be broadly classified by two critical features: 1. the identity of the two atoms involved within the “X → Y migration”, where X denotes the atom to which the migrating aryl group is initially bonded, and Y denotes the atom to which the aryl group is transferred; 2. the number of atoms “n” that the aryl group migrates between

in a “1, n migration,” with n denoting the number of atoms between X and Y, inclusively. For example, the first reported radical aryl migration was disclosed by Wieland in 1911 (Scheme 1).<sup>7</sup> Therein, the thermolysis of bis(triphenylmethyl)peroxide (**1-1**) resulted in a dimerized phenyl ether (**1-2**) which is classified herein as a C → O 1,2-aryl migration. Later investigations in the 1940s by Urry and Kharasch detailed the Grignard reaction of neophyl chloride (**1-3**) to an unexpected mixture of **1-4-1-6**.<sup>8</sup> This example constitutes the first C → C 1,2-aryl migration, which has subsequently become known as the “neophyl rearrangement.” During a steroid natural product synthesis, in 1972 Loven and Speckamp described a serendipitous S → C 1,4-aryl migration to **1-8** following debromination of an *N-p*-tolylsulfonyl protected intermediate (**1-7**).<sup>9</sup> This first example of the “radical Smiles-Truce” rearrangement along with several notable contributions from Motherwell<sup>10-13</sup> in the 1990s laid the foundations for further investigations which have dominated much of the contemporary research devoted to radical aryl migrations.

These radical aryl transfer methodologies are excellent alternatives to their polar counterparts because the associated radical intermediates are often more stable relative to the analogous ionic intermediates within polar variants. As a result, broader functional group tolerance and expanded substrate scopes can be achieved which expand synthetic utility and allow for unconventional retrosynthetic strategies for aromatic compounds.

Furthermore, there are a myriad of ways for synthetic chemists to arrive at the necessary radical intermediates of these transformations. While these earlier methods typically utilized high temperatures or stoichiometric quantities of radical initiators to effect homolysis, methods of radical generation relying upon photochemistry have also been disclosed. UV irradiation was utilized as early as 1979 by Zanardi and co-workers in radical aryl migration reactions towards biaryl synthesis.<sup>14</sup> Since then, developments in photochemical mediated electron-transfer processes—such as photoredox catalysis<sup>15-17</sup> and electron-donor acceptor complexes<sup>18, 19</sup>—have revolutionized the manner in which synthetic chemists generate radical intermediates. Under simple visible light irradiation, these methods access unique radical intermediates which are otherwise inaccessible or challenging to access through the use of more traditional harsh, unselective, or toxic stoichiometric oxidants and reductants. Consequently, both are well-disposed for integration with radical aryl migration strategies and, especially for photoredox catalysis, many developments have been recently disclosed demonstrating their beneficial synergy.

The core focus of this review is to detail the advancements in photoinduced radical aryl migrations since the first reports in this area of research in 2015. Special attention will be given to the scope of these transformations with respect to the migrating aryl group, the electronic, steric, or conformational factors that promote migration, and the mechanistic studies supporting these observations. Applications of methodologies to biologically active scaffolds along with demonstrations of the methodology on large (gram or greater) scale will also be covered in order to generate interest from the pharmaceutical industry. Finally, critical commentary will be applied to both accent notable contributions and advise researchers in addressing unresolved issues which hinder the methodologies under consideration. Many works are well-designed implementations of photoredox catalysis, others are more remarkable from the standpoint of the achieved aryl migration, while certain

exceptional works integrate excellence in both domains. It is the authors' hope that this review will both summarize the current state of the art in the field, promote greater research interest and efforts, and serve as a helpful guide in subsequent studies, especially for newcomers to either photoredox catalysis and/or radical aryl migration reactions. Previous relevant reviews on aryl migration strategies<sup>20, 21</sup> and the Smiles rearrangement<sup>22–24</sup> should be consulted for their valuable perspectives on these topics as well.

## 2. Aryl transfer from C to C

### a) 1,2-aryl transfer

The arylalkylation of allylic alcohols *via* photoredox catalysis was first accomplished by Yang and Xia in 2015 (Scheme 2).<sup>25</sup> Before discussing their contribution and the many subsequent reports that it inspired, it should be contextualized within the discovery of other transition-metal catalyzed allylic alcohol difunctionalization reactions around the same time by Sodeoka (utilizing Fe), Tu (utilizing Cu), and Tambar (utilizing Pd).<sup>26–28</sup> The accomplishments of Sodeoka and Tu in aryltrifluoromethylations can be more directly compared to Zhu (Scheme 5) and Cai (Scheme 17) below, whereas Tambar's work is similar to that of Yang and Xia here (Scheme 2) or Song and Li below (Scheme 3). This seminal photoredox example and all following examples within this C→C aryl transfer section ought to be appreciated considering the abundant examples from the chemical literature crossing synthetic subdisciplines at the time. These parallel developments likely informed and enriched each other.

In this specific work, the strongly reducing excited state of *fac*-Ir(ppy)<sub>3</sub> is oxidatively quenched by diethyl bromomalonate to furnish malonyl radical (CO<sub>2</sub>Et)<sub>2</sub>C•. Addition of this species to the olefin **2–1** yields the key alkyl radical **2–3**, which can undergo cyclization to the *ipso* position of an aryl ring to generate a spiro[2,5]octadienyl radical **2–4**, typical of neophyl-type rearrangements. Rearomatization of **2–4** results in 1,2-aryl migration while also giving a nucleophilic ketyl radical **2–5** capable of turning over Ir<sup>IV</sup> by single-electron reduction. Deprotonation of the resultant oxocarbenium **2–6** provides the desired ketone product **2–2** (Scheme 3). When the reaction was conducted in the presence of TEMPO, no **2–2** was detected in the reaction mixture, suggesting the presence of radical intermediates.

The scope of this transformation was mainly restricted to variations on the migrating arene (Scheme 2). Electron-rich and electron-deficient arenes were amenable to the optimized reaction conditions, yielding the corresponding ketones such as electron-rich (**2–2h**) in 71% yield and electron-deficient (**2–2j**) in 92% yield. For the diaryl allylic alcohol substrates with different aryl groups, two 1,2 aryl migration products were possible. In general, it was demonstrated that electron-deficient aryl rings migrated chemoselectively over electron-rich rings such as in the  $\alpha$ -aryl ketone (**2–2i**). In this case, migration occurs from the electron-deficient 4-Cl substituted ring. However, mixtures of both possible 1,2 migration products were obtained, especially when the electronics of each ring were not sufficiently discriminated. *ortho*-Substituted aryl rings were not competent migratory groups (see **2k–m**), likely due to the increased steric crowding these rings would introduce to the strained intermediate spirocycle **2–4** above. Notably, a monoaryl allylic alcohol substrate in which

a methyl group has replaced an aryl group underwent the transformation to methyl ketone product (**2-2o**) in 54% yield. Finally, the utility of this strategy was demonstrated in the formal synthesis of the natural product ( $\pm$ )-sequirin D.<sup>29</sup> The key intermediate (**2-2h**) was arrived at in high yield under the reported methodology with further elaboration from this intermediate demonstrated in the literature. In all, this work laid the foundation for further advancement in photoredox mediated 1,2 aryl migration strategies. However, the long reaction times (5 days for the fastest substrate reported) and limited scope of alkyl radical precursor remained important areas for improvement.

Shortly following the report by Yang and Xia, Song and Li reported a comparable method effecting the arylalkylation of  $\alpha$ -aryl allyl alcohols **4-1** with activated alkyl bromides **4-2** using the strongly reducing excited state of *fac*-Ir(ppy)<sub>3</sub> (Scheme 4).<sup>30</sup> However, some key differences allowed the authors to overcome the primary limitations of the prior work. Namely, photocatalyst loading was lower (2 mol%), the inorganic base Ag<sub>2</sub>CO<sub>3</sub> was used, and the reactions were conducted in MeCN at 50 °C under irradiation of 36 watt CFL bulbs. Although isolated yields of the arylalkylation products **4-3** were slightly lower, the scope of electron withdrawing groups on the alkyl bromide fragment was expanded considerably to include ketones (**4-3a**), esters (**4-3b**),  $\beta$ -ketoesters (**4-3c**), and tertiary amides (**4-3d**). Overall, formation of both 1,2-aryl migration products **4-3e-4-3i** in unsymmetric substrates was consistent with the trends described by Yang and Xia. However, the present system was more sensitive to electronic and steric perturbations, so selectivity for the major regioisomer (listed in parentheses) was higher. Finally, most reactions gave good yields within 18 hours and all reported reactions were conducted within 24 hours.

Concurrent with the above carboarylations using activated bromides, another radical addition-neophyl rearrangement sequence was disclosed by the Zhu group towards the synthesis of *fluorinated* 1,5-dicarbonyl compounds.<sup>31</sup> Such compounds are highly valuable due to the beneficial effects on important pharmacological properties such as that fluorination imparts to drug candidates and pharmaceuticals.<sup>32</sup> The activated ester BrCF<sub>2</sub>CO<sub>2</sub>Et served as a  $\bullet$ CF<sub>2</sub>COOEt radical synthon following single-electron reduction by the excited-state of the *fac*-Ir(ppy)<sub>3</sub> catalyst. The remainder of the mechanism following radical addition to **5-1** is identical to the previous report from Yang and Xia (compare Scheme 3 above and Scheme 6 below) The presence of base was crucial for the success of the transformation, while less-reducing Ir and Ru photocatalysts were detrimental to the reaction outcome. Addition of the radical trap TEMPO to the reaction completely inhibited the reaction, supporting the presence of radical intermediates (Scheme 6).

In line with observations of the preceding works, unsymmetrical  $\alpha,\alpha$ -diaryl allylic alcohols typically displayed a preference for migration of the most electron-deficient aryl substituent (Scheme 5). Low chemoselectivity was observed in cases such as (**5-2r**) where a 2:1 mixture of the possible 1,2 migration products was observed. In unsymmetrical substrates in which one of the rings was *ortho*-substituted, the *ortho*-substituted arene was less likely to migrate even if it was more electron-deficient than the other aryl substituent as in (**5-2o**) and (**5-2p**). This result demonstrates the importance of sterics in the highly-congested neophyl rearrangement step of this mechanism. The morpholine acetamide derived from ethyl bromodifluoroacetate was competent in the transformation, providing product (**5-2g**) in

high yield. Finally, several examples of trifluoromethylarylation of the allylic alcohols were demonstrated. Interesting  $\alpha$ -aryl, $\beta$ -CF<sub>3</sub> aryl ketone products (**5–2h**)–(**5–2l**) were obtained in excellent yield when CF<sub>3</sub>I was used as a trifluoromethyl radical source in the presence of Ru(bpy)<sub>3</sub>(PF<sub>6</sub>)<sub>2</sub> photocatalyst. Impressively, these conditions furnished an  $\alpha$ -quaternary ketone (**5–2i**) in 77% yield. Thus, this protocol served as an excellent gateway to both difluoro- and trifluoromethylated carbonyl-containing compounds, expanding the scope of the previous carboarylation reactions.

In a work similar to that of Zhu above, in 2018 the Cai group disclosed a carbotrifluoromethylation of allylic alcohols featuring a 1,2 aryl migration.<sup>33</sup> This protocol resulted in the synthesis of many  $\alpha$ -aryl, $\beta$ -CF<sub>3</sub> aryl ketone products derived from either symmetric or unsymmetric  $\alpha,\alpha$ -diaryl allylic alcohols. Unlike the existing precedent at that time, this reaction avoids the use of transition-metal catalysts, stoichiometric quantities of harsh oxidants/reductants, and does not require elevated temperature.<sup>34</sup> Fortunately, using the organic fluorophore 1,2,3,5-tetrakis (carbazol-9-yl)- 4,6-dicyanobenzene (4CzIPN) ( $E_{1/2}(P^*/P^-) = +1.35$  V vs. SCE), this method was able to achieve these transformations in a catalytic regime under very mild conditions.<sup>35</sup>

Compared to the 4 examples reported earlier by Zhu, a much wider variety of  $\alpha$ -aryl, $\beta$ -CF<sub>3</sub> aryl ketones were synthesized herein (Scheme 7). These included several examples from symmetrical substrates including migrating aryl groups with electron-withdrawing groups such as (**7–2g**) and halides such as **7–2e** and (**7–2j**). Alkyl substituted **7–2b** was isolated in 71%. A reduced yield of 50% was observed for the strongly electron-donating 4OMe-substituted (**7–2c**) in alignment with previous neophyl rearrangements of this type. Underlining the delicate steric requirements incumbent upon the congested spiro-transition state/intermediate structure of this aryl migration, the substrates which generated  $\alpha$ -quaternary center containing  $\alpha$ -aryl ketones such as (**7–2h**) and (**7–2i**) suffered reduced yields. Other sterically demanding substrates such as (**7–1a**) were unable to undergo the desired rearrangement.

Several observations from the scope of the unsymmetrical allylic alcohol substrates agreed with previous results as well: 1. The most electron-deficient aryl group migrated preferentially as in (**7–2m**)–(**7–2o**), 2. Low chemoselectivity was observed for substrates where the electronics of the aryl rings were similar as in (**7–2j**), 3. *ortho*-Substituted aryl systems were recalcitrant towards migration as in (**7–2p**)–(**7–2t**) and 4. Heteroaromatic aryl groups chemoselectively migrated over benzene derived aryl systems as in (**7–2u**). Gratifyingly  $\alpha$ -aryl, $\beta$ -CF<sub>3</sub> alkyl ketone products (**7–2v**) and (**7–2w**) were obtained in high yield from substrates in which an aryl group was replaced with an alkyl group.

An important mechanistic detail differentiating this work from the literature precedent is the manner in which the photoredox catalysis cycle is conducted (Scheme 8). In the former cases, the catalytic cycles began with *oxidative quenching* of the photocatalyst and were turned over by single electron reduction from a ketyl radical intermediate. On the other hand, this transformation begins with *reductive quenching* of the excited state of 4CzIPN\* with Langlois' reagent (CF<sub>3</sub>SO<sub>2</sub>Na). As in the previous works, intermolecular radical addition and 1,2 aryl migration results in ketyl radical **7–5**, however, the 4CzIPN

radical anion resulting from the initial reductive quench is unable to oxidize **7-5**. Thus, an external oxidant is required to turn over the catalyst and/or oxidize **7-5**.

Cleverly, Cai discovered that simply conducting the reaction under an atmosphere of N<sub>2</sub> gas containing 0.5 mol% of O<sub>2</sub> provided enough oxidant in the form of O<sub>2</sub>. The formation of oxocarbenium **7-6** upon oxidation by molecular O<sub>2</sub> or peroxide dianion (O<sub>2</sub><sup>2-</sup>) gives product **7-2** upon deprotonation. The 4CzIPN radical anion can be returned to its neutral ground state upon oxidation by O<sub>2</sub> or superoxide (O<sub>2</sub><sup>•-</sup>) (Scheme 8).

Indeed, this modification improved reaction yields from 65% to 79% for product **7-2a**. On the other hand, when the reaction was conducted under an exclusively O<sub>2</sub> atmosphere, oxidation of the **7-1a** to benzophenone **8-1b** was observed, demonstrating the importance of controlling the amount of oxidant present in the reaction mixture. Despite the similarities of the overall transformation to previous protocols and its somewhat more complicated redox cycle and setup, the diversity of products synthesized in this work along with its mild conditions and inexpensive •CF<sub>3</sub> radical precursor are quite meritorious.

In a follow-up report to the earlier 1,2 aryl migrations towards the synthesis of  $\alpha$ -aryl, $\beta$ -CF<sub>3</sub> ketones detailed above, the Cai group reported an innovative, synergistic approach to unique  $\alpha$ -aryl, $\gamma$ -methylsulfinyl ketones.<sup>36</sup> Sulfoxides are noted for their pharmaceutical relevance, including being featured in top-selling drugs like Esomeprazole.<sup>37</sup> However, traditional methods to access the sulfoxide moiety have been restricted to harsh oxidations of sulfides.<sup>38</sup> Milder conditions such as those employed in this work represent a welcome advance in the synthesis of sulfoxide-containing compounds.

Symmetric allylic alcohols yielded the corresponding  $\alpha$ -aryl, $\gamma$ -methylsulfinyl ketones in high yields (Scheme 9). Electron-deficient, halogen, and alkyl substituted aryl groups migrated efficiently to give (**9-2a**)–(**9-2j**) in good to excellent yields. *meta*- versus *para*-Substitution did not seem to affect the desired transformation.  $\alpha$ -quaternary center ketones (**9-2h**)–(**9-2j**) were also synthesized. Electron-rich migrating aryl group examples were not reported. As for unsymmetrical substrates, preferential electron-deficient aryl group migration, low chemoselectivity for non-electronically differentiated migrating aryl groups, and reluctance of *ortho*-substituted aryl groups to migrate were observed as in other works described herein. Interesting  $\alpha$ -aryl, $\gamma$ -methylsulfinyl aryl ketones with a variety of post-functionalization synthetic handles such as halogen-substituted (**9-2r**)–(**9-2v**), ester-substituted (**9-2q**), and cyano-substituted (**9-2p**) were synthesized. Alkyl ketone products were furnished with replacement of an aryl group by a cyclohexyl or cyclopentyl group as in **9-2z** and **9-2aa**, in 83% and 86% yield, respectively.

The mechanism was proposed to begin with oxidative quenching of the excited state of 4CzIPN by the *in situ* formed **9-5** to yield a purported iodanyl radical **9-6** (Scheme 10). This radical was assumed to perform a rate-limiting C–H abstraction from DMSO to yield 2-iodo-1,3,5-trimethoxybenzene **11-1**, benzene, and  $\alpha$ -sulfinyl radical **9-7**. The remainder of the mechanism follows the same pattern of other neophyl rearrangements from allylic alcohols: radical addition of **9-7** to **9-1**, aryl transfer from **9-9** to **9-10**, and deprotonation to **9-2**.

Mechanistic experiments supported the above hypothesis, especially regarding the role of **9–5** in the reaction (Scheme 11). An equimolar mixture of **9–3** and **9–4** allowed for independent synthesis of **9–5** which was converted to 2-iodo-1,3,5-trimethoxybenzene (**11–1**) upon visible-light irradiation in the presence of 4CzIPN and DMSO. Furthermore, subjection of **9–5** to the optimized reaction conditions with **9–1a** resulted in identical yields to the protocol using *in situ*-formed **9–5** outlined in Scheme 9. These data suggest that *in situ* formation of **9–5** is indeed responsible for the novel C–H abstraction chemistry. Perhaps the most interesting result is the primary kinetic isotope effect ( $KIE = k_H/k_D = 9.4$ ) obtained for a reaction run in an equimolar solution of DMSO and DMSO- $d_6$ , as determined by the relative ratio of products **9–2a** and **9–2a-d<sub>5</sub>**. This large primary KIE suggests that the rate-determining step of this mechanism is  $\alpha$ -sulfinyl C–H abstraction. Experimental confirmation of benzene- $d_1$  by NMR or MS analysis when the reaction is run in DMSO- $d_6$  would corroborate the proposed HAT step by the iodanyl radical.

In all, this synergistic merging of photoredox catalysis with hypervalent iodine(III) chemistry is commendable; however, the atom-economy and super-stoichiometric amount of generated waste from this process are areas of potential improvement.

Chen, Xiao, and coworkers applied Zard's pioneering work on  $\beta$ -scission of iminyl radicals to the neophyl rearrangement by leveraging modern photocatalytic methods to generate the requisite iminyl radicals from cyclobutanone oximes.<sup>39</sup> 1,2-aryl migration following C–C bond homolysis in 3,3-disubstituted cyclobutanone oximes **12–1** afforded branched  $\alpha,\beta$ -unsaturated nitriles **12–2**. The aryl migration was suppressed in 3-monosubstituted systems and in most 3-aryl-3-alkyl disubstituted systems. *O*-benzoyl oximes were selected as N-centered radical precursors because they reliably undergo reductive mesolytic cleavage by excited photoredox catalysts under mild conditions.<sup>40–42</sup> Thorough screening led the authors to identify *fac*-Ir(ppy)<sub>3</sub> as the optimal photoreductant together with the tertiary amine base DABCO. Control reactions excluding light or photocatalyst did not produce any product, but exclusion of DABCO still allowed the product to be isolated in 53% yield. The presented substrate scope showed variability only in the identity of the substituents at the 3-position of the cyclobutanone oxime. All 3,3-diarylcyclobutanone oximes were converted *via* the neophyl rearrangement to acrylonitriles; within this class of substrates, little electronic differentiation of either the migrating or stationary arene was demonstrated. However, differences in steric repulsion of the two arenes exerted dramatic effect on the product distribution: while reduction of an oxime bearing phenyl and *p*-tolyl groups led to a 1.3:1 mixture of regioisomers **12–2d** and **12–2d'**, an oxime with phenyl and *o*-tolyl groups under the same conditions produced exclusively nitrile **12–2e**. This result shows that more sterically hindered arenes have significantly higher migratory aptitudes in this system. Only one substrate without 3,3-diaryl substitution could rearrange to its corresponding unsaturated nitrile product (**12–2g**). Otherwise, such compounds only underwent C–C bond cleavage and reduction to give 3,3-substituted butyronitriles **12–3**.

The mechanism proposed by the authors (Scheme 13) is consistent with prior work on similar transformations. In the first step, single-electron reduction of the *O*-acyl oxime **12–1** by the photoexcited catalyst results in expulsion of a benzoate species and concomitant formation of iminyl radical **12–4**.  $\beta$ -scission of **12–4** driven by strain release and C $\equiv$ N triple



bond formation produces primary alkyl radical **12–5**. Neophyl rearrangement *via* spirocycle **12–6** constructs the new Csp<sup>3</sup>–Csp<sup>2</sup> bond, and the resulting tertiary radical **12–7** is oxidized by the quenched photocatalyst to the cation **12–8**. Regioselective deprotonation *alpha* to the nitrile gives the acrylonitrile product **12–2**.

In 2018, Li and Zhou were able to demonstrate an alkylarylation of allylic alcohols relying on generation and addition of an  $\alpha$ -cyano radical succeeded by a neophyl rearrangement.<sup>43</sup> In design, the protocol is similar to the alkylarylation developed by the Cai group towards  $\alpha$ -aryl, $\gamma$ -methylsulfinyl ketones—a C–H abstraction generates the key radical which then undergoes the addition-migration sequence. However, the 5-*oxo*-pentanenitriles synthesized in this work rely on C–H abstraction to an  $\alpha$ -cyano radical rather than a  $\alpha$ -sulfinyl radical. The C–H abstraction step relies on cyclobutanone oxime ring opening much in the same fashion as described by Chen and Xiao above.

As such, MeCN was chosen as the ideal nitrile to test the desired chemistry. A variety of cyclobutanone oximes were screened as additives which could form C–H abstracting radicals upon the action of the organic photocatalyst eosin Y. *O*-(4-trifluoromethyl)benzoyl oxime **14–4** was found to be the ideal additive giving 78% of the desired product **14–2a** under the optimized conditions, whereas without an additive the desired transformation could not occur. This gives good evidence for the C–H abstraction of MeCN to an  $\alpha$ -cyano radical being accomplished by **14–4**. High temperatures (100 °C) were optimal for the desired transformation, with lower –but still elevated– temperatures (80 °C) resulting in a decreased yield (63%) of **14–2a**.

A scope consisting of both symmetric and unsymmetric  $\alpha,\alpha$ -diaryl allylic alcohols resulted in a bevy of 5-*oxo*-pentanenitrile products. Examples from symmetric substrates gave halogen substituted **14–2d** and **14–2e**, electron-rich **14–2b**, and alkyl substituted **14–2f** all in excess of 70% yield. Several trends already addressed within this review with respect to the chemoselectivity of the aryl migration were again observed here. Aryl rings containing electron-withdrawing groups migrated in preference to more electron-rich rings as in **14–2s** and **14–2t**. Steric considerations resulted in decreasing aryl migration for rings substituted in the following order *para* > *meta* > *ortho* due to the highly strained intermediate **14–9**. Sometimes, these electronic and steric considerations competed as is evident in **14–2j** versus **14–2p**. The propensity of heterocyclic aromatic groups such as 2- and 4-pyridyl to migrate over a phenyl group resulted in products **14–2x** and **14–2y** as single regioisomers. The authors attributed this selection to the lower aromaticity of these systems due to their lower resonance energy, important factors when forming the dearomatized spiro intermediate **14–9**.<sup>5</sup> This may explain why product **14–2aa** could be synthesized from the mono  $\alpha$ -aryl allylic alcohol in moderate 45% yield, while the analogous phenyl substituted product could not be synthesized. This rationale invoking preferential migration of the aryl system with the lowest aromatic character was not observed in product **14–2z**, where the 2-naphthyl ring did not migrate compared to the more aromatic phenyl ring. However, in this case, the steric requirements for the transfer of the 2-naphthyl group could override the electronic considerations of aromaticity. In addition to MeCN, the utilization of pentanenitrile and malononitrile gave **14–2h** and **14–2g** in 70% and 85% yield, respectively.

A mechanistic proposal begins with oxidative quenching of the excited state of eosin Y by oxime **14-4** resulting in N–O bond cleavage to a stabilized benzoate and iminyl radical **14-5**. Following strain-driven homolysis of **14-5** to yield C-centered radical **14-6**, the key C–H abstraction between **14-6** and the  $\alpha$ -methylene of the nitrile starting material proceeds. The  $\alpha$ -cyano radical **14-7** undergoes intermolecular radical addition to allylic alcohol **14-1** followed by the 3-*exo*-trig cyclization to give spiro[2,5]octadienyl **14-9**. Upon rearomatization, the 1,2-aryl transfer is accomplished to yield ketyl radical **14-10**. Oxidation of **14-10** to the final oxonium intermediate **14-11** by the radical cation of Eosin Y is followed by deprotonation to give the 5-*oxo*-pentanenitrile product **14-2**. The oxidation completes the photoredox catalytic cycle. As in the earlier work of Cai, a very large primary kinetic isotope effect ( $k_H/k_D=12.3$ ) was obtained when an equimolar mixture of MeCN and MeCN- $d_3$  was used under the optimal reaction conditions, implicating the C–H abstraction as the rate-determining step. Gratifyingly, this C–H abstraction strategy utilizing oxime **14-4** was also able to generate  $\alpha$ -keto radicals, with a lone reaction using acetone as the alkyl fragment of the addition giving **15-2a** in 66% yield. The inclusion of more complicated carbonyl-containing addition partners would add to the versatility of this methodology. No post-functionalization reactions upon the installed nitrile moiety were performed.

While many of the neophyl-type rearrangements or other 1,2-aryl migration reactions detailed previously have utilized diaryl allylic alcohols as the migration substrate, a recent work from the Shi group has instead opted for a class of olefins bearing a vinyl-substituted all-carbon quaternary center.<sup>44</sup> Impressively, the transformation forges 2 new C–C bonds across the olefin.

A wide variety of fluorinated alkyl fragments could be integrated into the final rearranged products **16-2a–16-2g** in high yields (Scheme 16). Gratifyingly, two examples of non-fluorinated alkyl groups gave ester and nitrile **16-2h** and **16-2i**, respectively. Homologation of the alkene tether to an allyl or homoallyl group resulted in *ortho*-cyclization products **16-2t** and **16-2v** in good yields rather than aryl transfer, underscoring the delicate conformational requirements of radical aryl migration reactions. A variety of useful post-transformation functionalization reactions from **16-2b** gave further densely functionalized molecules **17-1–17-6** in high yields (Scheme 17).

In terms of the scope of the migrating aryl group, the transformation accommodated both electron-deficient and electron-rich aryl groups to give products **16-2j–16-2r** in high yields. In fact, both electron-deficient and electron-rich systems migrated better than the corresponding unsubstituted phenyl group. 2-naphthyl (**16-2o**) and 2-thienyl (**16-2r**) rearrangement products were achieved in 67% and 80% yield, respectively. No examples of migrating phenyl systems with *ortho*-substitution were demonstrated. All examples required that the substrate's vinyl quaternary-center bear two strongly electron-withdrawing groups. Besides diesters, a nitrile (**16-2s**) and a barbituric acid derivative (**16-2u**) were synthesized in acceptable yields.

While the mechanism of the transformation is still under investigation, their current paradigm begins with generation of a fluoroalkyl radical group (**R<sub>F</sub>**) by single electron reduction from the excited Ir<sup>III\*</sup> (Scheme 18). Radical addition to the vinyl group then

gives alkyl radical **16-3** and Ir<sup>IV</sup>. **16-3** can undergo either the desired aryl transfer or an undesired atom transfer radical addition (ATRA) pathway to byproduct **18-2**. Suppression of the latter pathway was achieved by the unique combination of organic bases, solvent, and photocatalyst. A drastic selectivity switch to favor the ATRA pathway could be achieved when no photocatalyst was added to the reaction (Scheme 18, bottom). This suggests that direct excitation of a perfluoroalkyl iodide–nitrogenous base EDA complex can also generate the fluoroalkyl radical **R<sub>f</sub>** and that a propagative radical chain pathway can sustain ATRA. A quantum yield of  $\Phi = 1.8$  also lends credence to propagative radical chain pathways. Subjection of ATRA product **18-2a** to the reaction conditions did not lead to aryl transfer product **16-2a**, suggesting ATRA products are not intermediates *en route* to aryl transfer products.

In any event, stabilized radical **16-5** is proposed to undergo a radical combination with an H-atom which was generated from  $\beta$ -scission of the solvent derived ketyl radical **18-3** to finally give product **16-2**. This radical **18-3** in turn could result from an amine radical cation, which was generated in the turnover of Ir<sup>IV</sup>. The observation of hemiacetals **18-6** and **18-5** (when the reaction was run in MeOD) is used as evidence to support the formation of **18-4** following the proposed  $\beta$ -scission. Direct HAT from **18-4** by **16-5** instead of a difficult to achieve radical combination between H• and **16-5** would also be consistent with the observed hemiacetals. On the other hand, there are several features of the reaction that suggest that single-electron reduction of **16-5** followed by protonation of the resultant carbanion forms the new C–H bond. These features include: 1. The attenuation of desired reactivity with utilization of less-strongly reducing photocatalysts; 2. The necessity of two strongly electron withdrawing groups at the quaternary center of the substrate; 3. Deuterium incorporation when the reaction is run in MeOD. All these features are consistent with protonation of a carbanionic intermediate. Therefore, studies are needed to clarify the formation of the C–H bond in the rearrangement product. In particular, a primary kinetic isotope effect experiment could provide useful information as to C–H bond formation as a HAT, deprotonation, or radical combination event.

In all, this cascade sequence constitutes a very welcome variation on the photoredox mediated neophyl rearrangement, diverging from the typical reliance on allylic alcohols as substrates. An expansion of the methodology to encompass further radical groups besides fluoroalkyl groups would be of benefit.

#### b) 1,4- and 1,5-aryl transfer

In 2017, Zhu and coworkers made a landmark contribution to the repertoire of aryl transfer reactivity. They disclosed both a 1,4- and 1,5-aryl migration between two carbon atoms that resulted in the dicarbofunctionalization of alkenes leading to distally functionalized aryl ketones from tertiary alcohols.<sup>45</sup> This report will not be discussed in this Review, as it does not involve photoredox catalysis. However, it is a seminal publication that inspired related work within the scope of this Review. Later in 2017, the same research group envisioned that intramolecular HAT from an alkyl group to an alkoxy radical could trigger a 1,4-aryl migration in a similar manner as the first report to achieve  $\delta$ -heteroarylation of ketones beginning from tertiary alcohols (Scheme 19).<sup>46</sup> Tertiary alcohols **19-1** containing

both a branched alkyl group and a migratory aryl group at the 1-position were synthesized to test this idea.  $\gamma$ -Arylated ketones **19–2** were successfully isolated from the reaction using reagents known to form alkoxy radicals from alcohols, thereby validating the authors' hypothesis. Parallels to the neophyl rearrangement in the reaction design are clear: C–C bond cleavage between the migrating aryl group and the “leaving” carbon atom overcomes thermodynamic penalties through stabilizing effects of the adjacent alcohol and through formation of a strong C=O bond. Optimized conditions from a model system produced the desired ketone in 82% isolated yield and required superstoichiometric quantities of  $K_2S_2O_8$  and 50 mol% of  $NBu_4Cl$  together with an iridium photocatalyst under blue LED irradiation. Exclusion of light or any single chemical reagent completely prevented product formation. Fukuzumi's catalyst (9-mesityl-10-methylacridinium perchlorate) gave the desired product in a decreased 42% yield. Other common transition metal photocatalysts with lower excited state oxidation potentials were ineffective. The role of  $NBu_4Cl$  was not elucidated, although it could not be substituted by either the phase-transfer catalyst sodium dodecyl sulfate or the inorganic base  $K_3PO_4$ . However, replacement of  $NBu_4Cl$  by  $NBu_4H_2PO_4$  resulted in only a slight yield reduction. The scope of the reaction was presented to emphasize functional group tolerance and diversity of C–H bonds which could undergo successful 1,5-HAT. Migration of a 2-benzothiazolyl unit could proceed to cyclic and acyclic, secondary and tertiary  $sp^3$  carbons as well as  $\alpha$ -ethereal carbons (**19–2g**). 2-thiazolyl (**19–2e**) and 2-pyridyl (**19–2f**) moieties could also migrate, but less effectively. Migration of substituted benzenes was not observed, regardless of their electronic or steric properties.

To establish a reactivity trend, the authors synthesized three 1-benzothiazolyl-1,1-dialkylmethanol compounds in which the two alkyl units contained different types of  $\delta$  C–H bonds (Scheme 20, left). Based on product distribution,  $3^\circ$  alkyl C–H bonds were most reactive, followed in descending order by  $2^\circ$  alkyl,  $2^\circ$  benzylic, and  $1^\circ$  C–H bonds. This competition experiment also showed that 1-aryl-1,1-dialkyl alcohols could give aryl migration products in the first place; no examples of such products were given in the main substrate scope. A quantum yield  $\Phi$  for the reaction of 0.86 was calculated and presented as evidence against a radical chain pathway. Stern-Volmer luminescence quenching studies indicated that oxidative quenching of the photocatalyst's excited state by  $K_2S_2O_8$  could occur, and cyclic voltammetry experiments suggested that direct oxidation of the substrate by the photocatalyst likely could not occur. The authors therefore postulate a concerted proton-coupled electron transfer (PCET) pathway involving oxidation of **19–1** by an  $Ir^{IV}$  intermediate to arrive at the key alkoxy radical **19–3**, but do not expound on the interaction between the substrate and the proton acceptor (Scheme 20, right). Following 1,5-HAT and 1,4-aryl migration, the  $\alpha$ -hydroxy radical **19–5** is oxidized to give ketone **19–2**.

The limited scope of migrating aryl groups in the  $\delta$ -arylation of benzylic alcohols described by Zhu and coworkers led the same authors to interrogate heterocycles without nitrogen atoms for their migratory aptitude (Scheme 21).<sup>47</sup> At the outset of this study, (benzo)thiazole-, (benz)imidazole-, benzoxazole-, quinoline-, and pyridine-containing compounds had all been demonstrated as competent substrates for radical 1,4-aryl migration between carbon atoms. Non-aromatic formyl, iminyl, alkynyl, and alkenyl groups had previously been shown to migrate as well.<sup>48, 49</sup> However, (benzo)furans and

(benzo)thiophenes had yet to be investigated, and a general ranking of migratory aptitude was not yet established. The authors therefore synthesized a series of bis-homoallylic alcohols with two different aryl groups at the 1-position. Addition of trifluoromethyl radical to the alkene would trigger the aryl migration to the product radical. The authors selected Togni's reagent II as the trifluoromethyl radical source and evaluated several photocatalysts as radical initiators.

Notably, both strong excited-state reductants such as *fac*-Ir(ppy)<sub>3</sub> and strong excited-state oxidants such as Fukuzumi's acridinium catalyst could generate the trifluoromethyl radical and facilitate the aryl migration in good yields. The authors therefore employed Fukuzumi's catalyst in all subsequent trifluoromethylations. The success of such a potent photooxidant in accomplishing the reductive cleavage of Togni's reagent II was surprising, so luminescence quenching experiments were conducted and revealed that the tertiary alcohol **21-1** could quench the catalyst's excited state. The authors concluded that a small amount of **21-1** could act as a sacrificial reductant of the excited photocatalyst to access its reducing neutral radical form Acr-Mes• (Scheme 22). Reductive cleavage of Togni's reagent II would release the first trifluoromethyl radical species into the system. Following •CF<sub>3</sub> addition to the alkene and 1,4-aryl migration to radical **21-3** through spirocycle **21-4**, the α-hydroxy radical **21-5** could be oxidized by the excited photocatalyst to give the product. Stabilized mono- and difluoroalkyl halides were also amenable to the addition/migration cascade, but *fac*-Ir(ppy)<sub>3</sub> was necessary to produce their corresponding fluoroalkyl radicals. The broad scope of the reaction validated (benzo)furan and (benzo)thiophene as competent migratory arenes. To construct a ranking of migratory aptitude, the authors prepared bis-homoallylic alcohols with two potential migrating groups to systematically compare the ratio of products corresponding to the migration of each aryl group. For example, a tertiary alcohol containing a 2-furyl group and a 2-thiazolyl group delivered a 1:1 ratio of trifluoromethyl ketones corresponding to migration of both groups. This finding led the authors to conclude that furan and thiazole possess comparable migratory aptitudes. Through these competition studies the authors derived the following ranking of migratory aptitude (in descending order): benzofuran > benzothiazole > furan ≈ thiazole > benzothiophene > thiophene. Density functional theory calculations were in good agreement with the experimental results; they illustrated lower activation barriers for the aryl migration step in the benzo-fused analogues of each heterocycle. Ultimately, computational comparisons of aryl migration activation energy between all heterocycles in the study resulted in the same migratory aptitude ranking as did the synthetic experiments. This work will likely be useful to other researchers who wish to design efficient aryl migration methodologies.

Seeking to design new aryl migrations, Gu and coworkers were inspired by prior achievements in C–H functionalization that generate radicals by HAT from alkanes and ethers to oxygen-centered radicals. Such alkyl radicals had already been merged with concomitant neophyl rearrangement of allylic alcohols.<sup>50, 51</sup> The authors sought to extend the reactivity of α-oxy radicals to homologated olefinic alcohols by effecting 1,4- and 1,5-aryl migrations between carbon atoms (Scheme 23).<sup>50, 52</sup> Tertiary *bis*-homoallylic alcohols **23-1** were synthesized with the expectation that additions of alkyl radicals derived from

HAT of ethers **23–2** would provoke aryl migration to provide  $\delta$ -alkylated ketones **23–3**. Successful radical addition/rearrangement of **23–1** was accomplished using the heteroleptic iridium photocatalyst Ir[dF(CF<sub>3</sub>)ppy]<sub>2</sub>(dtbbpy)PF<sub>6</sub> and K<sub>2</sub>S<sub>2</sub>O<sub>8</sub> as the HAT reagent. The scope of the reaction displayed migration of substituted benzothiazoles **23–3a–3c**, imidazole **23–3d**, and pyridine **23–3e**. Various ethers were successfully functionalized, including tetrahydrofuran **23–3f** and methyl *tert*-butyl ether **23–3g**. Unexpected regioselectivity of the HAT event was demonstrated with methyl benzyl ether; the stronger methyl hydrogen atom was abstracted rather than the weaker benzylic hydrogen atom (**23–3h**).

The proposed mechanism (Scheme 24) involves reduction of K<sub>2</sub>S<sub>2</sub>O<sub>8</sub> by the excited photocatalyst to yield sulfate radical anion SO<sub>4</sub><sup>•-</sup>. The radical anion can abstract a hydrogen atom from ether **23–2** to give the  $\alpha$ -oxy alkyl radical **23–4**, which then adds to the 2-position of the migrating arene prior to the crucial C–C bond cleavage of **23–6**. The extruded  $\alpha$ -hydroxy radical **23–7** is oxidized by Ir<sup>IV</sup> to ultimately give the  $\delta$ -alkylated ketone product **23–3**.

In 2019, interest in acyl radical chemistry drove Ngai and coworkers to pursue acyl chlorides **25–2** as reagents for arylation of alkenes **25–1** with concomitant aryl migration from a distal tertiary alcohol (Scheme 25).<sup>53</sup> The accessible arylacylated products of the present reaction were predicted to be 1,4-, 1,6-, and 1,7-diketones **25–3** depending on the length of the tether between the alcohol and olefin. Optimized conditions to synthesize **25–3** used 1 mol% *fac*-Ir(ppy)<sub>3</sub> as the reductant for the aroyl chloride, though different solvent mixtures and reaction durations were necessary depending on tether length. A satisfactory aroyl chloride scope was exhibited (**25–3a–d**), but we perceive the primary strength of this work to lie in the rich variety of competent migrating groups. Medicinally relevant pyrazine (**25–3h**), pyrimidine (**25–3i**), and substituted pyridine (**25–3j**) could migrate in good yield in addition to the more common (benzo)thiazole and (benzo)thiophene motifs (**25–3e–g**). Moreover, non-aromatic functional groups could migrate in good yields as well: one example each was provided for the transposition of cyanide, an aldehyde/formyl group, an oxime, and an alkene (**25–3m–p**).

Stern-Volmer luminescence quenching studies showed that aroyl chlorides were strong quenchers of the photocatalyst, and the authors used this finding to support their proposed mechanism (Scheme 26). Single-electron reduction of the aroyl chloride by the excited photocatalyst gives the acyl radical **25–4**, which adds to the alkene in the substrate to give alkyl radical **25–5**. The alkyl radical adds to the *pi* system of the migrating unit to arrive at intermediate **25–6**. Elimination of the secondary  $\alpha$ -hydroxy radical **25–7** follows, and sequential electron and proton transfers deliver the final diketone product. The authors further demonstrated that the migration could proceed with a moderate degree of chirality transfer to access enantioenriched quaternary centers if starting with an enantiopure tertiary alcohol **25–1q**. Finally, they carried out condensations of the diketone products to obtain functionalized pyrrole **25–8** and furan **25–9**. Because 1,4 diketones are typically synthesized with umpolung chemistry such as the Stetter reaction and 1,6- and 1,7-diketones have few general methods for their preparation, we view this work as a valuable and enabling synthetic advancement.

Their previous work on dearomative alkyl radical spirocyclizations onto furoic amides led Reiser and coworkers to investigate whether other aromatic systems could participate in similar reactions.<sup>54</sup> Benzamides were of particular interest because the spirocyclic intermediates were not envisioned as stable, so subsequent aryl migrations could conceivably lead to aryethylamines or benzo-fused lactams depending on the arene substitution or tether length. The authors began their study on *N*-protected benzamides **27-1** bearing an ethylene bridge to an *N*-acyloxyphthalimide as an alkyl radical precursor (Scheme 27). Use of 1 mol% of [Ir(ppy)<sub>2</sub>(dtbbpy)]PF<sub>6</sub> in 40:1 MeCN/H<sub>2</sub>O under blue LED irradiation produced  $\beta$ -phenethylamines **27-2** as products of a sequential decarboxylation, 1,4 aryl migration and a second decarboxylation.<sup>55</sup> When water was exchanged for alcohols, the second decarboxylation event could not occur, and the corresponding carbamates were isolated instead (**27-2e**). The scope of the phenethylamine synthesis encompassed mostly electron-rich arenes, although a few examples of electron-neutral arenes were reported in acceptable yields as well. Very electron-rich systems with multiple *meta*- and *para*-substituted methoxy groups underwent regioselective Friedel-Crafts acylation instead of a second decarboxylation to generate dihydroisoquinolinones such as **27-2g**. The authors also discovered that *N*-Boc benzylamines could participate in the aryl migration in addition to benzamides. Once extruded, the methylene carbon was oxidized and lost as formaldehyde. The lower oxidation state in the benzylamines was crucial to permit the rearrangement of substrates with  $\alpha$ -amino alkyl substitution, which converted to Boc-protected amphetamines **27-2h** and **27-2i** in good yields. A homologated propylene tether between the nitrogen atom and *N*-acyloxyphthalimide enabled direct addition of the alkyl radical to the *ortho* position of the benzamide. Rearomatization then gave benzo-tetrahydroazepinone products **27-3** in modest yields. For all substrates in this work, bulky *tert*-butyl or Boc groups were required to bias the substrates' conformations to achieve a productive rearrangement.

This report is notable not just for its unconventional aryl migration from an acyl group, but also for its unique mechanism (Scheme 28). Stern-Volmer luminescence quenching experiments suggested that benzamide **27-1c**, which successfully converts to the corresponding phenethylamine, is a competent quencher of the photocatalyst's excited state. In contrast, *n*-octyloxyphthalimide **27-4** does not quench the excited state of the photocatalyst. The same finding applied to compound **27-5**, which lacks an *N*-*tert* butyl group that would bias the amide conformation to bring the phthalimide in spatial proximity to the migrating arene. However, since **27-5** also contains a shorter tether, caution should be exercised when making a direct comparison between **27-5** and reactive benzamide **27-1c**. Finally, the authors note that the reaction can occur under UV irradiation without any photocatalyst present. With various reactivity modes in mind, the authors propose a mechanism for the aryl migration beginning with protonation of the phthalimide carbonyl and energy transfer from the excited photocatalyst to the protonated carbonyl. The excited carbonyl radical cation then undergoes intramolecular electron transfer (IET) from the benzamide arene to give an arene radical cation within intermediate **27-6**. The authors cite a thorough computational investigation that concludes such intramolecular electron transfers are possible.<sup>56</sup> The observation that electron rich substrates give higher yields is consistent with their increased ability to donate an electron in the IET step. In the two-carbon tether examples, N-O bond homolysis and decarboxylation from **27-6** gives

alkyl radical **27–7**, which adds *ipso* to the benzamide radical cation to give the spirocyclic Wheland intermediate **27–8**. Rearomatization of **27–8** causes Csp<sup>3</sup>–Csp<sup>2</sup> cleavage of the benzamide carbonyl to produce keteniminium ion **27–9**. This reactive species is decomposed by water with loss of CO<sub>2</sub> or converted to the carbamate by addition of an alcohol. With three-carbon tethers, *ortho* addition of the alkyl radical **27–10** is favored instead leading to the benztetrahydroazepinone **27–3**. This work is a rare example of aryl migrations from acyl groups. The *N-tert*-butyl groups could be reliably cleaved in TFA, permitting a formal synthesis of bronchodilating capsazepinoid **27–13** from phenethylamine **27–2j** and tetrahydroazepinone **27–3a**.

### 3. Aryl transfer from C to N

Nevado and coworkers disclosed a 1,4-aryl migration from a carbon atom to a nitrogen atom as an extension of precedent from Shi, Knowles, and Rovis on remote functionalization of alkyl amines. In the Shi work, a silver bipyridine catalyst was employed in conjunction with a hypervalent iodine oxidant to provoke aryl migration to an N-centered radical in 3,3-diarylpropylamines. The remaining benzylic radical was then oxidized to the cation and trapped by an oxygen nucleophile to accomplish a formal  $\gamma$ -oxygenation of an N-alkyl aniline.<sup>57</sup> In the Knowles and Rovis works, 1,5-HAT to N-centered radicals from an *N*-alkyl group enabled  $\delta$ -alkylation of alkyl amines with Michael acceptors.<sup>58, 59</sup> The Nevado group hypothesized that similar N-centered radicals could instead provoke the homolysis of distal unstrained C–C bonds and allow new bonds to be constructed in their place. As proof of this concept, triflyl-protected 3,3-diarylpropylamines **29–1** were subjected to a combination of base and photocatalyst that would provide an N-centered radical intermediate. 1,4-Migration of one of the aryl groups to the nitrogen atom proceeded smoothly, and the benzylic radical leaving group was capped with a Michael acceptor **29–2** to terminate the cascade and give the N-aryl triflamide **29–3** (Scheme 29).<sup>60</sup> The reaction worked best in a ternary solvent mixture of 1:1:1 PhCF<sub>3</sub>:PhCl:H<sub>2</sub>O with K<sub>2</sub>HPO<sub>4</sub> as the base and Ir[dF(CF<sub>3</sub>)ppy]<sub>2</sub>(dtbbpy)PF<sub>6</sub> as the photocatalyst. The authors assembled a substrate scope that exhibits the chemoselective nature of the aryl migration. In unsymmetric diaryl systems, the more electron-rich arene migrated preferentially even with minor electronic differentiation. For instance, compound **29–1e** containing phenyl and *p*-ethylphenyl substituents was converted to a mixture of the two possible migration products in a 6:1 ratio favoring *p*-ethylphenyl migration (**29–3e**) over phenyl migration. This trend was consistent with a polarity-matched aryl transfer to an electron deficient sulfonamidyl radical. Amines with less electron-withdrawing acyl, trifluoroacyl, and benzenesulfonyl protecting groups did not rearrange, suggesting that the lower p*K*<sub>a</sub> conferred to the N–H bond by perfluoroalkylsulfonyl groups is beneficial.

In their mechanistic proposal (Scheme 30), the authors suggest that the triflamide is deprotonated by the base, then the sulfonamidyl anion **29–4** is oxidized by the excited state of the photocatalyst to the *N*-centered radical **29–5**. Trapping of the radical by one of the arenes on the alkyl chain leads to the dearomatized spirocyclic intermediate **29–6**. C–C bond cleavage from **29–6** releases benzylic radical **29–7**, which adds to the Michael acceptor **29–2**. In most examples, the Michael acceptor is a substituted allyl sulfone **29–2a**



and, as such, undergoes  $\beta$ -elimination of a sulfinyl radical to convert to the product **29-3**. Reduction of the sulfinyl radical to its anion by the reduced Ir<sup>II</sup> photocatalyst completes the photocatalytic sequence. The authors further enriched this method by terminating the cascade with either a hydrogen atom source (iPr<sub>3</sub>Si)SH or a bromine atom source (BrCCl<sub>3</sub>) to give the corresponding reduced (**29-9**) or brominated (**29-10**) product,

In 2018, Liu and co-workers disclosed a practical, effective (N+3) ring-expansion methodology towards the synthesis of 8 to 11-membered lactams (Scheme 31 and Scheme 32).<sup>61</sup> Medium-sized ring lactams are featured in a variety of pharmaceuticals, natural products, and other biologically active scaffolds, but the thermodynamic challenges associated with medium-sized ring construction are formidable obstacles for synthetic chemists to overcome.<sup>62</sup> The key (N+3) ring-expansion step in the reaction features a rare, C→N bond migration enabled by the reactivity of an electrophilic amidyl radical. This radical is itself accessed from a synergistic merging of photoredox catalysis with hypervalent iodine(III) chemistry.

Beginning from 6-membered ring precursors, the method smoothly delivered the ring-expanded 9-member lactams (Scheme 31). Various electronic variations on the anilide moiety gave electronically diverse N-aryl lactams **31-2a-31-2f** in 40–85% yield. Changing the tetralone precursor used to synthesize the starting material alcohols allowed for variations in the identity of the migrating aryl group. These products encompassed halogen-substituted lactams **31-2g-31-2i**, providing the opportunity for further cross-coupling chemistry. Alkyl substitution was also tolerated in **31-2j**, but the *ortho*-substituted **31-2k** gave reduced yield (44%) likely due to the steric constraints imposed in the migration step by the *o*-methyl group. Heteroaryl migrating groups were also competent, giving interesting heteroaryl-fused lactams with pyridyl (**31-2l-31-2m**), quinolinyl (**31-2o-31-2q**), and even thienyl (**31-2n**) functionality, albeit in low yield for **31-2n**. In addition to 9-membered rings, the even more difficult 8, 10, and 11-membered ring analogues could be synthesized by beginning with 5, 7, or 8-membered ring precursors. These examples **31-2r-31-2t** further bolster the impressive scope of accessed scaffolds. Post-transformation functionalization included N-aryl deprotection to a free N-H lactam (**32-2-NH**) in two steps and a further, simple (N+4) ring-expansion step to access imposing 13 to 15-membered macrocycles (**32-2a-32-2c**).

The mechanism underlying this robust transformation relies upon generation of an amidyl radical-**31-6**. Fluorescence quenching studies confirmed that acetoxybenziodoxolone-**31-3** (BIOAc-**31-3**) could oxidatively quench Ru<sup>II\*</sup> to form the iodanyl radical **31-4** (BI•-**31-4**) and an equivalent of acetic acid (Scheme 33). This combination of **31-4** and acid, in turn, was shown in cyclic voltammetric studies to be a potent oxidant (> +2.0 V vs. Fc<sup>+</sup>/Fc) and is proposed to oxidize the anilide moiety of starting material **31-1** to its amidyl radical **31-6**, liberating 2-iodo-benzoic acid **31-5** which can aid in oxidation of further **31-1**. From **31-6**, a 1,4-aryl migration occurs giving tricyclic intermediate **31-7** with the new C<sub>Ar</sub>-N bond which upon rearomatization provides the lactam core in ketyl radical intermediate **31-8**. Finally, catalyst turnover is achieved by single-electron oxidation of **31-8** by Ru<sup>III</sup> generated during oxidative quenching. Facile deprotonation of the oxocarbenium ion generated from this previous step furnishes the desired lactam product **31-2**. The intermediacy of amidyl

radical **31-6** was supported by the hydroamination reaction accomplished utilizing the same photoredox-hypervalent iodine(III) reagents to form lactam **33-2a** from **33-1a**. Furthermore, a competition experiment demonstrated the faster reactivity of more electron-rich anilide starting materials (Scheme 33, bottom). Such anilide electronics would help stabilize the intrinsic electrophilicity of an amidyl radical and lead to a faster overall reaction.

In all, this protocol stands as a powerful synthetic application of radical aryl migration strategies to access interesting lactam products. Further studies utilizing the pairing of photoredox catalysis with hypervalent iodine(III) chemistry in the context of aryl migration should follow on the excellent precedent of this report.

#### 4. Aryl transfer from N to C

In 2018, Stephenson and coworkers devised a new aryl migration strategy to streamline the synthesis of aminoalkylated thiophenes.<sup>63</sup> Such products could be prepared in good yield by Smiles-Truce rearrangements of thiophenesulfonamides, and synthesis of such substrates on small scale is indeed trivial owing to the commercial abundance of the sulfonyl chloride precursors. However, the authors cited inefficient preparations of the sulfonyl chlorides from aminothiophenes that damage the efficiency of the route when applied on larger scales. Therefore, an *ipso* substitution of the aromatic amine by a carbon atom would eliminate several steps and concisely produce 3-thienyl propylamines. Examples of radical aryl migrations from nitrogen atoms to carbon atoms are sparse in the literature.<sup>14, 64-67</sup> Nonetheless, the authors chose to pursue their hypothesis because the migration products could be easily elaborated to medicinally relevant thieno-fused azepinones.<sup>68</sup> Protecting groups on the nitrogen atom would be expected to delocalize the N-centered radical leaving group and attenuate the thermodynamic penalty of such an aryl migration. To evaluate their hypothesis, the authors synthesized N-tosyl aminothiophene **34-1a** containing a terminal alkyl iodide as an alkyl radical precursor (Scheme 34). Blue light irradiation of **34-1a** in MeCN in the presence of [Ir(ppy)<sub>2</sub>(dtbbpy)]PF<sub>6</sub> and DIPEA afforded the desired C-N bond cleavage product **34-2a** in 87% yield. The isophthalonitrile-derived organic photocatalyst 4CzIPN gave similar yields when the light source was switched to purple LEDs, but it was challenging to later separate from the aryl migration products by chromatography. Although the alkyl iodide could rearrange successfully, the analogous alkyl bromides **34-1b** did not react productively due to the more negative reduction potential of the C-Br bond. The authors therefore developed a one-pot Finkelstein/Smiles-Truce reaction sequence by adding 1.0 equiv. of NaI together with the photocatalyst and amine. In this way, the desired reactivity was achieved and **34-2a** could be isolated in 55% yield. When the reaction was heated to 60 °C and the loadings of NaI and DIPEA were reduced to 0.5 equiv. and 3.0 equiv., respectively, isolated yields of **34-2a** increased to 95%.

The tosyl protecting group could be exchanged for either *p*-trifluoromethylbenzenesulfonyl (**34-2b**) or Boc groups (**34-2d**), but isolated yield decreased in both cases (Scheme 35). The scope of the rearrangement with respect to the arene was limited mostly to thiophenes, with no other heterocyclic examples and only one successful benzene derivative (**34-2f**). However, non-aromatic sp<sup>2</sup> carbons in  $\alpha,\beta$ -unsaturated  $\beta$ -amino esters could migrate successfully to give valuable  $\beta$ -alkyl enoate esters (**34-2g** and **34-2h**). Lastly, a substrate

with a butylene linker between the nitrogen and halogen atoms—a one-carbon homologated analogue—successfully participated in an atypical 1,5-aryl migration to give **34–2i** in 85% yield.

The proposed mechanism (Scheme 36) entails an initial S<sub>N</sub>2 displacement of 1° alkyl bromide **34–1** with iodide to form alkyl iodide **34–3** *in situ*. Single-electron oxidation of DIPEA by the photoexcited iridium catalyst gives the amine radical cation and an Ir<sup>II</sup> intermediate that reduces the alkyl iodide to the alkyl radical **34–4**. The iodide released by the reduction can then re-enter the catalytic cycle to participate in another bromide substitution. The alkyl radical displaces the aromatic amine in intermediate **34–5** to give an amidyl radical **34–6**, which then abstracts a hydrogen atom from the amine or its radical cation. Although α-amino radicals are competent chain-carrying agents in reductive dehalogenation chemistry and could conceivably exist in the reaction medium as transient intermediates, a possible chain mechanism was not discussed. Synthetic application of aryl migration product **34–2a** was illustrated by a two-step hydrolysis/amidation sequence to synthesize thienoazepinone **34–8** in 58% yield.

Clayden and coworkers sought to develop a new alkene difunctionalization strategy through a radical addition/polar aryl migration cascade of a vinyl urea (Scheme 37).<sup>69</sup> They pursued this idea by reacting electron-rich *N*-vinyl ureas **37–1** with electrophilic fluoroalkyl (R<sub>F</sub>•) radicals. If the R<sub>F</sub>• species was generated by photocatalytic oxidation of a fluoroalkyl sulfinate salt **37–2**, the product α-amino radical after addition to the olefin could be reduced to a carbanion and induce an anionic Smiles-Truce rearrangement. The Clayden group's prior work on aryl migrations from *N*-aryl ureas stresses the significant influence of the urea's conformational rigidity on the success of concerted anionic Smiles-Truce rearrangements.<sup>70</sup> Inclusion of CF<sub>3</sub>SO<sub>2</sub>Na as the trifluoromethyl radical source with 5 mol% of the organic photocatalyst 4CzIPN did not lead to productive reactivity at first. The authors observed undesired side products arising from premature oxidation of the α-amino radical. SO<sub>2</sub> generated during the sulfinate reduction was suspected as the oxidant in these cases. When Cs<sub>2</sub>CO<sub>3</sub> was included as an additive to scrub excess SO<sub>2</sub> from the reaction medium, the desired products could be isolated in good yields. The authors varied the reaction solvent depending on the electronics of the substrate, noting that electron-rich arene migrations performed well in DMF. Both electron-rich and electron-poor benzene derivatives could undergo migration (**37–3a–d**). The stationary vinylic substituent was limited only to aromatic groups, but within this restriction electronically varied substituted benzenes and thiophenes were compatible (**37–3e–i**). Several fluoroalkyl sulfinate salts were successful as radical precursors (**37–3j–l**). Sulfinate salts without α-fluorination did not yield any product, indicating that polarity matching between the vinyl urea and the radical fragment in the initial coupling was crucial. Diaryl phosphine oxides could also be converted to their corresponding phosphonyl radicals without altering the reaction conditions, leading to phosphonylarylated products **37–3m** and **37–3n**.

The major uncertainty in the mechanism was the oxidation state of the carbon atom to which the arene migrates. Since a delocalized spirohexadienyl radical intermediate might abstract a hydrogen atom from the solvent, the authors conclude that the rearrangement is ionic based on deuterium labeling studies that show no arene deuteration occurs in deuterated solvents

(Scheme 38, left). Additionally, when *N,N*-dialkyl urea **37–4** lacking a migrating group was subjected to the optimal conditions in deuterated solvents, deuterotrifluoromethylation product **37–5** was produced in good yield. This finding indicates that the  $\alpha$ -amino anion can be generated in the reaction. The authors thus propose that the reaction begins by oxidation of the fluoroalkyl sulfinate **37–2** (Scheme 38, right). Desulfonylation liberates the fluoroalkyl radical  $R_F^\bullet$ , which adds to vinyl urea **37–1** to give  $\alpha$ -amino radical **37–6**. Reduction of **37–6** to the anion induces the 1,4-aryl migration, which ejects the deprotonated urea as the leaving group. A final protonation gives the difunctionalized product **37–3**.

## 5. Aryl transfer from O to C

Chen and coworkers realized a synthesis of hydroxybenzophenones **39–2** through the first reported acyl Smiles-Truce rearrangement (Scheme 39).<sup>71</sup> They achieved this reactivity with dual hypervalent iodine and photoredox catalysis to homolyze  $\alpha$ -ketoacids **39–1** in a departure from methods that rely on reductive cleavage of acyl chlorides or stoichiometric phosphine-mediated deoxygenation. Conversion of aromatic ketoacids **39–1** to the corresponding 2-hydroxybenzophenones **39–2** proceeded in good yields using the Fukuzumi acridinium photocatalyst and acetoxybenziodoxole (BI-OAc) as the hypervalent iodine species. When the iodine reagent was replaced by sodium carbonate, the desired benzophenone could still form in diminished yield. Other common organometallic photocatalysts and iodine(III) reagents were evaluated, but were deemed less effective. The broad scope of the reaction with respect to the migrating fragment is a hallmark of radical Smiles-Truce rearrangements that do not require delocalization of an ionic intermediate (**39–2a–f**). The transformation was also shown to be scalable, with little change to isolated yield of **39–2i** on 5.5 mmol scale. However, only one heteroaryl migration example is provided, and isolated yield of the corresponding product **39–2f** is relatively low (26%).

The authors also conducted several informative mechanistic experiments (Scheme 40). When a 4:1 mixture of the ketoacid **39–1k**—known to be unreactive without BI-OAc—and its corresponding benziodoxole complex **39–3** was subjected to reaction conditions excluding BI-OAc, benzophenone **39–2k** was still isolated in 80% yield. This result suggests that **39–3** could be a productive reaction intermediate, and that some intermediate in the reaction can engage excess ketoacid in the desired reaction pathway. When a superstoichiometric quantity of TEMPO was added to the reaction, TEMPO adduct **39–4** could be isolated in 26% yield as evidence for acyl radical intermediates. These findings were used to propose a mechanism for the transformation beginning from activation of the ketoacid **39–1** with BI-OAc to form the complex **39–5**. Single-electron oxidation of **39–5** by the photoexcited acridinium dye would restore the benziodoxyl fragment to reunite with the displaced acetate ligand. Simultaneously, decarboxylation of the carboxyl radical **39–6** would produce the acyl radical **39–7**. 1,4-aryl migration from the *ortho*-disposed aryl ether (**39–8**) constructs the benzophenone moiety and displaces the more stable phenoxy radical **39–9**. Single-electron reduction by the neutral acridinium radical completes the photocatalytic cycle and yields the product **39–2** following protonation.

Inspired by the Chen laboratory's work on aryl migrations to acyl radicals, Zeng and coworkers hypothesized that the triplet diradical character of a photoexcited aldehyde—

accessed by irradiation with ultraviolet light—could effect aryl migration from an *ortho*-disposed biaryl ether without need for photocatalysts or external photosensitizers (Scheme 41).<sup>72</sup> Such a strategy would allow expedient preparations of hydroxybenzophenones and substituted phenyl heteroaryl ketones **41–2** from *O*-aryl salicylaldehydes **41–1**. TFA was included as a stoichiometric additive to activate migrating pyridyl rings towards attack by the carbonyl carbon in a Minisci-like radical addition.<sup>73, 74</sup> Electronically varied heterocycles were all competent migrating groups, but migrations of electron-rich pyridines led to the highest yields (**41–2a–d**). More electron-deficient heterocycles pyrazine (**41–2e**) and benzothiazole (**41–2f**) could transfer without need for TFA. 1- and 2-quinolinyl units were unreactive as migrating groups, likely due to the redshifted UV absorbance of their extended aromatic systems *versus* the carbonyl  $\pi$ -system.

A comparison of the yields of **41–2k** synthesized from **41–1k** and deuterated analog **41–2k-D** after a short reaction duration revealed a  $k_H/k_D$  ratio of only 1.2, implying that C–H abstraction is not the rate-limiting step of the transformation (Scheme 42). Additionally, the reaction outcome was not affected in the presence of radical scavenger TEMPO; crossover products indicative of intermolecular aryl or aroyl radical reactivity were not observed. The authors therefore propose a mechanism detailed in Scheme 42: If present, the heterocyclic base in **41–1** is protonated by TFA to give the ionic intermediate **41–1-H**.  $\pi \rightarrow \pi^*$  Excitation of the carbonyl by UV light gives the excited state diradical **41–3**, which then attacks the C2 position of the protonated heterocycle to give dearomatized spirocycle **41–4**. Elimination of a more stabilized phenoxy radical from **41–4** gives intermediate **41–5**. Benzylic 1,5-HAT to the phenoxy radical gives the diradical **41–6**—essentially the protonated excited state of the neutral product **41–2**. This method cleverly exploits the well-studied photochemical behavior of ketones to funnel their excited state diradicals into productive aryl transfer reaction pathways.

Due to their ubiquity within biologically active molecules, the preparation of nitrogen heterocycles is a pressing challenge to synthetic chemists.<sup>75</sup> The functionalization of these cores *via* radical addition has developed many advantages since the seminal reports of Minisci.<sup>76</sup> However, the regioselectivity of such processes is an enduring challenge. For pyridines, these traditional methods typically yield regioisomeric mixtures of C2- and C4-functionalized products. Motivated by these factors, the Hong group developed an intramolecular trifluoromethylpyridylation reaction of alkenes with C2 regioselectivity on the pyridine core (Scheme 43).<sup>77</sup>

Their strategy utilizes pyridine *N*-oxides with a tethered terminal alkene radical acceptor (Scheme 43, **43–1**). Complete C2 selectivity was observed in most cases, although mixtures of C2 and C6 regioisomers were also observed for C3 halogen-substituted **43–2i–43–2n**. More electron-rich pyridine systems such as in **41–2b** gave slightly attenuated isolated yields. In addition to simple pyridine cores (**43–2a–43–2d**), bipyridine, phenylpyridine, quinoline, isoquinoline, gave products **43–2p–43–2s** in good to high yields. Notably, no C4 alkylation was observed in contradistinction to the popular Minisci alkylation which favors these C4 isomers. C2-functionalized pyridines bearing  $\alpha$ -quaternary centers – challenging synthetic targets – were also obtained in **43–2t–43–2v** with little observed decrease in reactivity. Changing the length of the alkene tether had a dramatic effect on the outcome of

the desired difunctionalization. The products derived from 7-*endo*-trig cyclization during the aryl migration gave the highest yields, with 5, 6, and 8-*endo*-trig derived products **43-2w**–**43-2y** giving lower yields. The same trends in the trifluoromethylative method were seen in the phosphorylative functionalization giving an array of P-functionalized pyridines **43-2z** and **43-2aa**–**43-2ad**, including two (**43-2ac** and **43-2ad**) derived from aryl-substituted H-phosphine oxides in 41% and 43% yield, respectively.

The mechanism is proposed to begin with reductive quenching of the organic photocatalyst Eosin Y by Langlois' reagent to generate a  $\bullet\text{CF}_3$  radical (Scheme 44). Radical addition onto the terminal alkene of **43-1** gives carbon-centered radical **43-3**, which is well-disposed for *ortho* addition via 6,7, or 8-*endo*-trig cyclization (depending on the length of the *N*-oxide tether) onto the pyridinium core giving radical cation **43-4**. At this point, two pathways are possible with respect to the rearomatization of **43-4**. Either pathway results in the desired C2 selective aryl migration. Due to a quantum yield of  $\Phi=5.1$ , there is likely a radical chain pathway in which radical cation **43-4** is deprotonated to yield the alkoxy radical **43-7**. The acidity of this C2 proton is increased due to the neighboring nitrogen radical cation in addition to the ability to rearomatize by N-O bond cleavage. Oxidation of Langlois' reagent by **43-7** initiates the next radical chain, while protonation of the resulting alkoxy **43-6** yields the desired functionalized pyridine product **43-2**.

On the other hand, radical cation **43-4** can be reduced by the radical anion of Eosin Y, completing the photoredox catalysis cycle and yielding alkoxy **43-6** after rearomatization *via* deprotonation at C2. A primary KIE of  $k_{\text{H}}/k_{\text{D}} = 1.1$  indicates that deprotonation during rearomatization occurs after the rate-determining step of the reaction (Scheme 44 bottom). As before, a final protonation gives the desired difunctionalized product **43-2**. This same mechanistic paradigm was applied to phosphinoyl radicals derived from H-phosphine oxides to give net alkene phosphonopyridylation products with the same C2 regioselectivity. Key to this process was engaging Eosin Y with a radical precursor source that was a faster reductive quencher than the N-O bond of the pyridinium *N*-oxide.

The unique C2 selectivity of this protocol demonstrates the ability of radical aryl migration strategies to install and manipulate aryl functionality with great precision. Existing Minsci alkylation methodologies have yet to achieve the regioselectivity observed herein. Furthermore, the work also complements Smiles-Truce aryl migration strategies which are typically selective for *ipso* rather *ortho* addition to aryl systems. This report should inform future *ortho*-selective aryl migration strategies. Lastly, the work should also be commended for its delicate handling of the initial reductive quenching of either the  $\text{CF}_3$  or P-radical source in the presence of a sensitive, redox-active N-O bond of the *N*-oxide tether.

## 6. Aryl transfer from O to N

The Murphy group has disclosed a radical cation Smiles rearrangement O $\rightarrow$ N 1,4 aryl migration methodology (Scheme 45).<sup>78</sup> This work constitutes one of the first examples of photoredox catalysis in effecting an O to N aryl migration. In their protocol, a variety of aryloxy alkylamines were smoothly transformed to their corresponding aniline compounds under mild conditions. They cited inspiration primarily from the radical cation

$S_NAr$  C–N coupling protocol of Nicewicz. In that work, a C–N coupling was achieved in an intermolecular sense between a variety of primary amines and anisole derivatives. Murphy, however, was interested in extending this chemistry to an intramolecular variant which makes the transformation a variant of the Smiles rearrangement. Central to both methodologies, however, is the generation of an arene radical cation **45–5** *via* single-electron oxidation by the excited state of an acridinium photocatalyst **Acr**<sup>+</sup> (Scheme 46). In the original report of Nicewicz, this species was intermolecularly trapped by an amine whereas here the tethered amine reacts as an intramolecular nucleophile.<sup>79</sup> Generation of the corresponding [2,5]-spirocyclic octadienyl radical cation intermediate **45–6** can furnish the substituted aniline product **45–2** upon elimination of the oxy leaving group in **45–7** and single-electron reduction of arene radical cation **45–8**. The radical of the acridinium photocatalyst **Acr**<sup>•</sup> is returned to its cationic ground state in reducing **45–8**. Mechanistic studies, however, have not been conducted and it is likely that the tethered amines and arene portions of the substrates could both reductively quench the excited state of the acridinium photocatalyst ( $E_{1,2} = \sim +1.6$  V and  $\sim +1.8$  V vs. SCE, respectively).

The scope of the rearrangement was amenable to electron-neutral and electron-rich substituted arenes such as **45–2a–45–2g** (Scheme 45). The homologated **45–2i** which proceeds *via* the more challenging 1,5 aryl migration was also isolated in a gratifying 83%. The most electron rich 4-OMe substituted **45–2f** however, was only isolated in 4% yield whereas 2-OMe substitution in **45–2h** gave 74% yield. Electron-deficient arenes such as a nitro-substituted substrate did not give the desired Smiles rearrangement product, which is not surprising given the higher oxidation potentials of such systems. A secondary amine substrate **N-Me-45–1a** could undergo the desired rearrangement in low yields to give **45–2j** and was accompanied by *N*-demethylated product **45–2a**. This result contrasts with the intermolecular chemistry of Nicewicz, which could not accommodate secondary amine nucleophiles.

The products detailed above resulting from *ipso* substitution of the phenol are only one of the scaffolds accessible under this methodology. If the arene is substituted with a methoxy group *ortho* to the tethered amine as in **45–3**, tetrahydroquinolines are accessible in good to excellent yields (Scheme 45). Both electron-rich **45–4e** and electron-deficient arenes **45–4e** could undergo the *ortho* substitution, albeit with a lower 38% yield for **45–4c**. A medicinally valuable imidazo[1,2-*a*]quinoline **45–4f** was isolated in 80% yield.

This report is an initial foray into O→N aryl transfers utilizing organic photoredox catalysis and offers a good alternative to net phenol to aniline rearrangements achieved under different radical generation methods.<sup>80</sup> The versatility of this intramolecular rearrangement to either *ipso* or *ortho* substitution is a benefit, especially in the latter's access to tetrahydroquinoline derivatives. The scope of this transformation, however, will surely be limited by the oxidation potential of the arene and is unlikely to work well with electron-deficient arenes.

## 7. Aryl transfer from O to O

In 2017, two O → O radical Smiles rearrangement of 2-aryloxybenzoic acids to their corresponding aryl-2-hydroxybenzoates (aryl salicylates) were independently reported by groups led by Gonzalez-Gomez (Scheme 47) and Li (Scheme 49 below).<sup>81,77</sup> These methods enable access to a diverse scope of salicylate products, which are ideal precursors to salicylamide drugs such as niclosamide along with being UV-filtering additives in various materials. The processes are further distinguished by being overall redox-neutral reactions, obviating the need for external oxidants or reductants. The work of Gonzalez-Gomez will be addressed first, although it must be noted that it was published several months after the initial discovery of Li. In Gonzalez-Gomez's work, the use of the inexpensive acridinium photocatalyst (Fukuzumi's catalyst) and a scale-up demonstration of the process in a flow reactor are material and energy-saving attributes which should attract attention from an industrial standpoint (Scheme 47, 47–2a).

The Ullmann coupling of 2-halo benzoic acids with the corresponding phenol coupling partner facilitated the synthesis of a wide array of the 2-aryloxybenzoic acid starting materials. Variations on the migrating aryl group allowed for electronically diversified salicylates, including halogen-substituted derivatives such as 47–2b and 47–2f in high yields along with more electron-rich derivatives such as 47–2e. It is also apparent that sterically demanding *ortho*-substituted migrating aryl groups such as the previously mentioned 47–2f did not suffer from decreased reactivity. Oxidatively sensitive functionality such as allyl-substituted 47–2i was amenable to the reaction as well, giving the desired product in a high 75% yield. Both 1- and 2-naphthyl were efficient migrating groups, giving 47–2m and 47–2l in 75% and 80% yield, respectively. It is important to note, however, that migrating aryl rings containing the electron-donating 2- or 4-OMe group necessitated the addition of 10 mol% (PhS)<sub>2</sub> in order to achieve synthetically useful yields (yields for 47–2e and 47–2h with additive indicated above). Various substitutions along the benzoic acid core were well-tolerated in the optimized conditions, allowing for a variety of substituted aryl salicylate scaffolds (47–2n–47–2t). As previously mentioned, flow scale-up of the reaction was able to increase material throughput by an order of magnitude, decreasing the reaction times from 16 hours to less than 1 hour for 47–2a.

Extensive mechanistic studies were conducted to corroborate the hypotheses of the authors (Scheme 48). While the reaction could be conducted without base, substoichiometric amounts of Na<sub>2</sub>CO<sub>3</sub> were beneficial to both conversion and yield. This observation is in agreement with cyclic voltammetric and fluorescence quenching experiments, demonstrating that the tetrabutylammonium carboxylate salt ( $E_{1/2} = +1.77$  V vs. SCE) of the starting benzoic acid 47–1a was a better reductive quencher of the excited state of the acridinium photocatalyst ( $E_{1/2} = +2.12$  V vs. SCE) than the benzoic acid alone ( $E_{1/2} = +2.0$  V vs. SCE). In fact, the quenching of [Mes-Acr]<sup>++</sup> by carboxylate 47–3 was found to be near the diffusion limit ( $5.3 \times 10^9$  M<sup>-1</sup>s<sup>-1</sup>). Crossover experiments with an equimolar mixture of 47–1b and 47–1n did not yield crossover products, indicating the intramolecular nature of the rearrangement, while addition of TEMPO to the reaction inhibited product formation demonstrating its radical nature. A quantum yield of  $\Phi = 0.012$  ruled out appreciable radical chain mechanism behavior.



Supported by these observations, the mechanism proceeds with deprotonation of **47-1a** by sodium carbonate followed by rapid single electron transfer to the excited state of [Mes-Acr]<sup>+</sup> to yield benzyloxy radical **47-4**. This O-centered radical undergoes 1,5 aryl migration by *ipso* attack to the migrating phenolic moiety in a 6-*exo*-trig cyclization giving spiro intermediate **47-5**. Rearomatization completes the aryl transfer and gives phenoxyl radical **47-6** which can turn over both the reduced photocatalyst [Mes-Acr]<sup>•</sup> and return the carbonate base. The lack of examples for the rearrangement with strongly-electron deficient migrating phenol groups such as NO<sub>2</sub>- or CF<sub>3</sub>-substituted is a drawback of the protocol. Perhaps this is due to the base-sensitivity of the corresponding salicylate products under the reaction conditions. Or, perhaps, the barrier to aryl transfer is higher for the electron-deficient migrating aryl rings.

Shortly before the report of Gonzalez-Gomez, an analogous work was disclosed by Li and Cao (Scheme 49). While the former work utilized Fukuzumi's catalyst ([Mes-Acr]<sup>+</sup> ClO<sub>4</sub><sup>-</sup>), this work relied heavily upon the on perylene diimide-based photosensitizer **49-3**.<sup>82</sup> However, the methodology also worked with Fukuzumi's catalyst, with higher yields being achieved with it for several substrates including **49-2o-49-2r**. The mechanism of this work is nearly identical to that of Gonzalez-Gomez, with formation of the carboxyl radical **49-4** from reductive quenching of the excited state of **49-3**\* eventually leading to 1,5 aryl transfer from the ether linkage to the new ester bond in **49-7**. Reduction of this phenoxyl radical **49-6** by the **49-3** radical anion and protonation gives the expected salicylate **49-2** while turning over the photosensitizer catalyst. Cyclic voltammetry and fluorescence quenching experiments were in good agreement with those conducted by Gonzalez-Gomez above.

Some notable differences between the two works, however, should be addressed. Longer reaction times were required for this transformation. Indeed, the previously mentioned reactions giving **49-2o-49-2r** utilizing Fukuzumi's catalyst rather than **49-3** proceeded in shorter reaction times as well (26 hours rather than 48 hours). However, a greater diversity in the aryl salicylate products was obtained under these conditions. Most notably, a wide-variety of electron-deficient migrating aryl groups were amenable to the reaction conditions, especially in the *meta* position of the migrating aryl ring (**49-2k-49-2r**). However, these same groups could not occupy the *ortho* or *para* position of the migrating aryl ring as in the report of Gonzalez-Gomez. The steric bulk of the migrating aryl group was found to have little effect on the desired reactivity, even with 2-*t*-butyl and 2,6-dimethyl substituted products **49-2w** and **49-2aa** obtained in 90% and 80% yield, respectively. Strongly electron-donating groups were tolerated in the *para*- and *ortho*- position of the migrating ring (**49-2f** and **49-2u**) without necessitating additives in contrast to the report by Gonzalez-Gomez. This report also tolerated a variety of substitutions on the benzoic acid portion of the starting material yielding **49-2ac-49-2an**. A gram scale, one-pot, two-step synthesis of the anti-inflammatory drug guacetisal was conducted in 92% overall yield, demonstrating the scalability of this protocol. In all, the similar ether-to-ester O→O radical Smiles rearrangements of Gonzalez-Gomez and Li and Cao represent good precedent for further C–O bond-forming radical aryl migration methodologies and complement each other's respective disadvantages.

Ye and coworkers accomplished a Smiles rearrangement of *O*-aryl salicylaldehydes **46–1** through a merger of oxidative NHC catalysis with organic photoredox catalysis (Scheme 46).<sup>83</sup> A similar transformation had been previously reported by the Glorius laboratory, but the scope of the migrating arene in that work was limited to electron-deficient (hetero)arenes which could better stabilize anionic Meisenheimer intermediates.<sup>84</sup> By modifying the reaction conditions such that one-electron processes could operate, the scope with respect to the migrating arene was expanded. Ideal conditions were established using Fukuzumi's acridinium catalyst, a triazolium NHC precursor, substoichiometric quantities of NaI as a secondary electron transfer agent, and 1.5 equivalents of DABCO under an oxygen atmosphere with blue light irradiation. In this system, electron-neutral and moderately electron-rich benzene derivatives could partake in the migration (**46–2a–46–2c**). Steric encumbrance was also tolerated in the case of a mesityl group (**46–2d**). However, no examples of strongly electron-rich nor strongly electron-withdrawn aryl migrations were provided. The non-migrating benzene ring could contain strong electron-donating and weakly electron-withdrawing groups (**46–2e–46–2g**). Heteroaryl migration was not demonstrated.

The proposed mechanism is complex and intermingles oxidative processes by both molecular oxygen and the photoexcited acridinium dye (Scheme 51). The authors propose that *in situ* generated NHC **50–3** reacts with the aldehyde **50–1** to form the Breslow intermediate **50–4**. Oxidation of **50–4** with oxygen co-catalyzed by excited acridinium/NaI gives radical cation **50–5**, which is deprotonated by superoxide to afford the zwitterionic radical **50–6** and hydroperoxyl radical. **50–6** is then oxidized by hydroperoxyl radical to generate hydroperoxide and acyl triazolium **50–7**. This species is hydrolyzed to liberate the NHC catalyst and benzoic acid **50–8**. Deprotonation of benzoate and oxidation by the photoexcited acridinium catalyst produces a benzoyloxy radical **50–9** which performs the *ipso* substitution of the adjacent aryloxy moiety (**50–10**). The more stable phenoxyl radical **50–11** is reduced by the neutral acridinium radical to regenerate the cationic salt, then finally protonated to give the aryl salicylate product **50–2**. The role of DABCO is never explicitly assigned, and no other bases nor amines were evaluated. Although it likely acts as a proton shuttle, tertiary amines are also known reductive quenchers of photoexcited acridinium salts.<sup>85</sup>

## 8. Aryl transfer from O to S

Two papers from Nicewicz and coworkers have disclosed a photoredox mediated Newman-Kwart rearrangement (NKR).<sup>86, 87</sup> This particular aryl migration strategy converts *O*-aryl-carbamothioates to *S*-aryl-carbamothioates (Scheme 52).<sup>88, 89</sup> As such, it represents an important strategy in the synthesis of thiophenols from their corresponding phenols. Classically, the rearrangement is thermally activated with reported reaction temperatures often in excess of 200 °C. The formation of the strained, spirocyclic-thietane Meisenheimer intermediate explains the forcing conditions due to the high entropic and enthalpic barriers associated with the transition state of the rearrangement.

Unfortunately, these harsh thermal conditions can limit the utility of the transformation due to decomposition or undesired side reactivity. Furthermore, the  $S_NAr$  mechanism of

the classical NKR constrains the scope of the reaction to sufficiently electron-deficient aryl systems; electron-rich aryl rings are difficult to transfer as they discourage nucleophilic attack of the thione moiety in the starting material.<sup>90</sup> Both of these drawbacks were mitigated in the present strategy of Nicewicz, which inverts the mechanistic paradigm to what is better described as an  $S_EAr$  process (Scheme 53). The reaction begins with single-electron oxidation of the thione moiety within the O-aryl-carbamothioate **52-1** to its corresponding radical cation **52-4** by the pyrylium photocatalyst **52-3**. Importantly, the authors confirmed that oxidation indeed occurs at the thione rather than the arene; irrespective of arene electronics, fluorescence quenching and cyclic voltammetry experiments gave similar  $k_q$  ( $\sim 1.6 \times 10^{10}$ ) and  $E_{1/2}$  ( $\sim +1.2$  V vs. SCE) values. Furthermore, it was shown that alkene Z to E isomerization for **53-Z/54-3** could be effected in the presence of **52-4/52-1a**, likely due to reversible thiyl radical addition followed by rotation to a more stable *s-trans*-conformation (Scheme 50). This conformer eliminates the thiyl radical cation **52-4** to form **53-E/54-3-E**, giving further evidence of an S-centered radical cation rather than an arene radical cation. Reaction duration dependent isomerization of the pendant Z-alkene in **54-1** was also demonstrated in support of **52-4**. In both experiments, alkene isomerization inhibited the desired NKR significantly (Scheme 54).

**52-4** is electrophilic at sulfur, and, in the absence of competing side reactions with olefins, nucleophilic attack of the arene forms a spirocyclic-thietane intermediate **52-5**. Significant positive charge buildup within the arene during the transition state of this step was shown in a Hammett study and helps to explain the inverse reactivity favoring migration of electron-rich arenes in this protocol versus the opposite trend in the thermal NKR.  $C_{Ar}-O$  bond cleavage to radical cation **52-6** forms the critical  $C_{Ar}-S$  bond. **52-6** can be reduced to the desired product **52-2** by either pyranyl radical **52-3•** to complete the photocatalytic cycle, or chain-propagation can occur with **52-1** to give another equivalent of **52-4**.

Synthetically, the strategy allowed for the synthesis of many S-aryl-carbamates, especially those bearing electron-donating groups in the *ortho* or *para* position of the migrating aryl ring. For example, **52-2a**, **52-2d**, and **52-2g** were all accessible in excellent yields at high reaction concentrations of 0.5 or 0.12 M. Products **52-2f** and **52-2k** with less electron-rich rings were also synthesized in high yields, albeit with dilution of the reaction mixture to 0.06 M. These examples required longer reaction times to avoid off-cycle intermolecular thiyl radical cation coupling to disulfides or back-electron transfer to **52-3•**. These intermolecular pathways compete kinetically with a slow intramolecular aryl migration. Isolation of trifluoroborate **52-2l** in 80% yield is a notable achievement, along with quantitative yield of ( $\pm$ )-tocopherol derivative **52-2m**. Unsuccessful substrates typically bore electron-withdrawing groups, sterically demanding groups in the *ortho* position, or electron-donating groups in the non-resonance stabilizing *meta* position. The mechanistic study paper found that, in general, these recalcitrant substrates all had product S-aryl-carbamates with  $E_{1/2}$  +1.7 V (vs. SCE). An endergonic reaction for such substrates is borne of the fact that the sum of the oxidation potential of the starting materials **52-1** ( $\sim +1.15$  V vs. SCE = -26 kcal/mol) and the bond enthalpy change from an O-carbamothioate to S-aryl-carbamothioates ( $\sim -13$  kcal/mol) is -39 kcal/mol, or +1.7 V (vs. SCE). Thus, the oxidation potential of the desired product, which can be determined from DFT calculations or from

existing electrochemical data, provides a good model for predicting whether the radical cation rearrangement will be thermodynamically favorable. In all, this protocol enables the synthesis of a variety of aryl thiophenols under extremely mild conditions which would otherwise be inaccessible under traditional NKR conditions. A bevy of mechanistic studies bolstered the development of the optimal reaction conditions by informing parameters such as reaction concentration and provided a useful predictive model for the success of the transformation.

## 9. Aryl transfer from P to C

Most Smiles-Truce rearrangements rely on the extrusion of  $\text{SO}_2$  following aryl transfer and, as such, the substrates of such rearrangements are typically arylsulfonyl-containing compounds.<sup>22, 23</sup> The liberation of  $\text{SO}_2$  coupled with the exchanging of a weak  $\text{C}_{\text{Ar}}\text{-S}$  bond for a stronger  $\text{C}_{\text{Ar}}\text{-C}$  bond are favorable entropic and enthalpic factors, respectively. However, the expansion of radical aryl migration strategies beyond arylsulfonyl containing precursors would provide synthetic chemists with greater retrosynthetic freedom and perhaps enable the synthesis of otherwise inaccessible functionalities. A good example of such an advancement has been recently disclosed by Belmont and Brachet.<sup>91</sup> Therein, they describe the first reported radical “phospho”-Smiles-Truce rearrangement, utilizing a migration from the  $\text{C}_{\text{Ar}}\text{-P}$  bond of an arylphosphonohydrazone rather than the more common  $\text{C}_{\text{Ar}}\text{-S}$  bond of an analogous arylsulfonamide (Scheme 55). In fact, this novel development is largely indebted to their previous 2016 work detailing the synthesis of benzhydrylphthalazines from arylsulfonohydrazones through an identical  $\text{C-N/C-C}$  bond forming cascade. In the present case, however, the rearrangement substrate is now an arylphosphonohydrazone. These substrates incorporate both a nitrogen radical precursor and migrating aryl group within the phosphonohydrazone, which can be accessed from a 4-step convergent synthesis terminating with condensation of a 2-(arylethynyl)-benzaldehyde with a diarylphosphonohydrazine.

Many of the benzhydrylphthalazine products accessed through this method were also detailed in their 2016 report (see Scheme 63 below). The modulation of the aryl groups of the diarylphosphonohydrazone allowed for a variety of migrating aryl rings. A modest collection of migrating aryl systems contained halogen substitution (**55-2m** and **55-2n**), electron-rich aryl rings (**55-2q** and **55-2r**), and simple alkyl substituted rings in (**55-2o** and **55-2p**). The sterically demanding *ortho*-substituted **55-2p** was recalcitrant to transfer as shown by its low 32% yield. Migration of heterocyclic or electron-deficient phenyl systems was not described. In addition to substrate modifications resulting in the migration of different aryl groups, variations on the benzylidene core or pendant alkyne also provided diverse benzhydrylphthalazine products. Halogen-substituted **55-2g-55-2i** could be accessed, with debromination of **55-2i** accounting for its lower yield. Interesting indole and benzofuran containing products (**55-2j** and **55-2k**) provided access to otherwise synthetically challenging tricycles. Finally, the modification of the terminal group on the alkyne even allowed for alkyl-substituted **55-2f** amongst some other examples with aryl substitution (**55-2a-55-2e**) in adequate yields.

The mechanism largely coincides with their earlier 2016 report (Scheme 56 and **Scheme 65 below**). Deprotonation of the phosphonohydrazone **55-1** by hydroxide gives the N-anion **55-3** capable of reductively quenching the excited state of the optimal Ru(bpy)<sub>3</sub>(Cl)<sub>2</sub>•6H<sub>2</sub>O photocatalyst. This reductive quenching step had been disclosed by Belmont and Brachet for phosphoramidates and provided them with inspiration for a cascade amination/phospho-Smiles-Truce reaction.<sup>92</sup> The resulting N-centered radical **55-4** undergoes 6-*exo*-dig cyclization onto the internal alkyne functionality to yield an intermediate vinylic radical **55-5**. *ipso* Substitution on the migrating aryl group within the phosphonohydrazone of **55-5** yields intermediate **55-6**. Rearomatization of **55-6** results in aryl migration and generation of P-centered radical intermediate **55-7**, which is proposed to be reduced by Ru<sup>I</sup> and protonated by the solvent to give intermediate **55-8**. Ethanoylsis of the P–N bond of **55-8** gives the desired benzhydrylphthalazine product-**55-2** and an *H*-phosphinate byproduct **55-9**, which was isolated and characterized.

Significant optimization efforts were conducted in order to favor the full amination-aryl migration sequence over a simpler hydroamination process. This latter process is easily explained by the competitive reduction of **55-5** by Ru<sup>I</sup> followed by protonation from solvent rather than the desired 5-*exo*-trig cyclization. Indeed, dilution of the reaction to 0.01875 M proved optimal, favoring the desired intramolecular sequence to **55-2** over the competitive hydroaminative process to **55-11** and **55-12**.

In all, this protocol represents an important demonstration of a radical Smiles-Truce rearrangement not utilizing an arylsulfonyl precursor for the aryl migration. The novelty of the transformation lies more in the C<sub>Ar</sub>–P to C<sub>Ar</sub>–C migration than the benzhydrylphthalazine products that it accesses. These products were obtained in comparable or higher yields in their previous 2016 report (see Scheme 63 below). However, the expansion of radical aryl migration to encompass phospho-containing precursors should not be discounted. Of note in this regard is the more atom-economic synthesis of title product **55-2a** from a monoarylphosphonohydrazone rather than the diarylphosphonohydrazone, albeit in a reduced yield of 34% versus the optimal 65%. Finally, future utilization of chiral phosphorus(V) containing aryl groups introduces the possibility of asymmetric rearrangement reactions.

## 10. Aryl transfer from S to C

A seminal publication by Nevado and coworkers in 2013 detailed the cascade reactivity of *N*-arylsulfonyl acrylamides upon conjugate addition of trifluoromethyl radical to produce either trifluoromethylated oxindoles or amides.<sup>93</sup> The auxiliary nitrogen substituent selectively dictated the product identity such that mixtures of products were observed only in rare cases. Because complex molecules could be rapidly constructed from simple substrates, this report prompted several groups to contribute additional methodologies involving a myriad of radical precursors. To that end, Yang, Xia, and coworkers in 2015 were the first to apply photoredox catalysis to generate radicals for conjugate addition to the *N*-arylsulfonyl acrylamide scaffold (Scheme 53).<sup>94</sup> The authors used trifluoromethanesulfonyl chloride as the trifluoromethyl radical source together with the photocatalyst Ru(bpy)<sub>3</sub>Cl<sub>2</sub>•6H<sub>2</sub>O to convert acrylamides **57-1** to oxindoles **57-2** or amides **57-3**. The reaction optimization

process revealed no benefit from the more strongly reducing photocatalyst *fac*-Ir(ppy)<sub>3</sub>. Relatively high photocatalyst loading (5 mol%) was necessary for satisfactory yields. Although a base was needed to convert the *N*-alkyl substrates to oxindoles, the *N*-aryl substrates did not require a base to give satisfactory yields of the corresponding amides. Electronic manipulation of the sulfonyl-substituted arene did not significantly alter the isolated yields of the oxindoles **57–2b** and **57–2c**. *ortho*-Substituted *N*-alkyl substrates gave complex mixtures of products rather than the anticipated oxindoles. *Meta*-substituted aryl sulfonamides could cyclize to regiosomeric oxindoles: C–N bond formation in the rearrangement of **57–1e** preferentially occurs *para* (**57–2d'**) rather than *ortho* (**57–2d**) to the existing substituent, but this selectivity is not very high. More electron-rich *N*-aryl compounds performed slightly better in the amide synthesis, but the given substrate scope does not permit a definitive conclusion to be drawn.

The proposed mechanism (Scheme 58) for the reaction first involves a single-electron reduction of trifluoromethanesulfonyl chloride, which then desulfonylates to liberate •CF<sub>3</sub>. Conjugate addition of this radical to the acrylamide olefin **57–1** produces the α-amido radical **57–4**, which participates in a Smiles-Truce rearrangement (**57–5**) to give amidyl radical **57–6** following desulfonylation. The reaction diverges at this point depending on the nitrogen substituent R in accordance with Nevado's findings. If R = aryl, then HAT from the solvent terminates the cascade and delivers amide **57–3**. If R = alkyl, the less stabilized amidyl radical is trapped by the arene to give the dearomatized radical intermediate **57–7**. Oxidation by the oxidized photocatalyst gives a Wheland intermediate which is rapidly deprotonated and rearomatized by the base to give **57–2**. This report is notable because it is the first of many applications of photoredox catalysis to accomplish a Smiles-Truce rearrangement. Tang, Sheng and coworkers later expanded the scope of this transformation to include multiple perfluoroalkyl iodide radical precursors.<sup>95</sup>

In 2016, Wan and Zhang disclosed a wholly intramolecular method to synthesize substituted *N*-aryl-2-arylamides **59–2** from *N*-arylsulfonyl 2-bromoacetamides **59–1** (Scheme 59).<sup>96</sup> In contrast with procedures that trigger analogous 1,4-aryl migration by intermolecular radical conjugate additions to *N*-arylsulfonyl acrylamides, the present method achieves the aryl migration by reductive dehalogenation of an activated alkyl bromide already present in the substrate. An analogous copper-mediated reductive dehalogenation/1,4-aryl migration sequence was first reported by Clark et. al. in 2009.<sup>97</sup> However, the present strategy did not require superstoichiometric amounts of a reductant, instead relying on photoexcited *fac*-Ir(ppy)<sub>3</sub> to reduce the substrate directly. When inorganic bases were included as additives instead of water, the reactions proceeded to slightly lower conversions and dramatically lower assay yields. The substrate scope with respect to the amide portion was restricted to tertiary or fluoroalkyl bromides; secondary and primary alkyl bromides did not react. Interestingly, when the optimized conditions were adjusted such that 1 equivalent of Li<sub>2</sub>CO<sub>3</sub> was used instead of water, compound **59–2d** could be isolated in 34% yield while compound **59–2e** remained elusive. The scope of the migrating arene encompassed both electron-rich and electron-deficient benzene rings, although strong electron-withdrawing groups (**59–2b**) and electron-donating groups (**59–2c**) resulted in decreased yields. Thiophene was also competent as a migrating group (**59–2g**). The scope of the *N*-aryl substituent R<sup>2</sup>

accommodated more electronic variation without impacting yield. Notably, no product was formed when N-alkyl substituents were present in place of aryl groups (**59–2j**). Such substrates were reported by other groups to convert to oxindoles, but the authors do not state whether the same is true in their own system.<sup>93, 98, 99</sup>

The mechanistic proposal (Scheme 60) invokes an  $\alpha$ -carbonyl radical **59–3** generated *via* oxidative quenching by the activated alkyl bromide **59–1**. A 1,4-aryl migration (**59–4**) triggers N-desulfonylation and the resulting amidyl radical **59–5** abstracts a hydrogen atom from the solvent. The authors suggest that the catalytic cycle closes by direct oxidation of DMF by the Ir<sup>IV</sup> intermediate. This hypothesis conflicts with the fact that the reported oxidation potential of DMF (2.26 V vs. SCE) is significantly greater than that of the Ir<sup>IV/III</sup> redox pair in *fac*-Ir(ppy)<sub>3</sub> (0.77 V vs. SCE).<sup>100</sup> Another possible pathway to close the catalytic cycle is oxidation of the carbamoyl radical byproduct from the HAT event. The resultant keteniminium species would quickly decompose in the presence of water.

To circumvent an inefficient benzylic fluorination step in the preparation of ORL-1 inhibitor fragment **61–1**, Stephenson and coworkers developed a radical Smiles-Truce rearrangement of bromodifluoroethyl sulfonate esters **61–2** to synthesize 2,2-difluoroarylethanol **61–3** (Scheme 57).<sup>101</sup> These substrates were ultimately derived from the parent sulfonyl chloride and inexpensive ethyl bromodifluoroacetate as the difluoromethyl source. The substrate scope was demonstrated on a variety of (hetero)arylsulfonates, including thiophene **61–3a**, quinoline **61–3b**, furan **61–3c**, and thiazole **61–3d**. Styrenyl sulfonate **61–2e** underwent a vinylogous Smiles-Truce rearrangement to give the corresponding vinylene-homologated difluoroethanol **61–3e**. Pyridine, pyrazole, and benzene derivatives underwent the aryl migration but with diminished yields (**61–3g–61–3i**). Building on well-established reductive dehalogenation strategies, the authors paired Ru(bpy)<sub>3</sub>Cl<sub>2</sub>•6H<sub>2</sub>O with *in situ* generated tributylammonium formate as a sacrificial reductant. DMSO was found to be the superior solvent for the reaction, and relatively high dilution (0.07M) was beneficial to prevent premature decomposition of the sulfonate ester. Interestingly, catalyst loading as low as 0.01 mol% was tolerated without decreasing yield for the model substrate nor appreciably lengthening the duration of the reaction. This observation was consistent with a radical chain mechanism, but the authors did not provide further evidence for this hypothesis in their initial publication.

A more thorough mechanistic study conducted in a subsequent report clarified several details and more definitively concluded that a chain mechanism was operative (Scheme 62).<sup>102</sup> Specifically, an induction period was consistently observed when the reaction mixture was not completely degassed. Furthermore, the reaction could proceed in the absence of photocatalyst altogether if the reaction mixture was rigorously degassed. Without sufficient degassing, greater quantities of unwanted elimination products were isolated. To account for these findings, the authors proposed that a thermal or photochemical homolysis of the C–Br bond in **61–2** could induce the aryl migration (**61–4**, **61–5**), and that the photocatalyst could act as a residual oxygen scavenger if any were present after the degassing process. Formate could act as the hydrogen atom source for the rearranged sulfinyl radical **61–6**, and the resulting carboxyl radical anion could act as the reductant for another molecule of substrate. Finally, as part of the separate mechanistic study, a

100-gram scale batch reaction was executed successfully to give **61-3a** in 64% yield. The advantages of this aryl migration approach compared with C–H fluorination or metal-catalyzed fluoroalkylation include the inexpensive reagents, mild conditions, low catalyst loadings, orthogonal thiophene functionalization regioselectivity, and impressive scalability. However, the authors concede that the scalability of the system in batch is due in part to the highly propagative mechanism and is not generalizable to all photochemical processes. They also caution that the photocatalyst-free conditions were unsuccessful on other analogues of **61-2** besides **61-2a**.

An elegant tandem C–N/C–C bond forming methodology towards the synthesis of benzhydrylphthalazine derivatives was realized by the Brachet and Belmont groups in 2016 (Scheme 63).<sup>103</sup> This work would form the basis for their later investigations into a similar reaction utilizing arylphosphonohydrazones (see Scheme 55 above). The unique heterocyclic scaffolds achieved in this report were synthesized *via* a photoredox mediated cascade hydroamination-Smiles-Truce rearrangement sequence. The novelty of this sequence along with the beneficial biological properties (anti-cancer, anti-bacterial, etc.) of the phthalazine products demand special attention.<sup>104, 105</sup> The starting material integrated both the nitrogen radical precursor as well as the migrating aryl group. Such materials could be traced back to the simple condensation reactions of the corresponding arylsulfonyl chlorides and 2-arylethynyl ketones.

Following the desired transformation, a wide variety of benzhydrylphthalazines were obtained. Electronic variations on the aryl portion of the internal alkyne within the starting materials allowed for both electron-rich aryl containing benzhydrylphthalazine **63-2e** in 60% yield along with electron-deficient derivative **63-2b** in 55% yield. Interestingly, starting materials bearing a 2-(alkylethynyl)benzylidene moiety were also competent in the reaction allowing for enyne-derived product **63-2h** in 66%. Diversification of the migrating aryl ring of the arylsulfonylhydrazone also yielded a wide array of phthalazine derivatives. The electron-rich or deficient character of the migrating aryl ring did not affect the efficiency of the desired transformation, with electron-rich **63-2i** and electron-poor **63-2j** giving nearly identical yields. A 5-methylthiophene aryl ring was also able to act as a migrating group, enabling the synthesis of a unique heterocyclic substituted phthalazine derivative **63-2o** in 71% yield. However, it must be noted that the sterics of the migrating aryl system played an integral role in determining the success of the overall transformation. Sterically encumbered aryl rings such as in *ortho*-substituted **63-2n** were detrimental to the desired transformation, yielding only 30% of the desired phthalazine. 1-naphthyl was also incompetent as a migrating aryl group giving 0% of the desired product **63-2m**. These previous two considerations highlight the strict steric requirements characteristic of the strained spiro intermediates of Smiles-Truce rearrangements. Unsurprisingly, a mesylsulfonylhydrazone was not amenable to the optimized reaction conditions giving 0% yield of **63-2p**.

Interesting elaborations on the benzylidene core of the starting materials for the rearrangement allowed for diverse phthalazine derivatives including 3-substituted **63-2v** and **63-2w** in good to high yields. A 3-chloro substituted starting material gave its corresponding product **63-2s** in 46% yield. The Cl handle was used for post-functionalization in a Buchwald-Hartwig amination to yield an even more structurally sophisticated heterocycle



**64-1** in good yield (Scheme 64). Pyridazine **63-2q** and pyridopyrazine **63-2r** were accessible in 71% and 64% yield, respectively, under the optimized conditions. Finally, the starting material synthesis reaction followed by the title transformation was demonstrated in a one-pot, two-step procedure for several substrates.

Both cyclic voltammetric and fluorescence quenching experiments indicated that only the *N*-deprotonated sulfonylhydrazone is capable of reductively quenching the excited state of the optimal Ru(bpy)<sub>3</sub>(Cl)<sub>2</sub>•6H<sub>2</sub>O photocatalyst. The reaction mechanism is similar to the earlier described cascade from Belmont and Brachet utilizing arylphosphonohydrazones. In this case, however, the S-leaving group of SO<sub>2</sub> is extruded as a gas whereas the P-leaving group of the previous method requires basic solvolysis for removal. Otherwise, the manner in which the C–N and three C–C bonds is formed is the same in this work as in the arylphosphonohydrazone work (compare Scheme 56 above with Scheme 65 below). Notably, no side products due to competitive reduction of the vinylic radical to a vinyl anion were observed in this work in comparison to the arylphosphonohydrazone method. This is good evidence that the intramolecular cyclization/aryl transfer step is faster with the SO<sub>2</sub> leaving group in this method rather than the P-leaving group of the previous work.

Quantitative deuterium incorporation at the triarylmethine position was achieved in product **63-2a-d1** (68% yield) when the reaction was conducted in MeOH-*d*<sub>4</sub>, confirming the role of solvent as the proton source in the final step. This observation is also consistent with the poor performance of this methodology in aprotic solvents. A low quantum yield of  $\Phi = 0.33$  was measured, suggesting that significant radical chain reactivity was not operative. This work is a powerful example of the ability of photoredox mediated radical aryl migrations to rapidly construct intriguing aryl-containing architectures.

An intricate cascade sequence from 1,8-enynes towards the construction of fluorinated tetracycles incorporating both indole and dihydroquinolinone moieties was reported by Li in 2017 (Scheme 66).<sup>106</sup> Building off 1,8-enyne radical cascades developed by Nevado, Li was able to initiate this 4-step sequence with photoredox mediated radical generation from ethyl bromodifluoroacetate avoiding the stoichiometric oxidants and heat necessitated in Nevado's work.<sup>107</sup> Conceptually, the reaction design relies upon oxidative quenching of the excited state of the Ir<sup>III</sup>\* photocatalyst by BrF<sub>2</sub>CO<sub>2</sub>Et in order to generate the desired difluoromethyl radical (Scheme 67). Intermolecular radical addition to the acrylamide moiety of **66-1** begins the serial cascade reactions, first proceeding with a Smiles-Truce rearrangement resulting in 1,4-aryl migration to **66-5** following rearomatization and extrusion of SO<sub>2</sub> from **66-4**. The subsequent *N*-centered radical can then undergo 6-*exo*-dig cyclization onto the appended internal alkyne resulting in vinyl radical **66-6**. This species adds into the *N*-aryl group of the acrylamide at its *ortho* carbon in a 5-*exo*-trig cyclization to give the stabilized cyclohexadienyl radical **66-7**. This species can return the oxidized Ir<sup>IV</sup> photocatalyst to ground state Ir<sup>III</sup> and give the final cationic intermediate **66-8**, which is easily rearomatized *via* deprotonation to the desired tetracyclic product **66-2**. The Na<sub>2</sub>HPO<sub>4</sub> base utilized in the reaction had a profound effect on reaction yield, giving 92% of title product **66-2a** while other bases failed to exceed 60% yield. While the reaction design is similar to earlier cascade reactions, it is notable as a redox neutral process and for its integration of the valuable -CF<sub>2</sub>COOEt handle into a complex molecular architecture.

A brief substrate scope focused mainly on differential substitution on the *N*-aryl and terminal aryl ring of the internal alkyne. Electron-rich and electron-deficient *N*-aryl substitution was tolerated giving excellent yields for a variety of substrates **66–2a–66–2f**. *ortho*-Substitution on this ring also resulted in good yields for **66–2g–66–2j**, with a reduced yield of 51% for the more sterically demanding 2-naphthyl substituted **66–2i**. *meta*-Substitution on this ring resulted in regioisomeric mixtures of **66–2k** and **66–2l**. Various aromatic functionalities including 2-thienyl (**66–2u**) could be accommodated as the terminal aryl group of the internal alkyne in high yields. Only two variations on the sulfonyl-linked migrating aryl group were demonstrated giving **66–2m** and **66–2n** in 85% and 87% yield, respectively. While this work is notable for forging 4 bonds in one pot, a more thorough investigation of the scope of migrating aryl groups would bolster its synthetic potential.

In a work like that reported by Li in 2017, the Zhang group recently disclosed a multi-step cascade sequence towards the synthesis of tetracyclic *N*-fused indoloisoquinolinones (Scheme 68).<sup>108</sup> In essence, the work bears much in common with the previous work of Li; whereas the latter begins with an intermolecular radical addition to an *N*-acrylamide moiety, this work arrives at a similar radical intermediate **68–1** (compare to **66–3**) by single electron reduction of the  $\alpha$ -bromo amide **68–1** by excited state Ir<sup>III</sup>\* (Scheme 68, bottom). The remainder of the mechanism is largely indistinguishable from that of Li (compare the bottom of Scheme 68 with Scheme 67).

Whereas the previous sequence detailed by Li results in the incorporation of a *gem*-difluoromethyl moiety within the isoquinolinone core, this method instead furnishes the analogous *gem*-dimethyl compounds. In fact, products lacking the *gem*-dimethyl group derived from the corresponding secondary or primary bromide substrates were not obtained in this reaction. Additionally, there are only two examples – alkyl-substituted **68–2l** and chloro-substituted **68–2k** – of products with substitution upon the migrating aryl group (Ar<sup>1</sup>). This limits the available complexity of the resulting isoquinolinone backbone. Despite these limitations, a variety of other products could be obtained through various substitutions on the terminal aryl group of the alkyne or *N*-aryl group. Such substitutions resulted in indole cores including electron-deficient (**68–2h**), halogen-substituted (**68–2d** and **68–2e**), and electron-rich (**68–2c**) examples in good yields. Adequate yield of thiophene containing **68–2j** in 45% integrated further heterocycle functionality.

Despite its access to unique tetracyclic *N*-fused indoloisoquinolinones, further variation on the scope of the migrating aryl group would augment the synthetic impact of this method.

Xia and coworkers reported a creative implementation of alkyne photochemistry to initiate a Smiles-Truce rearrangement of 3-aryl-*N*-(arylsulfonyl) propiolamides **69–1** to ultimately produce phenanthro-fused isothiazolone 1,1-dioxides **69–3** upon UV irradiation (Scheme 69).<sup>109</sup> The dilute reaction conditions were necessary to prevent photochemical [2+2] dimerization of the intermediate 4,5-diaryl isothiazolones **69–2**, which are the initial products of the rearrangement. Upon further irradiation, a photochemical oxidative cyclization of **69–2** (known as the Mallory reaction) ensues to give **69–3**.<sup>110</sup> *Para*-substituted sulfonamides could be converted to the corresponding phenanthrenes in good yields as single isomers (**69–3a–69–3c**). *Meta*-substituted sulfonamides give a single isomer of **69–**

**2** after the Smiles-Truce rearrangement, but the subsequent Mallory reaction can occur at two distinct positions to give a mixture of regioisomers (as seen for **69–3d**). *Ortho*-substituted sulfonamides, too, give single isomers of **69–2**. Once again, the Mallory reaction gives regioisomeric mixtures of dihydrophenanthrene intermediates. In one isomer—resulting from *ipso* addition to the carbon bearing the substituent—rearomatization of the dihydrophenanthrene involves loss of the substituent. This process is evidenced by the reaction of **69–1f** to give both **69–3f** and **69–3a** by loss of fluoride. Other N-alkyl ( $R^2$ ) groups besides methyl were tolerated, including a potentially reactive methallyl group (**69–3g**). Thiophene derivatives could also participate in the reaction (**69–3h**), but no other heterocycles were reported. By stopping the reaction sooner (0.5 hours *versus* 7 hours), **69–2h** could be isolated cleanly before **69–3h** could form.

A plausible mechanism for the process is provided in Scheme 70. Excitation of **69–1** with UV light generates the excited state diradical **69–1\***. Aryl migration to the proximal carbon atom in the alkyne of **69–1** leads to dearomatized spirocycle **69–4**. Rearomatization extrudes the aminosulfonyl radical in **69–5**, which combines with the vinyl radical on the distal carbon originating from the alkyne to give the isolable intermediate **69–2**. A second photoexcitation of the newly-formed *cis*-stilbene system induces cyclization to give *trans* 4a,4b-dihydrophenanthrene **69–6**. Trace oxygen is sufficient to oxidize **69–6** to **69–3**. During the optimization process using **69–1a** as the starting material, the authors noticed trace quantities of the unsubstituted phenanthrene hydrocarbon resulting from loss of the isothiazolone 1,1-dioxide motif. In a subsequent report from the same group, it was shown that in the presence of an amine additive, **69–6** could further undergo sequential 1,3-hydride shifts, C–S bond homolysis, *N*-desulfonylation, and elimination of an alkyl isocyanate to ultimately produce phenanthrene hydrocarbons.<sup>111</sup>

Ye and coworkers applied the rich chemistry of ynamides to a new reaction manifold involving a ketyl radical-ynamide coupling in a cascade sequence with a Smiles-Truce rearrangement to afford benzhydryl-functionalized indoles and isoquinolines (Scheme 71).<sup>112</sup> The authors cited the underexplored realm of radical ynamide functionalizations, a renaissance in catalytic ketyl radical generation methods, and the complexity-building Smiles-Truce rearrangement cascades popularized by Nevado as inspiration for their design. In *N*-sulfonylated ynamide substrates **71–1**, production of the ketyl radical initiated the desired cascade to yield indoles **71–2**. The scope of the acetylenic substituent  $R^3$  was mostly limited to benzene derivatives, although both moderately electron-donating and strongly electron-withdrawing groups were tolerated. Modification of the migrating arene was shown, but most examples involved electron-rich benzene derivatives (**71–2a–71–2i**). Homologated ynamides **71–1** could be transformed into the corresponding isoquinolines **71–3** under modified reaction conditions—most importantly, presence of oxygen was found to increase the isolated yields. Similar flexibility was shown in the identities of  $R^1$ ,  $R^2$ , and  $R^3$  as was seen in the indole synthesis (**71–3a–71–3d**).

Stern-Volmer luminescence quenching studies lent strong evidence to the hypothesis that a Hantzsch ester could undergo electron transfer with the photoexcited catalyst, while the ynamide could not. Based on this crucial finding, the authors proposed a mechanism starting with reductive quenching of the photocatalyst by the Hantzsch ester (Scheme 72).

The dihydropyridyl radical cation delivers a hydrogen atom to the carbonyl functionality in the substrate **71-1** to give the ketyl radical **71-4**. Regioselective cyclization onto the  $\alpha$ -carbon of the ynamide yields a nucleophilic vinyl radical **71-5**, which then displaces the sulfonamide in the aryl migration event to give radical **71-6** represented by N-centered- and C-centered radical resonance forms. This species undergoes formal HAT to give imine **71-7**, which could be isolated. Reduction of **71-7** by a second equivalent of the Hantzsch ester, followed by a dehydration through a spin-centered shift gives  $\alpha$ -iminyl radical **71-9**. Finally, protonation gives indole **71-2**. In the homologated substrates, a final oxidation—potentially by ambient molecular oxygen—generates the aromatic isoquinoline system **71-3**. This work represents a creative implementation of an unconventional radical coupling as a trigger of the Smiles-Truce rearrangement.

The Smiles-Truce rearrangement had long been known as a reliable method for arylethylamine synthesis by the time Stephenson and coworkers reported a novel aminoarylation methodology in 2018.<sup>113, 114</sup> However, substrates for effective Smiles-Truce rearrangements usually contained functionalized tethers that required additional steps to produce from commercial building blocks. The authors hypothesized that a radical coupling between a sulfonamide and an alkene would give an adduct prone to aryl transfer without need of a discrete radical precursor in either component (Scheme 73). Pioneering work by Nicewicz and coworkers describing the catalytic hydroamination of alkene radical cations inspired the authors to investigate whether these same electrophilic intermediates could intercept aryl sulfonamides and induce aryl migration.<sup>115</sup> In presence of the strongly oxidizing photocatalyst [Ir(dFCF<sub>3</sub>ppy)<sub>2</sub>(5,5'-dCF<sub>3</sub>bpy)]PF<sub>6</sub> and substoichiometric amounts of KOBz under blue light irradiation, arylsulfonylacetamides **73-1** reacted with electron-rich styrene derivatives **73-2** (R = H) to garner the desired diarylethylamines **73-3** in moderate yields. Carbamates could be substituted for the acetyl protecting group, but trifluoroacetyl protection shut down the reaction completely (**73-3a-73-3d**). Significant increases in yield were not observed until the alkene substrate **73-2** was changed to disubstituted *trans*-anethole (R = Me), which was converted to the corresponding aminoarylation product **73-3e** in 82% yield without any change to the reaction conditions. The improved performance of  $\beta$ -methyl styrenes can likely be ascribed to slower dimerization with their corresponding radical cations compared to monosubstituted styrenes.<sup>116</sup> Notably, the aminoarylation was highly diastereoselective in both cyclic and acyclic systems; only one diastereomer was detected for each product. The scope of the reaction with respect to the *N*-acylsulfonamide included a wide variety of heteroaromatic and polycyclic aromatic structures (**73-3e-73-3j**). Endocyclic alkenes granted access to complex compounds such as **73-3k**. The primary limitations of the method are the low reactivities of substituted benzenesulfonamides—likely due to the higher thermodynamic barrier for their dearomatization in the *ipso* substitution step—and the requirement of electron-rich styrene substrates.

The mechanism is supported by Stern-Volmer fluorescence quenching analysis and begins with single-electron oxidation of **73-2** by the excited photocatalyst (Scheme 74). The resultant alkene radical cation **73-4** likely reacts with the deprotonated sulfonylacetamide to give the neutral radical adduct **73-5**. Bond rotation in **73-5** occurs faster than the subsequent aryl transfer event, which explains both the high diastereoselectivity for the reaction and

the finding that both *cis*- and *trans*-anethole convert to the same diastereomer of **73-3**. *ipso*-Substitution of the sulfonyl group by the benzylic radical proceeds through the intermediate dearomatized spirocycle **73-6**. Reduction by the reduced Ir<sup>II</sup> complex, desulfonylation, and protonation yields the final diarylethylamine **73-3**.

An impressive advancement in photoredox mediated aryl migration strategies was disclosed by the Zhu group in 2018.<sup>117</sup> Their iododifluoromethylarylation of unactivated olefins utilized a bifunctional sulfonyl linked reagent- **75-1** containing both a difluoromethyl radical precursor along with the migrating aryl component (Scheme 75). The “docking-migration” strategy relied upon the traceless extrusion of the SO<sub>2</sub> linker between the difluoromethyl radical donor and migrating aryl group acceptor, much like the bifunctional sulfonylacetamide reagents described earlier by Stephenson (see Scheme 73). Initial efforts focused on addition of benzothiazolyl and iododifluoromethyl groups across activated alkenes, with the iodine functionality supplied by tetrabutylammonium iodide additive.

Addition of these groups across styrene in 82% yield (**75-2a**) under the optimized conditions led to an extensive scope of difunctionalized products. Electronic and steric variation upon the styrene aryl group was inconsequential to the outcome of the desired transformation, with examples **75-2a-75-2j** all being obtained in good to excellent yields. Even a pinacol boronic ester-substituted product **73-2d** was tolerated, albeit with a reduced yield of 56%. Product **75-2k** with a quaternary center was synthesized in 75% yield. Complete *syn*-diastereoselectivity was observed for **75-2l** derived from dialin. This was confirmed by x-ray crystallographic analysis of **73-2l**. The unique diastereoselectivity is due to kinetic control favoring the *syn*-delivery of the groups across the double bond in accord with the previous observations of Stephenson (see Scheme 74). Other activated alkenes including enol ethers and enamides gave products **75-2n** and **75-2m**, respectively in adequate to high yields.

This protocol especially shone, however, in its accommodation of unactivated alkenes. Terminal olefins distal to various sensitive functionalities such as ethers (**75-2p**), acids (**75-2q**), alcohols (**75-2r**), silanes (**75-2s**), halides (**75-2u**), nitro-groups (**75-2t**), and alkynes (**75-2v**) smoothly transformed to the desired difunctionalized products in synthetically useful yields. These results are certainly remarkable considering the patent difficulty in harnessing the unstabilized intermediate alkyl radical **75-5** resulting from initial radical addition to unactivated olefins. The capture of this radical in a Smiles-Truce rearrangement is a testimony to its excellent utility to effectively install aryl functionality. The application of this methodology to biologically relevant scaffolds in derivatives **75-2w** and **75-2x** is laudable. Impressive post-functionalization reactions included conversion of the benzothiazole to an aldehyde (**76-1**) in 3 steps in 63% yield. Suzuki and Heck cross-coupling yielded **76-2** and **76-3** in 90% and 64% yield, respectively. Substitution, elimination, oxidation, and reduction all yielded unique scaffolds (**76-4-76-6**) as well (Scheme 76).

Other heteroaryl migrating groups could be delivered using similar bifunctional sulfone reagents. Thiazolyl, benzoxazolyl, benzoimidazolyl, pyrimidyl, and quinolinyl groups were competent in this regard and afforded difunctionalized products **75-2y-75-2z** and **75-2aa-**

**75–2ac** albeit in reduced yields. No examples with phenyl group derived bifunctional sulfones were reported. The bifunctional sulfone reagents themselves could be synthesized in three steps from the corresponding heteroaryl mercaptans.

The elegance of this methodology revolves around the engagement of the bifunctional sulfone **75–1** within the mechanistic paradigm. The excited state Ir<sup>III\*</sup> photocatalyst is oxidatively quenched by the bromodifluoromethyl portion of **75–1**, unmasking the desired difluoromethyl radical **75–4**. This step is corroborated by both fluorescence quenching experiments and cyclic voltammetry with **75–1** ( $E_{1/2} = -0.71$  V vs. SCE). **75–1** can then engage the olefin reaction partner **75–3** in an intermolecular radical addition to give the transient alkyl radical **75–5**. 5-*exo*-trig cyclization to the *ipso* position of the appended aryl group gives spirocyclic *N*-centered radical intermediate **75–6**. Rearomatization of **75–6** ultimately results in 1,4-aryl migration along with extrusion of SO<sub>2</sub> to a difluoromethyl radical **75–7**. At this point, I<sub>2</sub> generated from the oxidation of tetrabutylammonium iodide by Ir<sup>IV</sup> can trap **75–7** to give the desired iododifluoromethylarylated product **75–2**. Generation of I<sub>2</sub> also completes the photoredox catalytic cycle. The trapping of **75–7** with groups other than I remains was not demonstrated. The authors state that the superstoichiometric amount of tetrabutylammonium iodide was necessary for starting material conversion, suggesting that this difluoromethyl radical **75–7** is difficult to capture otherwise. Although the iodide functionality was aptly transformed in various post-functionalizations, engagement of the radical **75–7** in cross-coupling or cascade cyclizations could be interesting advancements.

However, in two subsequent papers to the original report, the Zhu group demonstrated that their protocol could be adapted to accommodate a myriad of different di- and even trifunctionalization reactions of both unactivated and activated alkenes.<sup>118, 119</sup> Simply switching the initial reagent from difluoromethyl radical precursors to dialkyl radical precursors resulted in, for example, net heteroarylisopropylation reactions of many of the same alkene substrates as detailed above. Cyclopentyl or azetidynyl group incorporation could also be achieved from the corresponding bifunctional reagents. The heteroaryl group (typically benzothiazole or other *N*-heterocycles as above) was also replaced with an oximinyl radical precursor, which is a significant example of the expansion of this docking strategy to encompass alkene difunctionalization without arylation. Significantly, trapping of the intermediates of these reactions analogous to **75–7** in the initial report was demonstrated. Radical trapping with deuterium, acrylates, and S- or Se-radical trapping reagents led to an impressive scope of three-component reaction products. This adaptation is a worthy improvement upon the original work in which **75–7** could only be engaged with iodine. These three works of Zhu must be commended as some of the most synthetically diverse applications of radical aryl migration *via* photoredox catalysis and ought to serve as templates for further discovery. A convenient and comprehensive account of these 3 works and other radical migration strategies from the Zhu group should be consulted for a more thorough appreciation of this “docking-migration” strategy.<sup>120</sup>

The Greaney group has reported on a variety of ionic Smiles-Truce reactions,<sup>121</sup> but in 2019 their attention shifted to radical variants (Scheme 77).<sup>122</sup> Building from the precedent of Zard on aryl transfer of *N*-acylsulfonamides,<sup>123, 124</sup> a carbodifluoroalkylation of various

*N*-allyl sulfonylacetamides provided functionally rich, fluorinated acetamide products. Their original paradigm included a reductive photocatalytic regime, utilizing *fac*-Ir(ppy)<sub>3</sub> and ethyl bromodifluoroacetate to arrive at the •CF<sub>2</sub>CO<sub>2</sub>Et radical (Scheme 78). Addition of this radical to **77-1** arrived at alkyl radical **77-3**. The standard 1,4-aryl transfer sequence could then result from intramolecular *ipso* addition of **77-3** into the appended aryl group of the sulfonylacetamide followed by extrusion of SO<sub>2</sub> to give **77-5**. It is at this point that sacrificial reductant such as tetramethylethylenediamine (TMEDA) could turn over Ir<sup>IV</sup>. The subsequent amine radical cation provides an H-atom for **77-5** to furnish the acetamide product **77-2**. Alternatively, the amine could reduce **77-5** and act as a proton source to give **77-2**. The amine radical cations of tertiary amines have been demonstrated to act as either an H-atom or proton donor.<sup>125</sup>

The above paradigm guided initial reaction optimization, and it was found that 3 equivalents of TMEDA was optimal. Curiously and more importantly, however, control experiments revealed that the reaction proceeded in higher yields upon irradiation in the absence of photocatalyst (59% vs. 67% for title product **77-2b**). In the dark, or by simply heating, no rearrangement product was observed. These observations align with literature precedent of trialkylamines acting as *n*-sigma donors to electron-deficient halides in electron donor-acceptor (EDA) complexes.<sup>19</sup> <sup>19</sup>F-NMR and UV-Vis studies of mixtures of TMEDA with difluorobromoethyl acetate corroborated this EDA hypothesis as well. Consequently, the original photoredox catalyzed paradigm was discarded in favor of the photochemical EDA approach (Scheme 78).

The scope of the transformation was found to accommodate a small series of migrating aryl groups including electron-deficient (**77-2d-77-2g**), neutral (**77-2a** and **77-2b**), and electron-rich (**77-2c** and **77-2k**) aryl systems (Scheme 77). Yields were typically lower for electron-deficient migrating groups. Two sterically challenging *ortho*-substituted aryl rings produced products **77-2h** and **77-2k** in 49% and 69% yield, respectively. A homologated acetamide product **77-2j** could be synthesized in 41% yield, showcasing a more difficult 1,5 aryl transfer in understandably lower yields relative to the analogous 1,4 aryl transfer product (**77-2a**, 80%). A thiophene was also found to migrate in 56% yield (**77-2l**). This example should serve as a good early example of an EDA mediated Smiles-Truce rearrangement, an area of research which has been underexplored to date. Furthermore, the difunctionalized acetamide products are difficult to access otherwise and include the valuable difluoromethyl moiety with a useful ester synthetic handle.

In 2020, the Greaney group again turned their attention to Smiles-Truce chemistry (Scheme 79).<sup>126</sup> In this most recent report, a well-designed series of  $\gamma$ -arylsulfonylacetamido oxime esters (**79-1**) were shown to rearrange to their corresponding  $\beta$ -arylethylamine products (**79-2**) in a decarboxylative/desulfonylative Smiles-Truce sequence. The envisioned transformation was initiated through energy transfer between the excited state of Ir<sup>III\*</sup> and the diaryloxime ester moiety of starting material **79-1** (Scheme 80). This transfer delivers a diradical **79-3** which is poised to undergo N–O bond cleavage (**79-4**) followed by decarboxylation as has been described by Glorius.<sup>127</sup> Aryl migration by *ipso* substitution of resulting alkyl radical **79-5** followed by desulfonylation forges the new C<sub>sp</sub><sup>3</sup>–C<sub>sp</sub><sup>2</sup> bond in **79-7** with hydrogen atom transfer (HAT) from THF giving the desired final product

**79–2**. The iminyl radical **80–1** generated from N–O bond cleavage can also be quenched by HAT from the solvent to give imine byproduct **80–2**. An experiment demonstrating deuteration of the acetamide products and imine byproduct with a reaction run in THF- $d_8$  would provide evidence of the postulated HAT from solvent as the last step in the reaction. The extrusion of  $CO_2$  and  $SO_2$  provides strong driving forces forward and enables the synthesis of pharmaceutically relevant  $\beta$ -arylethylamines. This pharmacophore is featured in a variety of drugs that target the central nervous system such as agomelatine, baclofen, and methylphenidate.<sup>128–130</sup> Furthermore, energy transfer obviates the need for stoichiometric reductants.

A collection of oxime ester substrates could be easily prepared in three steps without purification from the corresponding ketoxime,  $\beta$ -amino acid, and arylsulfonyl chloride. These substrates delivered products such as **79–2g–79–2m** containing thiophene groups in good to excellent yields. Substitution on the ethylene backbone such as in **79–2k** gave increased yields, perhaps due to Thorpe-Ingold type conformational effects which would favor an aryl transfer reactive conformation over a non-reactive conformation.<sup>131</sup> No loss of enantiopurity from the parent  $\beta$ -amino acid core was observed in products **79–2k** and **79–2l**. 1-Naphthyl substituted arylethylamine **79–2f** could be accessed in 54% yield.

A variety of electron-deficient benzene derivatives were also competent for aryl migration under these reaction conditions. The use of 2,6-disubstituted phenyl groups as in products **79–2a** and **79–2b** seemed to facilitate the desired reactivity, as has been shown in similar observations by Truce.<sup>132</sup> Simple *ortho*-substitution was also able to promote the desired reactivity, giving **79–2c** and **79–2d** in 39% and 61% yield, respectively. Mesityl substituted **79–2e** was synthesized in 54% yield. Products bearing electron-donating groups on the migrating phenyl ring were not demonstrated, perhaps in line with other reports detailed within this review describing the greater migration efficiency of electron-deficient aryl systems.

To showcase the method's applicability in pharmaceutical synthesis, a protected  $\beta$ -2-thienyl-alanine **79–2m** was synthesized in high yield and high enantiomeric excess. This arylethylamine is used in the treatment of infant phenylketonuria, a brain-damaging malady when left untreated.<sup>133</sup> Lastly, the method could be run without the iridium photosensitizer when the applied wavelength was switched from 427 nm to 365 nm. The latter wavelength can directly excite oxime ester **79–1** to its diyl-**79–3** to initiate the rearrangement sequence. However, this protocol gave reduced yields compared to the photosensitized regime as seen in product **79–2j** (41% reagent free yield vs. 56% photosensitized yield).

A mechanism based upon energy transfer rather than N–O bond reduction is supported by several facts: 1. photosensitizers with similar reduction potentials to the iridium complex used herein could not promote the desired reactivity, 2. Stoichiometric reductants could not promote the desired reactivity, and 3. the reduction potential of the N–O bond in the substrates **79–1** ( $\sim -2.0$  V vs. SCE) is outside of the reduction potential of the iridium photosensitizer ( $Ir^{III*}/Ir^{IV} = -0.89$  V vs. SCE) used herein.



In all, this work comprises a welcome incorporation of energy transfer radical generation strategies into Smiles-Truce aryl transfer methodology development. There is much potential for deeper synergy between the two, and this work should guide further developments in the integration of these strategies. The lack of reactivity for a simple phenyl-substituted **79-1** and no products featuring electron-donating groups on the migrating aryl ring are drawbacks of this otherwise exemplary report.

Wu and coworkers designed a mechanistically distinct SO<sub>2</sub>-retaining Smiles-Truce rearrangement of *N*-arylsulfonyl propiolamides **81-1** (Scheme 81).<sup>134</sup> In this work, the extruded sulfonyl radical forms a new C-S bond by intramolecular conjugate addition, giving 4-aryl-5-acyl-isothiazolidinones **81-3**. Building upon previous work from the same laboratory, neutral eosin Y was used as a mild HAT reagent under blue LED irradiation in MeCN to generate acyl radicals directly from aldehydes or secondary phosphine oxides **81-2**.<sup>135</sup> A rich substrate scope was exhibited with respect to the aldehyde/phosphine oxide and the (hetero)aromatic sulfonamide (**81-3a-81-3l**).

Several informative mechanistic experiments were presented by the authors to elucidate key intermediates. To support the proposed intermediacy of acyl radicals, pivalaldehyde **82-2m** was used as the acyl source. Decarbonylation from the pivaloyl radical led to incorporation of a *tert*-butyl group into the resulting isothiazolidinone product **82-4**. Acyl radical addition to *N*-arylsulfonyl propiolamide **82-1g** containing an *N*-isobutyl group allowed 1,5-HAT to unfold instead of the anticipated Smiles-Truce rearrangement. The isobutyl radical could then add *via* conjugate addition to an enone, yielding lactam **82-5**. This experiment is presented as support for vinyl radical intermediates. When deuterated aldehyde **82-2a-d** was used as the acyl radical precursor, 42% of the isolated isothiazolidinone **82-3a** contained an incorporated deuterium at the tertiary benzylic carbon. When D<sub>2</sub>O was added, the extent of benzylic deuteration increased to 98%; in anhydrous MeCN-d<sub>3</sub> no deuterium was incorporated. This observation led the authors to infer that H-D exchange between eosin Y and D<sub>2</sub>O could occur following HAT from **82-2**, in accordance with similar exchange mechanisms for decatungstate HAT reagents.<sup>136</sup> A complete mechanism is provided in Scheme 82 and begins by photoexcitation of eosin Y by blue light. HAT to this species from an aldehyde produces acyl radical **82-6**, which adds to the propiolamide **82-1**. Aryl migration to the incipient vinyl radical **82-7** results in elimination of the sulfonyl radical **82-9** through spirocycle **82-8**. Rather than desulfonylation, **82-9** undergoes 5-endo-*trig* ring closure. The cyclic product **82-10** abstracts a hydrogen atom from [eosin Y]-H to afford the final product **82-3**. The reaction is easily scaled, but the long reaction time (48 hours) at elevated temperatures (80 °C) limit its general synthetic utility.

Studer and coworkers implemented reductive photoredox catalysis to synthesize quaternary  $\alpha$ -arylated amides **83-2** from *ortho*-iodinated benzenesulfonamides **83-1** (Scheme 83).<sup>137</sup> This work is a rare instance of a photoinduced aryl transfer that relies on radical generation on the migrating arene itself.<sup>138</sup> The same group has previously achieved similar rearrangements of sulfonate esters using silane reductants.<sup>139</sup> Variations in the nitrogen substituent R<sup>1</sup> (**83-2a**, **83-2b**), the migrating arene (**83-2c-83-2e**), and the  $\alpha$ -amidyl substituents R<sup>2</sup> and R<sup>3</sup> (**83-2f-83-2j**) were all thoroughly demonstrated.

The reaction initiates by reduction of the aryl iodide **83-1** with photoexcited *fac*-Ir(ppy)<sub>3</sub> (Scheme 84). A 1,6-hydrogen atom transfer from the  $\alpha$ -amidyl position to the aryl radical in **83-3** leads to  $\alpha$ -amidyl radical **83-4**, which then participates in a Smiles-Truce rearrangement (**83-5**). The authors conducted two deuterium labelling experiments to determine whether the N-H proton in **83-2** originates from a hydrogen atom transfer to amidyl radical **83-6** or from a stepwise reduction and protonation. When the reaction of model compound **83-1k** was conducted in MeCN-*d*<sub>3</sub>, no *N*-deuterated product **83-2k-d** was observed. However, addition of excess D<sub>2</sub>O led to nearly complete *N*-deuteration. Because deuterium atom transfer from D<sub>2</sub>O is unlikely, the authors concluded that a second reduction by the photoexcited catalyst must occur to give **83-2** following protonation of the amidyl anion. Reduction of Ir<sup>IV</sup> by excess carbonate ion presumably restores the ground state Ir<sup>III</sup> photocatalyst.

In a recent groundbreaking work, the Nevado group has reported the first asymmetric radical Smiles-Truce rearrangement (Scheme 85).<sup>140</sup> The stereospecific transformation furnishes acyclic chiral amides bearing an  $\alpha$ -quaternary center from the corresponding *N*-arylsulfinyl acrylamides. Integrating their previous experience with radical Smiles-Truce rearrangement cascade reactions<sup>107</sup> with the achievements of Clayden in asymmetric polar Smiles-Truce rearrangements<sup>141</sup> suggested that a switch from an arylsulfonyl to an enantioenriched arylsulfinyl tether could allow access to valuable, bioactive scaffolds via stereocontrolled aryl migration. Furthermore, in addition to acting as the key chiral auxiliary and aryl group source, the sulfinyl tether was anticipated to be traceless through the release of an “SO” equivalent in analogy to the SO<sub>2</sub> extrusion typical of sulfonyl tethers.

The net alkene difunctionalization methodology coupled various radical group additions to the acrylamide starting materials followed by stereospecific aryl migration.  $\alpha$ -aryl,  $\beta$ -sulfonylaryl amides were synthesized in high yields and enantiomeric ratios (e.r.) from the starting arylsulfonylchloride and enantiopure acrylamides (Scheme 85). Both configurations of the newly created  $\alpha$ -quaternary center were accessible with (*S*)-sulfinylacrylamides starting materials giving the product (*R*)-enantiomer, and vice-versa. The scope with respect to the arylsulfonyl radical was quite broad irrespective of the electronics or sterics of the sulfonyl chloride (**85-2a-85-2i**). Even alkylsulfonyl chlorides were amenable to the reaction, giving **85-2k** and **85-2l** with only somewhat reduced yields while maintaining comparable e.r.

Varying the scope of the migrating aryl group derived from the enantioenriched sulfinamide gave diversified  $\alpha$ -arylation products **85-2r-85-2x**. While lacking examples of electron-deficient aryl migration products, unsubstituted (**85-2r**), electron-rich (**85-2s**), brominated (**85-2t**), sterically demanding (**85-2w** and **85-2x**), and hetero- or polycyclic aryl groups (**85-2u** and **85-2v**) all gave high yields and excellent e.r. It is worth noting that *ortho*-substitution as in **85-2w** and **85-2x** was beneficial for the desired migration.

Higher e.r. was observed for products **85-2y**, **85-2z**, and **85-2aa-85-2ae** derived from *N*-alkyl sulfinamines rather than *N*-aryl sulfinamines. Variations on the olefin moiety gave a variety of functionalized quaternary-center products, including valuable O and N protected **85-2ab** and **85-2ac** in 75% and 41% yield, respectively. Product **85-2ad** derived from an

unsubstituted acrylamide demonstrated that the methodology is applicable for constructing enantiopure tertiary amide products.

Finally, a variety of radical group precursors besides arylsulfonyl chlorides were amenable to the reaction conditions. Addition products **85-2m-85-21** from fluoroalkyl, alkyl, and acyl radical equivalents were synthesized in high yields with somewhat decreased e.r. for fluorinated products **85-2n** and **85-2o**. This radical group diversity widely expands the synthetic utility of the transformation, giving densely difunctionalized products in a stereocontrolled manner. Post-reaction functionalization (Scheme 86) gave a variety of interesting enantioenriched scaffolds without loss of e.r., including 3,3-disubstituted oxindole **86-5** in 90% yield (97:3 e.r.).

DFT calculations surrounding the transformation gave a robust mechanistic picture, including rationale for the observed enantioselectivity (Scheme 87). Single electron reduction of the radical group precursor such as an arylsulfonyl chloride followed by radical addition to acrylamide (**S**) **85-1** gives C-centered  $\alpha$ -amidyl radical **85-3**. This radical can undergo the stereospecific 1,4-aryl transfer *via* 5-*exo*-trig cyclization onto the *ipso* carbon of the arylsulfonamide giving **TS-85-4**. Notably, the aryl transfer was calculated to be a *concerted* process – no stable radical Meseinheimer-type intermediate was found on the calculated reaction profile. The concerted nature of the rearrangement is in line with other reports, giving further evidence of concerted nucleophilic aromatic substitution reactivity.<sup>142, 143</sup> Concerted reactivity is also invoked to explain the observed electronic variety of migrating aryl groups; stepwise processes would likely involve prohibitively higher energy intermediates depending on the electronic nature of the migrating ring. A stereoselection model for the reaction was proposed in which the conformation (of **TS-85-4**) adopted in **85-6** is thermodynamically favored compared to **85-7** in which there is unfavorable steric repulsion between the former acrylamide residue and the migrating aryl group. From **TS-85-4**, the concerted, enantioselective transfer results in S-centered radical intermediate **85-5** which in the presence of water undergoes a highly exergonic single-electron reduction to give H<sub>2</sub>SO<sub>3</sub> and the desired enantioenriched amide product (**R**) **85-2**. This is in line with the observation that neither SO nor SO<sub>2</sub> gas were detected in the headspace of the reaction vessels.

In all, this work has confronted perhaps the longest-standing unaddressed shortcoming of radical aryl migration reactions: asymmetric aryl transfer. The elegant utilization of the arylsulfonamide as a traceless chiral auxiliary resulted in unprecedented enantioselective radical aryl migration giving controllable access to either enantiomer of an  $\alpha$ -amide quaternary center. It is anticipated that this strategy could be applied to many previous methodologies utilizing arylsulfonyl group tethers in order to easily convert them to an enantioselective transformation. Further development of asymmetric Smiles-Truce and other radical aryl migration strategies remains a tantalizing goal, and this work should serve as an excellent template upon which to build subsequent research.

In an innovative work from 2019, a team of researchers led by Zhu pioneered difficult 1,5-aryl migrations towards the synthesis of diverse diaryl ketones *via* an acyl radical Smiles-Truce rearrangement (Scheme 88).<sup>144</sup> This strategy leveraged the emerging field of

photoredox-generated phosphorus radical cations to deoxygenate aromatic carboxylic acids to give the key acyl radical nucleophile (Scheme 89)

As demonstrated independently by Zhu<sup>145</sup> and Doyle<sup>146</sup>, the excited state of many common photoredox catalysts—including the iridium complex used herein—is sufficiently oxidizing to access the P-radical cation of various phosphorus functionalities including triphenylphosphine (Scheme 89). The nucleophilic capture of this P-radical cation by the benzoate **88-3** of benzoic acid starting material **88-1** results in a phosphoranyl radical **88-4**. This key intermediate undergoes  $\beta$ -scission, with formation of the strong P=O double bond providing a driving force to give triphenylphosphine oxide and the key acyl radical **88-5**. At this point, a 6-*exo*-trig cyclization onto the arylsulfonyl moiety gives spiro intermediate **88-6** which upon rearomatization and extrusion of SO<sub>2</sub> affords the uncommon 1,5-aryl transfer.<sup>147</sup> The subsequent stabilized *N*-centered radical **88-7** is reduced to its anion by Ir<sup>II</sup> giving the ground state Ir<sup>III</sup> and product **88-2** upon protonation. These hypotheses were supported by extensive DFT calculations, with extrusion of SO<sub>2</sub> and formation of the P=O double bond being the most exergonic steps. The method is notable for being an overall redox-neutral process, harnessing a nascent strategy for radical generation, and utilizing the unique acyl radical nucleophile in a challenging 1,5 aryl migration. On top of this, the 2-arylsulfonamidyl- and 2-arylsulfonyloxybenzoic acid starting materials were easily accessible from the corresponding 2-amino and 2-hydroxybenzoic acids and arylsulfonylchlorides in one step without purification. These substrates were smoothly transformed at room temperature to various diaryl ketone products, with over 60 examples reported (Scheme 88).

The scope in the migrating aryl group was largely insensitive to the electronic character of the ring for both sulfonamide and sulfonate substrates. Electron-deficient (**88-2e** and **88-2j**) as well as electron-rich (**88-2c**) migration products were all synthesized in high yields, with a 5 mmol scale up reaction towards **88-2b** giving 75% yield. Halogen-substituted diaryl ketones were also obtained (**88-2d**, **88-2n**, and **88-2i**). Importantly, sterically encumbered *ortho*-substituted migrating groups were amenable to the methodology, perhaps due to the less strict steric requirements of the spiro-[5,5]undecadienyl radical (**88-6**) relative to other smaller spiro intermediates detailed in this Review. Consequently, products **88-2k**, **88-2l**, and **88-2q-88-2s** were synthesized in good yields. Lastly, a variety of heteroaromatic ketones including pyridine (**88-2p**), quinoline (**88-2y**), and benzo[d]thiazole (**88-2x**) were synthesized. Variations on the benzoic acid backbone resulted in many other diaryl ketones including **88-2z** and **88-2aa-88-2ac**.

Post-functionalization reactions to form a variety of 5 to 8-membered aromatic heterocyclic scaffolds proceeded in good yields (**89-1-89-5**), while a two-step, 64% yielding sequence to the natural product ( $\pm$ )-Yaequinolone A2 (**89-4**) could be accessed from product **88-2c**. Even the simpler diaryl ketone products accessed immediately from the reaction constitute an impressive achievement given the mild conditions, scope, novel radical generation method, and challenging 1,5 aryl migration of this work. Within the context of photoredox aryl migration strategies, this method represents an excellent template for the development of further 1,5 aryl transfers along with acyl radical nucleophile strategies.

## 11. Conclusion and outlook

The key strategic advantage of aryl migration is the efficient conversion of easily prepared substrates to complex products with bonds that would otherwise be challenging to construct. The works discussed in this Review collectively testify to this advantage. However, we perceive three areas of investigation in this field that merit further pursuit:

### (1) Radical generation from native functionality.

Although aryl migration is inherently an intramolecular process, the radical species immediately prior to the migration can be accessed either by intra- or intermolecular reaction designs. Intramolecular approaches relying on homolysis of deliberately installed radical precursors on the substrate do not take full advantage of the power of aryl migration because they require more highly functionalized starting materials. Intermolecular approaches—wherein the radical originates from a source other than the substrate undergoing rearrangement—are more modular. However, reliance on traditional radical precursors (alkyl halides, acyl/sulfonyl chlorides, sulfinates, etc.) in existing works has limited their novelty. Recent achievements in photoredox catalysis have provided chemists with new tools to homolyze unactivated C–H bonds as well as strong O–H and N–H bonds. Such advances are well-suited for integration into new radical aryl migration methodologies.

### (2) Discovery of new leaving groups and expansion of substrate architectures informed by mechanistic analysis.

Most radical aryl migrations involve displacement of sulfonyl groups or benzylic carbon atoms. Development of other functional groups into competent leaving groups broadens the scope of amenable substrates as well as the structures of accessible products. The asymmetric Smiles-Truce rearrangement of aryl sulfinamides realized by the Nevado laboratory is one such example of the synthetic benefits that innovation in this area can present. We further believe that improved mechanistic understanding—particularly of kinetic and thermodynamic barriers to spirocyclative dearomatizations proposed to occur in nearly all radical aryl migrations—can permit escape from restrictive 1,2- and 1,4-migration regimes that currently pervade the literature. This is especially the case when simple bond enthalpy calculations or the lack of clear thermodynamic driving forces (e.g. extrusion of SO<sub>2</sub> or CO<sub>2</sub>) would suggest against the thermodynamic favorability of a rearrangement, particularly between two heteroatoms as in sections 6 through 8 of this review. The diligence of Nicewicz and coworkers in developing a predictive model for a radical cation Newman-Kwart rearrangement based upon easily obtained thermodynamic parameters is a good example in this regard (see section 8 above).

### (3) Diversification of post-migration reactions.

After displacement, the radical leaving group typically undergoes HAT or a radical/polar crossover event to terminate the reaction. If useful bond formations could first occur involving the radical or ionic intermediates, the aryl migration could function as an intermediate step in a more elaborate cascade sequence and unlock an even larger swath of chemical space. Notable instances of this idea are seen in the works by the Nevado, Reiser, and Wu groups in the preparation of oxindoles, dihydroisoquinolinones, and

isothiazolidinones, respectively. These underutilized cascade strategies have the potential to amplify the complexity of aryl migrations.

Photoredox catalysis has reinvigorated the field of radical chemistry in the past decade. This renaissance has evolved aryl migration into a general tactic for complex molecule synthesis in turn. Looking forward, we anticipate that innovations of this method will further expand the aryl migration arsenal to bring about landmark synthetic accomplishments.

## Acknowledgments

The authors acknowledge financial support from the NIH-NIGMS (GM127774) and the University of Michigan. This work was also supported by an NSF Graduate Research Fellowship for A.R.A. (grant DGE 1256260).

## Biographies

Anthony R. Allen

Anthony R. Allen hails from Redford, Michigan and obtained a B.A. degree (High Honors in Chemistry, Philosophy) from Oberlin College in 2018 where he conducted undergraduate research on cascade Nazarov cyclization reactions with Professor Albert Matlin. In 2017, he also was an undergraduate researcher under Professor Song Lin of Cornell University as part of the CCMR REU summer research program. In 2018, he began graduate school at the University of Michigan in the lab of Professor Corey Stephenson working on photoredox reaction mechanism elucidation and methodology development.

Efrey A. Noten

Efrey Noten grew up in San Jose, California before obtaining his B.S. with Comprehensive Honors in Chemistry from the University of Wisconsin-Madison. His undergraduate research focused on the synthesis and catalytic activity of molybdenum carboxylate complexes in the laboratory of Prof. John Berry. Efrey's interests gradually shifted to synthetic organic chemistry following two summer internships at Promega Biosciences in San Luis Obispo, CA and at Merck & Co., Inc. in Rahway, NJ. In 2018, he began his graduate studies at the University of Michigan in Prof. Corey Stephenson's group, where he conducts research on novel photoredox catalysis methodology.

Corey R.J. Stephenson

Corey Stephenson was born in Collingwood, Ontario, Canada and received his undergraduate degree from the University of Waterloo in 1998. He completed graduate studies under the direction of Professor Peter Wipf at the University of Pittsburgh before joining the lab of Professor Erick M. Carreira at ETH Zürich. In September 2007, he joined the Department of Chemistry at Boston University as an Assistant Professor and was granted tenure and promoted to Associate Professor in February, 2013. In July 2013, he joined the Department of Chemistry at the University of Michigan as Associate Professor of Chemistry. In September 2015, Corey was promoted to full Professor.

## 14. References

1. Kekulé A, Sur la Constitution des Substances Aromatiques. Bull. Soc. Chim. Fr. 1865, 3, 98.
2. Erlenmeyer E, Studien über die s. g. aromatischen Säuren. Liebigs Ann. 1866, 137, 327–359.
3. Krygowski TM; Cyrański MK; Czarnocki Z; Häfelinger G; Katritzky AR, Aromaticity: a Theoretical Concept of Immense Practical Importance. Tetrahedron 2000, 56, 1783–1796.
4. Schleyer P. v. R., Introduction: Aromaticity. Chem. Rev. 2001, 101, 1115–1118. [PubMed: 11749368]
5. Krygowski TM; Cyrański MK, Structural Aspects of Aromaticity. Chem. Rev. 2001, 101, 1385–1420. [PubMed: 11710226]
6. Solà M, Why Aromaticity Is a Suspicious Concept? Why? Front. Chem. 2017, 5.
7. Wieland H, Über Triphenylmethyl-peroxyd. Ein Beitrag zur Chemie der freien Radikale. Ber. Dtsch. Chem. Ges. 1911, 44, 2550–2556.
8. Urry WH; Kharasch MS, Factors Influencing the Course and Mechanism of Grignard Reactions. XV. The Reaction of  $\beta,\beta$ -Dimethylphenethyl Chloride with Phenylmagnesium Bromide in the Presence of Cobaltous Chloride. J. Am. Chem. Soc. 1944, 66, 1438–1440.
9. Loven RS, W. N., A novel 1,4 arylradical rearrangement. Tetrahedron 1972, 13, 1567–1570.
10. Motherwell WB; Pennell AMK, A Novel Route to Biaryls via Intramolecular Free Radical *ipso* Substitution Reactions. J. Chem. Soc., Chem. Commun. 1991, 877–879.
11. da Mata MLEN; Motherwell WB; Ujjainwalla F, Observations on the Nature of the Tethering Chain in the Synthesis of Biaryls and Heterobiaryls *via* Intramolecular Free Radical *Ips* Substitution Reactions. Tetrahedron Lett. 1997, 38, 141–144.
12. da Mata MLEN; Motherwell WB; Ujjainwalla F, Steric and Electronic Effects in the Synthesis of Biaryls and their Heterocyclic Congeners Using Intramolecular Free Radical [1,5] *ipso* Substitution Reactions. Tetrahedron Lett. 1997, 38, 137–140.
13. Godfrey CRA; Hegarty P; Motherwell WB; Uddin MK, A Novel Route to Unsymmetrical Stilbene Derivatives *via* Intramolecular Free Radical *ipso* Substitution Reactions. Tetrahedron Lett. 1998, 39, 723–726.
14. Benati L; Spagnolo P; Tundo A; Zanardi G, Intramolecular Aromatic *ipso*-Substitution in the Photolysis of 2-Iodoazobenzenes. J. Chem. Soc., Chem. Commun. 1979, 141–143.
15. Narayanam JMR; Stephenson CRJ, Visible Light Photoredox Catalysis: Applications in Organic Synthesis. Chem. Soc. Rev. 2011, 40, 102–113. [PubMed: 20532341]
16. Prier CK; Rankic DA; MacMillan DWC, Visible Light Photoredox Catalysis with Transition Metal Complexes: Applications in Organic Synthesis. Chem. Rev. 2013, 113, 5322–5363. [PubMed: 23509883]
17. McAtee RC; McClain EJ; Stephenson CRJ, Illuminating Photoredox Catalysis. *Trends Chem.* 2019, 1, 111–125.
18. Lima CGS; de M. Lima T; Duarte M; Jurberg ID; Paixão MW, Organic Synthesis Enabled by Light-Irradiation of EDA Complexes: Theoretical Background and Synthetic Applications. ACS Catal. 2016, 6, 1389–1407.
19. Crisenza GEM; Mazzarella D; Melchiorre P, Synthetic Methods Driven by the Photoactivity of Electron Donor–Acceptor Complexes. J. Am. Chem. Soc. 2020, 142, 5461–5476. [PubMed: 32134647]
20. Chen ZM; Zhang XM; Tu YQ, Radical aryl migration reactions and synthetic applications. Chem. Soc. Rev. 2015, 44, 5220–45. [PubMed: 25954772]
21. Huynh M; De Abreu M; Belmont P; Brachet E, Spotlight on Photoinduced Aryl Migration Reactions. Chem. - Eur. J. 2021, 27, 3581–3607. [PubMed: 32996634]
22. Snape TJ, A Truce on the Smiles Rearrangement: Revisiting an Old Reaction—the Truce–Smiles Rearrangement. Chem. Soc. Rev. 2008, 37, 2452–2458. [PubMed: 18949118]
23. Henderson ARP; Kosowan JR; Wood TE, The Truce–Smiles rearrangement and related reactions: a review. Can. J. Chem. 2017, 95, 483–504.
24. Allart-Simon I; Gérard S; Sapi J, Radical Smiles Rearrangement: An Update. Molecules 2016, 21, 878.

25. Huang H-L; Yan H; Yang C; Xia W, Visible Light-Mediated Arylalkylation of Allylic Alcohols through Concomitant 1,2-Aryl Migration. *Chem. Commun.* 2015, 51, 4910–4913.
26. Egami H; Shimizu R; Usui Y; Sodeoka M, Iron-Catalyzed Trifluoromethylation with Concomitant C–C Bond Formation via 1,2-Migration of an Aryl Group. *Chem. Commun.* 2013, 49, 7346–7348.
27. Chen Z-M; Bai W; Wang S-H; Yang B-M; Tu Y-Q; Zhang F-M, Copper-Catalyzed Tandem Trifluoromethylation/Semipinacol Rearrangement of Allylic Alcohols. *Angew. Chem. Int. Ed.* 2013, 52, 9781–9785.
28. Yu Y; Tambar UK, Palladium-Catalyzed Cross-Coupling of  $\alpha$ -Bromocarbonyls and Allylic Alcohols for the Synthesis of  $\alpha$ -Aryl Dicarbonyl Compounds. *Chem. Sci.* 2015, 6, 2777–2781. [PubMed: 26229586]
29. Reddy MP; Rao GSK, Synthesis of 5-p-Hydroxybenzyl-5,6-dihydro-2-naphthol, ( $\pm$ )-Sequirin D. J. *Chem. Soc., Perkin Trans. 1* 1981, 2662–2665.
30. Li Y; Liu B; Ouyang X-H; Song R-J; Li J-H, Alkylation/1,2-aryl migration of  $\alpha$ -aryl allylic alcohols with  $\alpha$ -carbonyl alkyl bromides using visible-light photoredox catalysis. *Organic Chemistry Frontiers* 2015, 2, 1457–1467.
31. Xu P; Hu K; Gu Z; Cheng Y; Zhu C, Visible Light Promoted Carbodifluoroalkylation of Allylic Alcohols Via Concomitant 1,2-Aryl Migration. *Chem. Commun.* 2015, 51, 7222–7225.
32. Wang J; Sánchez-Roselló M; Aceña JL; del Pozo C; Sorochinsky AE; Fustero S; Soloshonok VA; Liu H, Fluorine in Pharmaceutical Industry: Fluorine-Containing Drugs Introduced to the Market in the Last Decade (2001–2011). *Chem. Rev.* 2014, 114, 2432–2506. [PubMed: 24299176]
33. Cai S; Tian Y; Zhang J; Liu Z; Lu M; Weng W; Huang M, Carbotrifluoromethylation of Allylic Alcohols *via* 1,2-Aryl Migration Promoted by Visible-Light-Induced Photoredox Catalysis. *Adv. Synth. Catal.* 2018, 360, 4084–4088.
34. Liu X; Xiong F; Huang X; Xu L; Li P; Wu X, Copper-Catalyzed Trifluoromethylation-Initiated Radical 1,2-Aryl Migration in  $\alpha,\alpha$ -Diaryl Allylic Alcohols. *Angew. Chem. Int. Ed.* 2013, 52, 6962–6966.
35. Shang T-Y; Lu L-H; Cao Z; Liu Y; He W-M; Yu B, Recent Advances of 1,2,3,5-Tetrakis(carbazol-9-yl)-4,6-dicyanobenzene (4CzIPN) in Photocatalytic Transformations. *Chem. Commun.* 2019, 55, 5408–5419.
36. Lu M; Qin H; Lin Z; Huang M; Weng W; Cai S, Visible-Light-Enabled Oxidative Alkylation of Unactivated Alkenes with Dimethyl Sulfoxide through Concomitant 1,2-Aryl Migration. *Org. Lett.* 2018, 20, 7611–7615. [PubMed: 30485102]
37. Scott LJ; Dunn CJ; Mallarkey G; Sharpe M, Esomeprazole. *Drugs* 2002, 62, 1503–1538. [PubMed: 12093317]
38. Rayner CM, Synthesis of Thiols, Sulfides, Sulfoxides and Sulfones. *Contemp. Org. Synth.* 1995, 2, 409–440.
39. Boivin J; Fouquet E; Zard SZ, Ring Opening Induced by Iminyl Radicals Derived from Cyclobutanones: New Aspects of Tin Hydride Cleavage of S-Phenyl Sulfenylimines. *J. Am. Chem. Soc.* 1991, 113, 1055–1057.
40. Dauncey EM; Morcillo SP; Douglas JJ; Sheikh NS; Leonori D, Photoinduced Remote Functionalisations by Iminyl Radical Promoted C–C and C–H Bond Cleavage Cascades. *Angew. Chem. Int. Ed.* 2018, 57, 744–748.
41. Yu X-Y; Chen J-R; Wang P-Z; Yang M-N; Liang D; Xiao W-J, A Visible-Light-Driven Iminyl Radical-Mediated C–C Single Bond Cleavage/Radical Addition Cascade of Oxime Esters. *Angew. Chem. Int. Ed.* 2018, 57, 738–743.
42. Li L; Chen H; Mei M; Zhou L, Visible-Light Promoted  $\gamma$ -Cyanoalkyl Radical Generation: Three-Component Cyanopropylation/Etherification of Unactivated Alkenes. *Chem. Commun.* 2017, 53, 11544–11547.
43. Wang Q-L; Chen Z; Zhou C-S; Xiong B-Q; Zhang P-L; Yang C-A; Liu Y; Zhou Q, Visible-Light-induced 1,2-Alkylarylation of Alkenes with  $\alpha$ -C(sp<sup>3</sup>)-H bonds of Acetonitriles Involving Neophyl Rearrangement Under Transition-Metal-Free Conditions. *Tetrahedron Lett.* 2018, 59, 4551–4556.
44. Li Z; Wang M; Shi Z, Radical Addition Enables 1,2-Aryl Migration from a Vinyl-Substituted All-Carbon Quaternary Center. *Angew. Chem. Int. Ed.* 2021, 60, 186–190.



45. Wu Z; Wang D; Liu Y; Huan L; Zhu C, Chemo- and Regioselective Distal Heteroaryl ipso-Migration: A General Protocol for Heteroarylation of Unactivated Alkenes. *J. Am. Chem. Soc.* 2017, 139, 1388–1391. [PubMed: 28098990]
46. Wu X; Wang M; Huan L; Wang D; Wang J; Zhu C, Tertiary-Alcohol-Directed Functionalization of Remote C(sp<sup>3</sup>)-H Bonds by Sequential Hydrogen Atom and Heteroaryl Migrations. *Angew. Chem. Int. Ed.* 2018, 57, 1640–1644.
47. Zhang H; Kou L; Chen D; Ji M; Bao X; Wu X; Zhu C, Radical-Mediated Distal Ipso-Migration of O/S-Containing Heteroaryls and DFT Studies for Migratory Aptitude. *Org. Lett.* 2020, 22, 5947–5952. [PubMed: 32701302]
48. Yu J; Wang D; Xu Y; Wu Z; Zhu C, Distal Functional Group Migration for Visible-light Induced Carbo-difluoroalkylation/monofluoroalkylation of Unactivated Alkenes. *Adv. Synth. Catal.* 2018, 360, 744–750.
49. Tang X; Studer A, Alkene 1,2-Difunctionalization by Radical Alkenyl Migration. *Angew. Chem. Int. Ed.* 2018, 57, 814–817.
50. Chu X-Q; Meng H; Zi Y; Xu X-P; Ji S-J, Metal-Free Oxidative Direct C(sp<sup>3</sup>)-H Bond Functionalization of Ethers with  $\alpha,\alpha$ -Diaryl Allylic Alcohols. *Chem. Commun.* 2014, 50, 9718–9721.
51. Zhao J; Fang H; Song R; Zhou J; Han J; Pan Y, Metal-free Oxidative C(sp<sup>3</sup>)-H Bond Functionalization of Alkanes and Alkylation-Initiated Radical 1,2-Aryl Migration in  $\alpha,\alpha$ -Diaryl Allylic Alcohols. *Chem. Commun.* 2015, 51, 599–602.
52. Gu L; Gao Y; Ai X; Jin C; He Y; Li G; Yuan M, Direct Alkylheteroarylation of Alkenes *via* Photoredox Mediated C-H Functionalization. *Chem. Commun.* 2017, 53, 12946–12949.
53. Sarkar S; Banerjee A; Yao W; V. Patterson E; Ngai M-Y, Photocatalytic Radical Aroylation of Unactivated Alkenes: Pathway to  $\beta$ -Functionalized 1,4-, 1,6-, and 1,7-Diketones. *ACS Catal.* 2019, 9, 10358–10364. [PubMed: 34040817]
54. Kachkovskiy G; Faderl C; Reiser O, Visible Light-Mediated Synthesis of (Spiro)annelated Furans. *Adv. Synth. Catal.* 2013, 355, 2240–2248.
55. Faderl C; Budde S; Kachkovskiy G; Rackl D; Reiser O, Visible Light-Mediated Decarboxylation Rearrangement Cascade of  $\omega$ -Aryl-N-(acyloxy)phthalimides. *J. Org. Chem.* 2018, 83, 12192–12206. [PubMed: 30153021]
56. Ledermüller K; Schütz M, Local CC2 Response Method Based on the Laplace Transform: Analytic Energy Gradients for Ground and Excited states. *J. Chem. Phys.* 2014, 140, 164113. [PubMed: 24784259]
57. Zhou T; Luo F-X; Yang M-Y; Shi Z-J, Silver-Catalyzed Long-Distance Aryl Migration from Carbon Center to Nitrogen Center. *J. Am. Chem. Soc.* 2015, 137, 14586–14589. [PubMed: 26523735]
58. Chu JCK; Rovis T, Amide-directed photoredox-catalysed C-C bond formation at unactivated sp<sup>3</sup> C-H bonds. *Nature* 2016, 539, 272–275. [PubMed: 27732580]
59. Choi GJ; Zhu Q; Miller DC; Gu CJ; Knowles RR, Catalytic alkylation of remote C-H bonds enabled by proton-coupled electron transfer. *Nature* 2016, 539, 268–271. [PubMed: 27732585]
60. Shu W; Genoux A; Li Z; Nevado C,  $\gamma$ -Functionalizations of Amines through Visible-Light-Mediated, Redox-Neutral C-C Bond Cleavage. *Angew. Chem. Int. Ed.* 2017, 56, 10521–10524.
61. Wang N; Gu Q-S; Li Z-L; Li Z; Guo Y-L; Guo Z; Liu X-Y, Direct Photocatalytic Synthesis of Medium-Sized Lactams by C-C Bond Cleavage. *Angew. Chem. Int. Ed.* 2018, 57, 14225–14229.
62. Hussain A; Yousuf SK; Mukherjee D, Importance and Synthesis of Benzannulated Medium-sized and Macrocyclic Rings (BMRs). *RSC Adv.* 2014, 4, 43241–43257.
63. Alpers D; Cole KP; Stephenson CRJ, Visible Light Mediated Aryl Migration by Homolytic C-N Cleavage of Aryl Amines. *Angew. Chem. Int. Ed.* 2018, 57, 12167–12170.
64. Grimshaw J; Hamilton R; Trocha-Grimshaw J, Electrochemical Reactions. Part 24. Reductive Cyclisation of *i*-(2-Halogenophenyl)-*j*-phenyl Compounds: a General Reaction. *J. Chem. Soc., Perkin Trans. 1* 1982, 229–234.
65. Lee E; Whang HS; Chung CK, Radical Isomerization *via* Intramolecular *ipso* Substitution of *N*-Arylamides: Aryl Translocation from Nitrogen to Carbon. *Tetrahedron Lett.* 1995, 36, 913–914.

66. Bacqué E; El Qacemi M; Zard SZ, An Unusual Radical Smiles Rearrangement. *Org. Lett.* 2005, 7, 3817–3820. [PubMed: 16092883]
67. Rey V; Pierini AB; Peñeñory AB, Competitive Reaction Pathways for *o*-Anilide Aryl Radicals: 1,5- or 1,6-Hydrogen Transfer versus Nucleophilic Coupling Reactions. A Novel Rearrangement to Afford an Amidyl Radical. *J. Org. Chem.* 2009, 74, 1223–1230. [PubMed: 19138117]
68. Garcin ED; Arvai AS; Rosenfeld RJ; Kroeger MD; Crane BR; Andersson G; Andrews G; Hamley PJ; Mallinder PR; Nicholls DJ, et al. , Anchored Plasticity Opens Doors for Selective Inhibitor Design in Nitric Oxide Synthase. *Nat. Chem. Biol.* 2008, 4, 700–707. [PubMed: 18849972]
69. Abrams R; Clayden J, Photocatalytic Difunctionalization of Vinyl Ureas by Radical Addition Polar Truce–Smiles Rearrangement Cascades. *Angew. Chem. Int. Ed.* 2020, 59, 11600–11606.
70. Costil R; Dale HJA; Fey N; Whitcombe G; Matlock JV; Clayden J, Heavily Substituted Atropisomeric Diarylamines by Unactivated Smiles Rearrangement of *N*-Aryl Anthranilamides. *Angew. Chem. Int. Ed.* 2017, 56, 12533–12537.
71. Li J; Liu Z; Wu S; Chen Y, Acyl Radical Smiles Rearrangement To Construct Hydroxybenzophenones by Photoredox Catalysis. *Org. Lett.* 2019, 21, 2077–2080. [PubMed: 30888188]
72. Dou Q; Li C-J; Zeng H, Photoinduced Transition-Metal- and External-Photosensitizer-Free Intramolecular Aryl Rearrangement via C(Ar)–O Bond Cleavage. *Chem. Sci.* 2020, 11, 5740–5744. [PubMed: 32864086]
73. Minisci F; Fontana F; Vismara E, Substitutions by Nucleophilic Free Radicals: A New General Reaction of Heteroaromatic Bases. *J. Heterocycl. Chem.* 1990, 27, 79–96.
74. Proctor RSJ; Phipps RJ, Recent Advances in Minisci-Type Reactions. *Angew. Chem. Int. Ed.* 2019, 58, 13666–13699.
75. Taylor RD; MacCoss M; Lawson ADG, Rings in Drugs. *J. Med. Chem.* 2014, 57, 5845–5859. [PubMed: 24471928]
76. Minisci F; Bernardi R; Bertini F; Galli R; Perchinummo M, Nucleophilic Character of Alkyl Radicals—VI: A New Convenient Selective Alkylation of Heteroaromatic Bases. *Tetrahedron* 1971, 27, 3575–3579.
77. Jeon J; He Y-T; Shin S; Hong S, Visible-Light-Induced *ortho*-Selective Migration on Pyridyl Ring: Trifluoromethylative Pyridylation of Unactivated Alkenes. *Angew. Chem. Int. Ed.* 2020, 59, 281–285.
78. Lawson CA; Dominey AP; Williams GD; Murphy JA, Visible Light-Mediated Smiles Rearrangements and Annulations of Non-Activated Aromatics. *Chem. Commun.* 2020, 56, 11445–11448.
79. Tay NES; Nicewicz DA, Cation Radical Accelerated Nucleophilic Aromatic Substitution via Organic Photoredox Catalysis. *J. Am. Chem. Soc.* 2017, 139, 16100–16104. [PubMed: 29068677]
80. Lardy SW; Luong KC; Schmidt VA, Formal Aniline Synthesis from Phenols through Deoxygenative *N*-Centered Radical Substitution. *Chem. - Eur. J.* 2019, 25, 15267–15271. [PubMed: 31535414]
81. Gonzalez-Gomez JC; Ramirez NP; Lana-Villarreal T; Bonete P, A Photoredox-Neutral Smiles Rearrangement of 2-Aryloxybenzoic Acids. *Org. Biomol. Chem.* 2017, 15, 9680–9684. [PubMed: 29119165]
82. Wang S-F; Cao X-P; Li Y, Efficient Aryl Migration from an Aryl Ether to a Carboxylic Acid Group To Form an Ester by Visible-Light Photoredox Catalysis. *Angew. Chem. Int. Ed.* 2017, 56, 13809–13813.
83. Xia Z-H; Dai L; Gao Z-H; Ye S, *N*-Heterocyclic Carbene/Photo-Cocatalyzed Oxidative Smiles Rearrangement: Synthesis of Aryl Salicylates from *O*-Aryl Salicylaldehydes. *Chem. Commun.* 2020, 56, 1525–1528.
84. Janssen-Müller D; Singha S; Lied F; Gottschalk K; Glorius F, NHC-Organocatalyzed CAr–O Bond Cleavage: Mild Access to 2-Hydroxybenzophenones. *Angew. Chem. Int. Ed.* 2017, 56, 6276–6279.
85. Margrey KA; Levens A; Nicewicz DA, Direct Aryl C–H Amination with Primary Amines Using Organic Photoredox Catalysis. *Angew. Chem. Int. Ed.* 2017, 56, 15644–15648.

86. Perkowski AJ; Cruz CL; Nicewicz DA, Ambient-Temperature Newman–Kwart Rearrangement Mediated by Organic Photoredox Catalysis. *J. Am. Chem. Soc.* 2015, 137, 15684–15687. [PubMed: 26645387]
87. Cruz CL; Nicewicz DA, Mechanistic Investigations into the Cation Radical Newman–Kwart Rearrangement. *ACS Catal.* 2019, 9, 3926–3935.
88. Kwart H; Evans ER, The Vapor Phase Rearrangement of Thioncarbonates and Thioncarbamates. *J. Org. Chem.* 1966, 31, 410–413.
89. Newman MS; Karnes HA, The Conversion of Phenols to Thiophenols via Dialkylthiocarbamates. *J. Org. Chem.* 1966, 31, 3980–3984.
90. Lloyd-Jones GC; Moseley JD; Renny JS, Mechanism and Application of the Newman-Kwart O→S Rearrangement of O-Aryl Thiocarbamates. *Synthesis* 2008, 2008, 661–689.
91. De Abreu M; Belmont P; Brachet E, Light-Enabled Radical 1,4-Aryl Migration Via a Phospho-Smiles Rearrangement. *J. Org. Chem.* 2021, 86, 3758–3767. [PubMed: 33439649]
92. De Abreu M; Selkti M; Belmont P; Brachet E, Phosphoramidates as Transient Precursors of Nitrogen-Centered Radical Under Visible-Light Irradiation: Application to the Synthesis of Phthalazine Derivatives. *Adv. Synth. Catal.* 2020, 362, 2216–2222.
93. Kong W; Casimiro M; Merino E. b.; Nevado C, Copper-Catalyzed One-Pot Trifluoromethylation/Aryl Migration/Desulfonylation and C(sp<sup>2</sup>)-N Bond Formation of Conjugated Tosyl Amides. *J. Am. Chem. Soc.* 2013, 135, 14480–14483. [PubMed: 24047140]
94. Zheng L; Yang C; Xu Z; Gao F; Xia W, Difunctionalization of Alkenes via the Visible-Light-Induced Trifluoromethylarylation/1,4-Aryl Shift/Desulfonylation Cascade Reactions. *J. Org. Chem.* 2015, 80, 5730–5736. [PubMed: 25955879]
95. Tang S; Yuan L; Deng Y-L; Li Z-Z; Wang L-N; Huang G-X; Sheng R-L, Visible-Light-Induced Perfluoroalkylation/Aryl migration/Desulfonylation Cascades of Conjugated Tosyl Amides. *Tetrahedron Lett.* 2017, 58, 329–332.
96. Li Y; Hu B; Dong W; Xie X; Wan J; Zhang Z, Visible Light-Induced Radical Rearrangement to Construct C–C Bonds via an Intramolecular Aryl Migration/Desulfonylation Process. *J. Org. Chem.* 2016, 81, 7036–7041. [PubMed: 27351977]
97. Clark AJ; Coles SR; Collis A; Debure T; Guy C; Murphy NP; Wilson P, 1,4-Aryl migration under copper(I) atom transfer conditions. *Tetrahedron Lett.* 2009, 50, 5609–5612.
98. Shi L; Wang H; Yang H; Fu H, Iron-Catalyzed Arylsulfonylation of Activated Alkenes. *Synlett* 2015, 26, 688–694.
99. He Z; Tan P; Ni C; Hu J, Fluoroalkylative Aryl Migration of Conjugated N-Arylsulfonylated Amides Using Easily Accessible Sodium Di- and Monofluoroalkanesulfonates. *Org. Lett.* 2015, 17, 1838–1841. [PubMed: 25839912]
100. Nicewicz D; Roth H; Romero N, Experimental and Calculated Electrochemical Potentials of Common Organic Molecules for Applications to Single-Electron Redox Chemistry. *Synlett* 2015, 27, 714–723.
101. Douglas JJ; Albright H; Sevrin MJ; Cole KP; Stephenson CRJ, A Visible-Light-Mediated Radical Smiles Rearrangement and its Application to the Synthesis of a Difluoro-Substituted Spirocyclic ORL-1 Antagonist. *Angew. Chem. Int. Ed.* 2015, 54, 14898–14902.
102. Douglas JJ; Sevrin MJ; Cole KP; Stephenson CRJ, Preparative Scale Demonstration and Mechanistic Investigation of a Visible Light-Mediated Radical Smiles Rearrangement. *Org. Process Res. Dev.* 2016, 20, 1148–1155.
103. Brachet E; Marzo L; Selkti M; König B; Belmont P, Visible Light Amination/Smiles Cascade: Access to Phthalazine Derivatives. *Chem. Sci.* 2016, 7, 5002–5006. [PubMed: 30155150]
104. Ibrahim HS; Eldehna WM; Abdel-Aziz HA; Elaasser MM; Abdel-Aziz MM, Improvement of Antibacterial Activity of Some Sulfa Drugs through Linkage to Certain Phthalazin-1(2H)-one Scaffolds. *Eur. J. Med. Chem.* 2014, 85, 480–486. [PubMed: 25113876]
105. Mohd I; Mohammad A, Study of Various Pyridazine and Phthalazine Drugs with Diverse Therapeutical and Agrochemical Activities. *Russ. J. Bioorg. Chem.* 2020, 46, 745–767.
106. Huang H; Li Y, Sustainable Difluoroalkylation Cyclization Cascades of 1,8-Enynes. *J. Org. Chem.* 2017, 82, 4449–4457. [PubMed: 28387113]

107. Fuentes N; Kong W; Fernández-Sánchez L; Merino E; Nevado C, Cyclization Cascades via N-Amidyl Radicals toward Highly Functionalized Heterocyclic Scaffolds. *J. Am. Chem. Soc.* 2015, 137, 964–973. [PubMed: 25561161]
108. Gao X; Li C; Yuan Y; Xie X; Zhang Z, Visible-Light-Induced Intramolecular Radical Cascade of  $\alpha$ -Bromo-*N*-benzyl-alkylamides: a New Strategy to Synthesize Tetracyclic *N*-Fused Indolo[2,1-*a*]isoquinolin-6(5*H*)-ones. *Org. Biomol. Chem.* 2020, 18, 263–271. [PubMed: 31829389]
109. Chen M; Yang C; Wang Y; Li D; Xia W, UV Light Induced Direct Synthesis of Phenanthrene Derivatives from a Linear 3-Aryl-*N*-(arylsulfonyl) Propiolamides. *Org. Lett.* 2016, 18, 2280–2283. [PubMed: 27115834]
110. Mallory FB; Mallory CW, Photocyclization of Stilbenes and Related Molecules. In *Organic Reactions*, 2005; pp 1–456.
111. Chen M; Zhao X; Yang C; Wang Y; Xia W, Further insight into the photochemical behavior of 3-aryl-*N*-(arylsulfonyl)propiolamides: tunable synthetic route to phenanthrenes. *RSC Adv.* 2017, 7, 12022–12026.
112. Wang Z-S; Chen Y-B; Zhang H-W; Sun Z; Zhu C; Ye L-W, Ynamide Smiles Rearrangement Triggered by Visible-Light-Mediated Regioselective Ketyl–Ynamide Coupling: Rapid Access to Functionalized Indoles and Isoquinolines. *J. Am. Chem. Soc.* 2020, 142, 3636–3644. [PubMed: 32003986]
113. Tada M; Shijima H; Nakamura M, Smiles-type free radical rearrangement of aromatic sulfonates and sulfonamides: syntheses of arylethanol and arylethylamines. *Org. Biomol. Chem.* 2003, 1, 2499–2505. [PubMed: 12956067]
114. Monos TM; McAtee RC; Stephenson CRJ, Arylsulfonylacetamides as bifunctional reagents for alkene aminoarylation. *Science* 2018, 361, 1369–1373. [PubMed: 30262501]
115. Nguyen TM; Manohar N; Nicewicz DA, anti-Markovnikov Hydroamination of Alkenes Catalyzed by a Two-Component Organic Photoredox System: Direct Access to Phenethylamine Derivatives. *Angew. Chem. Int. Ed.* 2014, 53, 6198–6201.
116. Groenewold GS; Chess EK; Gross ML, Structure of the Intermediate Formed in the Reaction of the Styrene Radical Cation and Neutral Styrene. *J. Am. Chem. Soc.* 1984, 106, 539–543.
117. Yu J; Wu Z; Zhu C, Efficient Docking-Migration Strategy for Selective Radical Difluoromethylation of Alkenes. *Angew. Chem. Int. Ed.* 2018, 57, 17156–17160.
118. Liu J; Wu S; Yu J; Lu C; Wu Z; Wu X; Xue X-S; Zhu C, Polarity Umpolung Strategy for the Radical Alkylation of Alkenes. *Angew. Chem. Int. Ed.* 2020, 59, 8195–8202.
119. Niu T; Liu J; Wu X; Zhu C, Radical Heteroarylalkylation of Alkenes via Three-Component Docking-Migration Thioetherification Cascade. *Chin. J. Chem.* 2020, 38, 803–806.
120. Wu X; Zhu C, Radical-Mediated Remote Functional Group Migration. *Acc. Chem. Res.* 2020, 53, 1620–1636. [PubMed: 32706572]
121. Rabet PTG; Boyd S; Greaney MF, Metal-Free Intermolecular Aminoarylation of Alkynes. *Angew. Chem. Int. Ed.* 2017, 56, 4183–4186.
122. Whalley DM; Duong HA; Greaney MF, Alkene Carboarylation through Catalyst-Free, Visible Light-Mediated Smiles Rearrangement. *Chem. - Eur. J.* 2019, 25, 1927–1930. [PubMed: 30536854]
123. Gheorghe A; Quiclet-Sire B; Vila X; Zard SZ, Synthesis of 3-Arylpiperidines by a Radical 1,4-Aryl Migration. *Org. Lett.* 2005, 7, 1653–1656. [PubMed: 15816775]
124. Gheorghe A; Quiclet-Sire B; Vila X; Zard SZ, Synthesis of Substituted 3-Arylpiperidines and 3-Arylpyrrolidines by Radical 1,4 and 1,2-Aryl Migrations. *Tetrahedron* 2007, 63, 7187–7212.
125. Dinnocenzo JP; Banach TE, Deprotonation of Tertiary Amine Cation Radicals. A Direct Experimental Approach. *J. Am. Chem. Soc.* 1989, 111, 8646–8653.
126. Whalley DM; Duong HA; Greaney MF, A Visible Light-Mediated, Decarboxylative, Desulfonylative Smiles Rearrangement for General Arylethylamine Syntheses. *Chem. Commun.* 2020, 56, 11493–11493.
127. Patra T; Mukherjee S; Ma J; Strieth-Kalthoff F; Glorius F, Visible-Light-Photosensitized Aryl and Alkyl Decarboxylative Functionalization Reactions. *Angew. Chem. Int. Ed.* 2019, 58, 10514–10520.

128. Sansone RA; Sansone LA, Agomelatine: a Novel Antidepressant. *Innov. Clin. Neurosci.* 2011, 8, 10–14.
129. Farokhnia M; Schwandt ML; Lee MR; Bollinger JW; Farinelli LA; Amodio JP; Sewell L; Lionetti TA; Spero DE; Leggio L, Biobehavioral Effects of Baclofen in Anxious Alcohol-Dependent Individuals: a Randomized, Double-Blind, Placebo-Controlled, Laboratory Study. *Transl. Psychiatry* 2017, 7, e1108–e1108. [PubMed: 28440812]
130. Kent MA; Camfield CS; Camfield PR, Double-Blind Methylphenidate Trials: Practical, Useful, and Highly Endorsed by Families. *Archives of Pediatrics & Adolescent Medicine* 1999, 153, 1292–1296. [PubMed: 10591309]
131. Bunnett JF; Okamoto T, Steric Acceleration through Regulation of Rotational Conformation: The Smiles Rearrangement. *J. Am. Chem. Soc.* 1956, 78, 5363–5367.
132. Truce WE; Ray WJ, Rearrangements of Aryl Sulfones. III. The Kinetics of the Reaction of o-Methyl diaryl Sulfones with n-Butyllithium. *J. Am. Chem. Soc.* 1959, 81, 484–487.
133. Al Hafid N; Christodoulou J, Phenylketonuria: a Review of Current and Future Treatments. *Transl. Pediatr.* 2015, 4, 304–317. [PubMed: 26835392]
134. Yan J; Cheo HW; Teo WK; Shi X; Wu H; Idres SB; Deng L-W; Wu J, A Radical Smiles Rearrangement Promoted by Neutral Eosin Y as a Direct Hydrogen Atom Transfer Photocatalyst. *J. Am. Chem. Soc.* 2020, 142, 11357–11362. [PubMed: 32543192]
135. Fan X-Z; Rong J-W; Wu H-L; Zhou Q; Deng H-P; Tan JD; Xue C-W; Wu L-Z; Tao H-R; Wu J, Eosin Y as a Direct Hydrogen-Atom Transfer Photocatalyst for the Functionalization of C–H Bonds. *Angew. Chem. Int. Ed.* 2018, 57, 8514–8518.
136. Dondi D; Fagnoni M; Molinari A; Maldotti A; Albin A, Polyoxotungstate Photoinduced Alkylation of Electrophilic Alkenes by Cycloalkanes. *Chem. - Eur. J* 2004, 10, 142–148. [PubMed: 14695559]
137. Radhoff N; Studer A, Functionalization of  $\alpha$ -C(sp<sup>3</sup>)-H Bonds in Amides Using Radical Translocating Arylating Groups. *Angew. Chem. Int. Ed.* 2021, 60, 3561–3565.
138. Nacsa ED; Lambert TH, Cross-Coupling of Sulfonic Acid Derivatives via Aryl-Radical Transfer (ART) Using TTMS or Photoredox. *Org. Chem. Front.* 2018, 5, 64–69.
139. Friese FW; Muck-Lichtenfeld C; Studer A, Remote C-H functionalization using radical translocating arylating groups. *Nat. Commun.* 2018, 9, 2808. [PubMed: 30022072]
140. Hervieu C; Kirillova MS; Suárez T; Müller M; Merino E; Nevado C, Asymmetric, Visible Light-Mediated Radical Sulfinyl-Smiles Rearrangement to Access All-Carbon Quaternary Stereocentres. *Nat. Chem.* 2021, 13, 327–334. [PubMed: 33833448]
141. Leonard DJ; Ward JW; Clayden J, Asymmetric  $\alpha$ -Arylation of Amino Acids. *Nature* 2018, 562, 105–109. [PubMed: 30283103]
142. Lennox AJJ, Meisenheimer Complexes in S<sub>N</sub>Ar Reactions: Intermediates or Transition States? *Angew. Chem. Int. Ed.* 2018, 57, 14686–14688.
143. Rohrbach S; Smith AJ; Pang JH; Poole DL; Tuttle T; Chiba S; Murphy JA, Concerted Nucleophilic Aromatic Substitution Reactions. *Angew. Chem. Int. Ed.* 2019, 58, 16368–16388.
144. Ruzi R; Ma J; Yuan XA; Wang W; Wang S; Zhang M; Dai J; Xie J; Zhu C, Deoxygenative Arylation of Carboxylic Acids by Aryl Migration. *Chem. - Eur. J.* 2019, 25, 12724–12729. [PubMed: 31441136]
145. Zhang M; Xie J; Zhu C, A General Deoxygenation Approach for Synthesis of Ketones from Aromatic Carboxylic Acids and Alkenes. *Nat. Commun.* 2018, 9, 3517. [PubMed: 30158628]
146. Stache EE; Ertel AB; Rovis T; Doyle AG, Generation of Phosphoranyl Radicals via Photoredox Catalysis Enables Voltage-Independent Activation of Strong C–O Bonds. *ACS Catal.* 2018, 8, 11134–11139. [PubMed: 31367474]
147. Fuss D; Wu YQ; Grossi MR; Hollett JW; Wood TE, Effect of the Tether Length Upon Truce-Smiles Rearrangement Reactions. *J. Phys. Org. Chem.* 2018, 31, e3742.

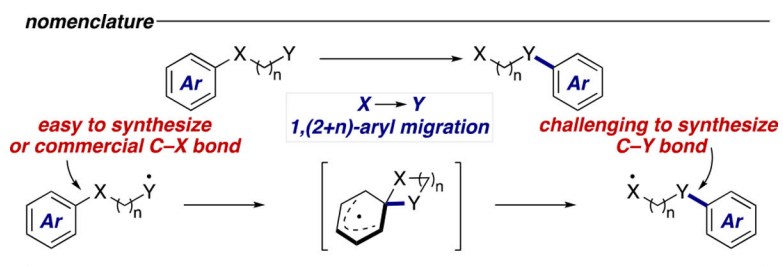
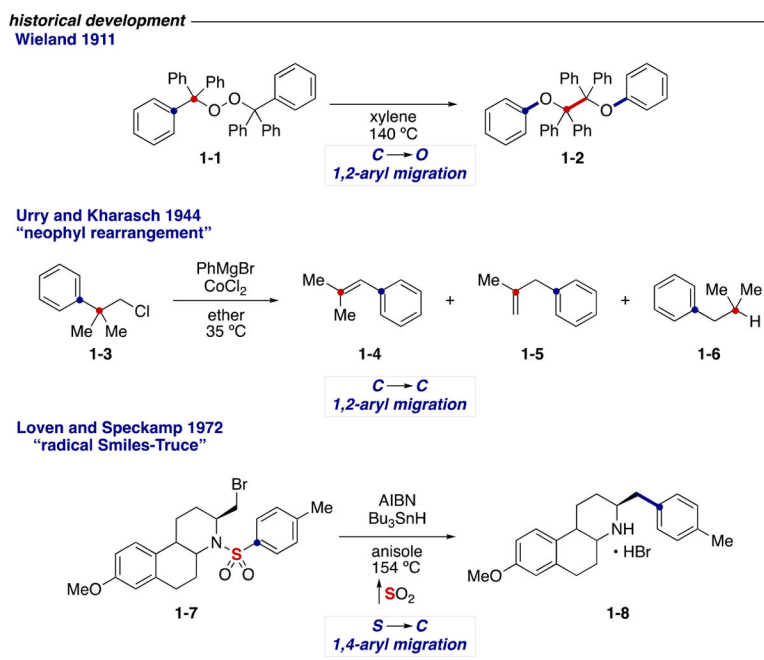
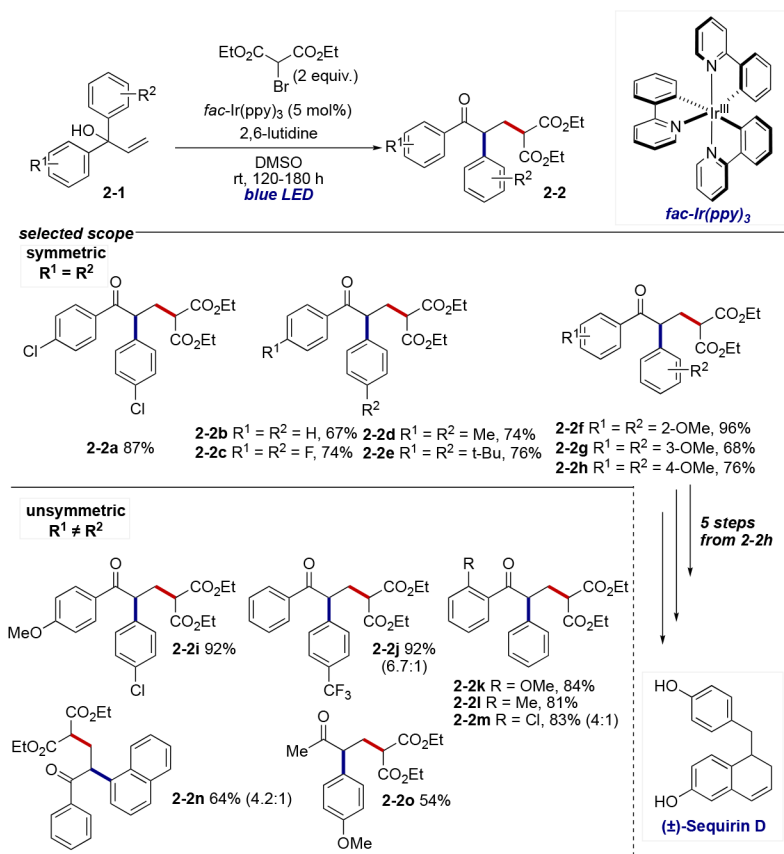


Figure 1.

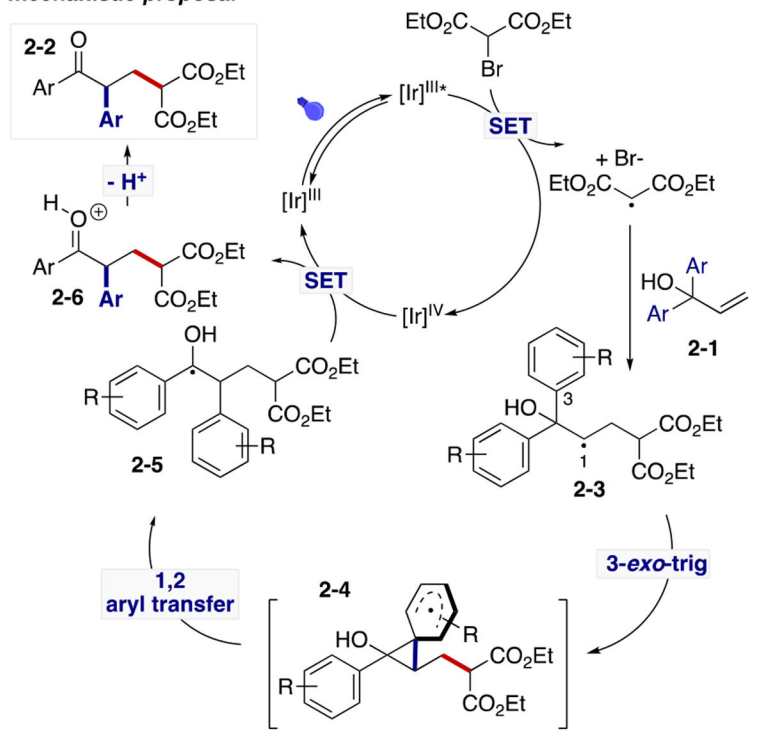


Scheme 1.

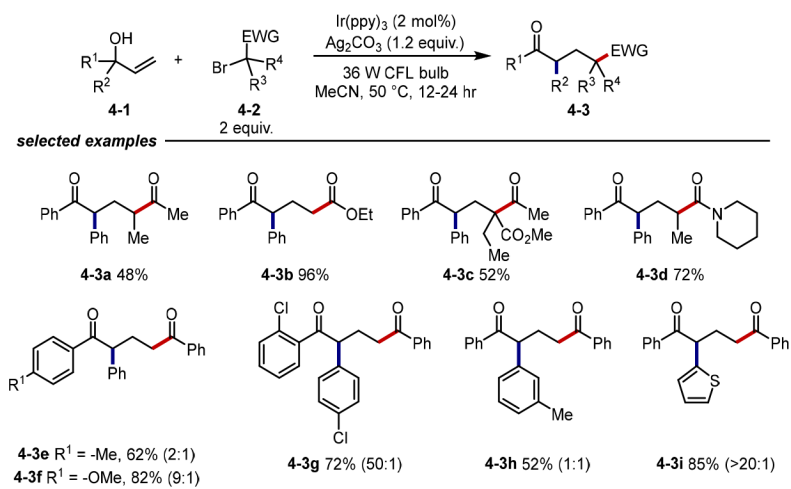


Scheme 2.

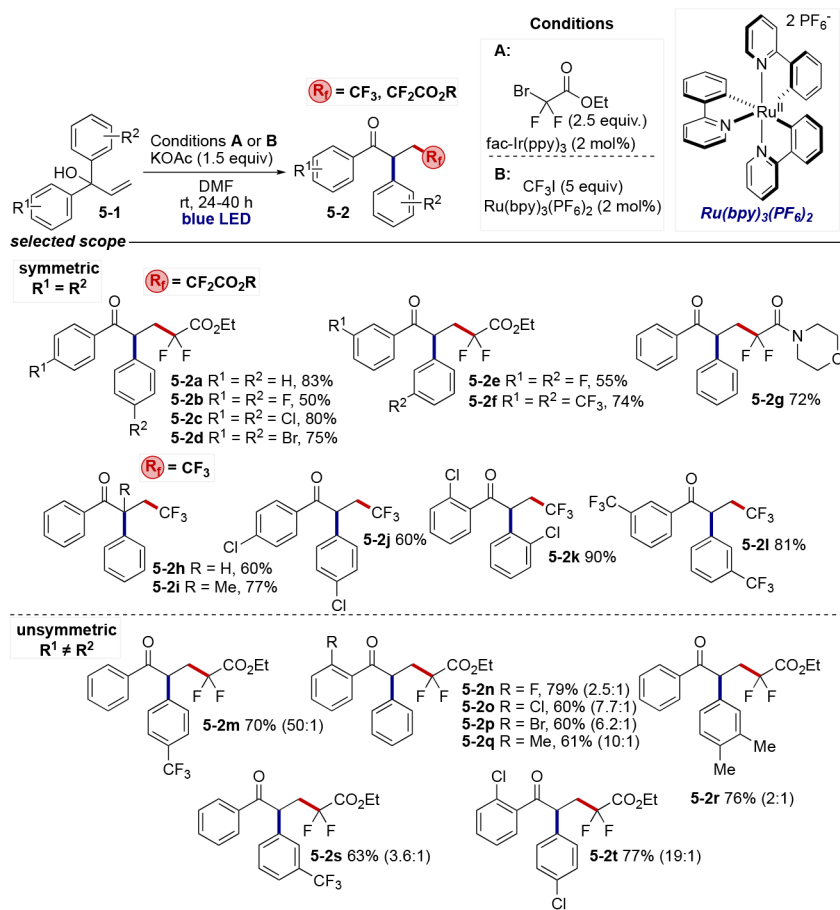


**mechanistic proposal**

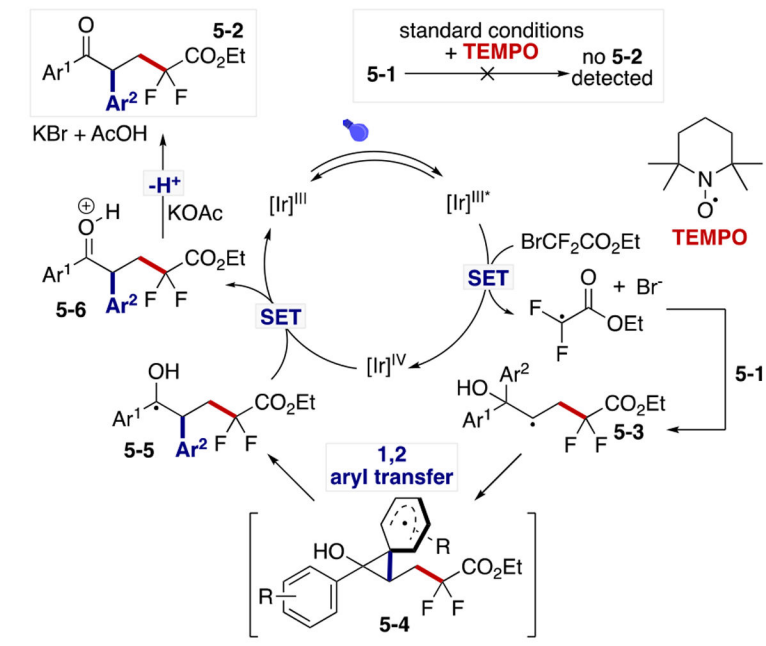
Scheme 3.



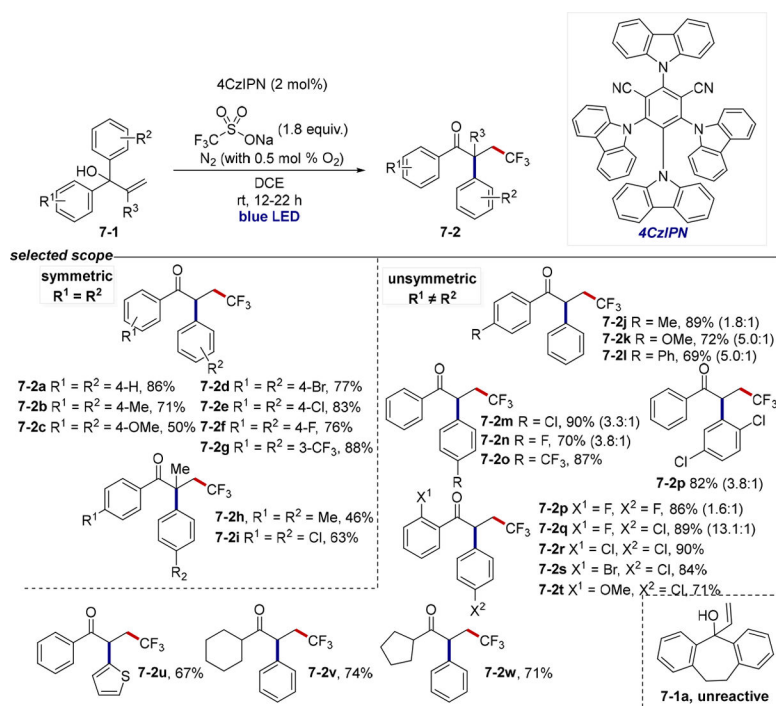
Scheme 4.



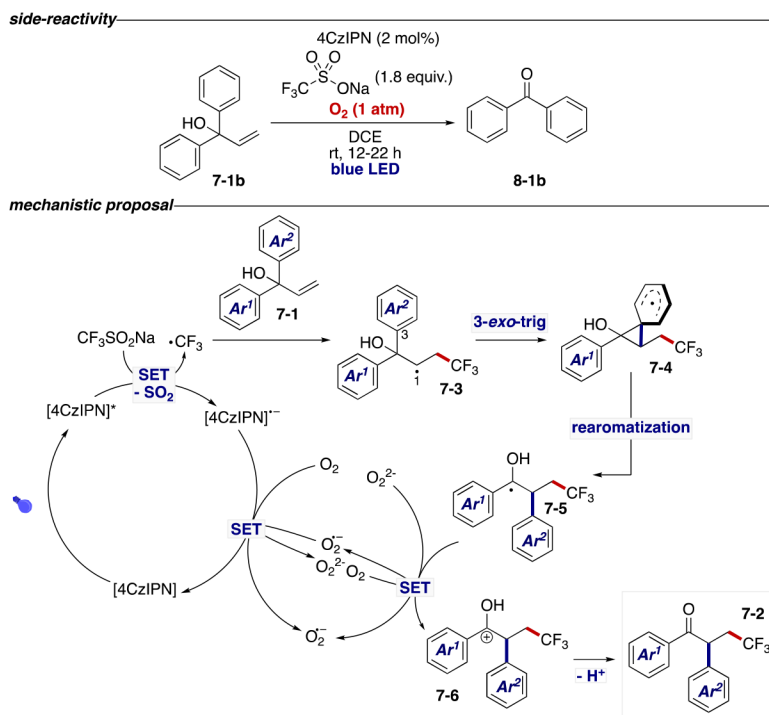
Scheme 5.

*mechanistic proposal*

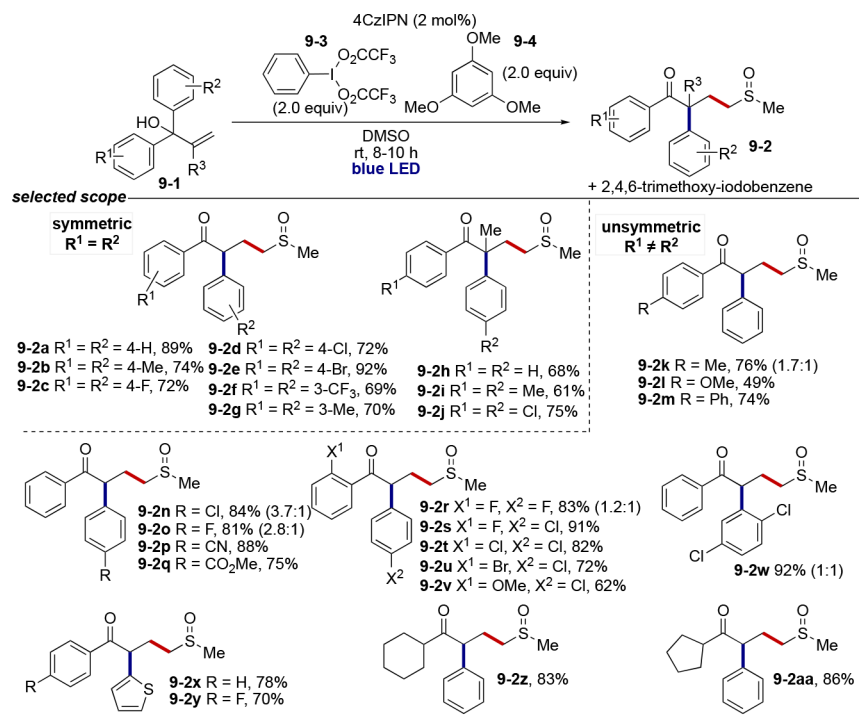
Scheme 6.



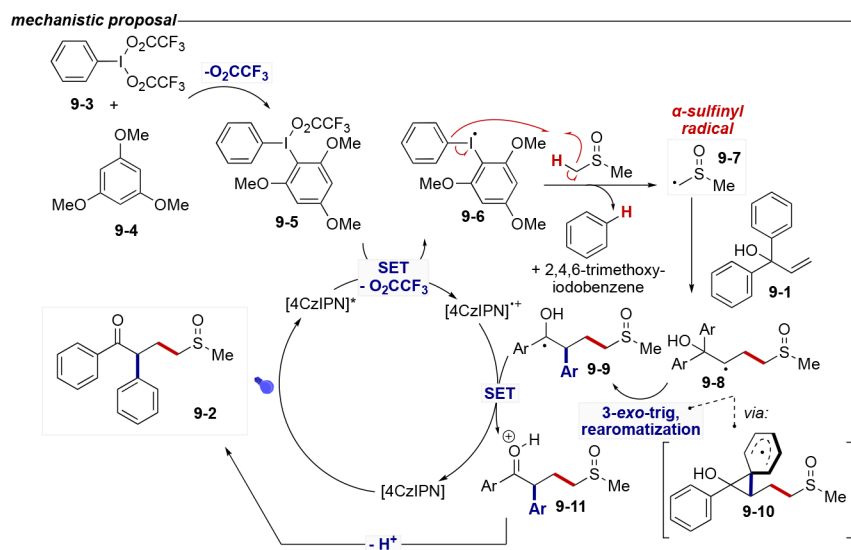
Scheme 7.



Scheme 8.



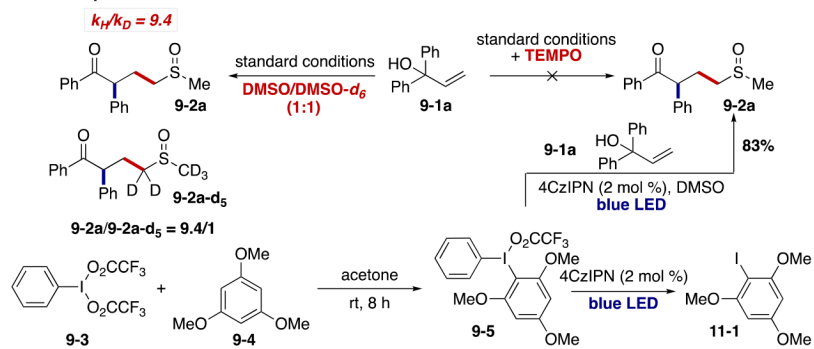
Scheme 9.



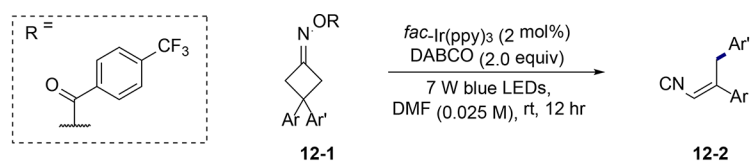
Scheme 10.



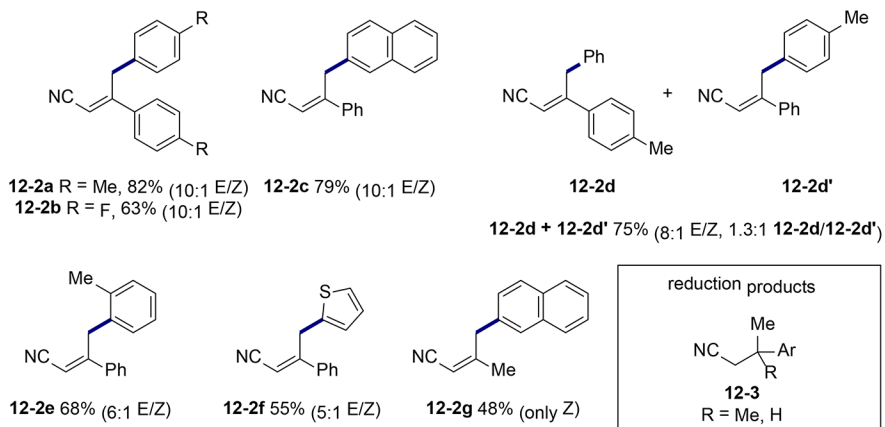
## mechanistic experiments



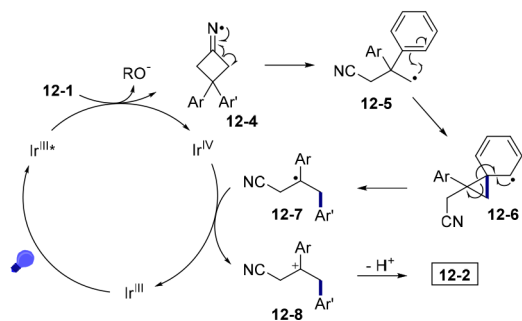
Scheme 11.

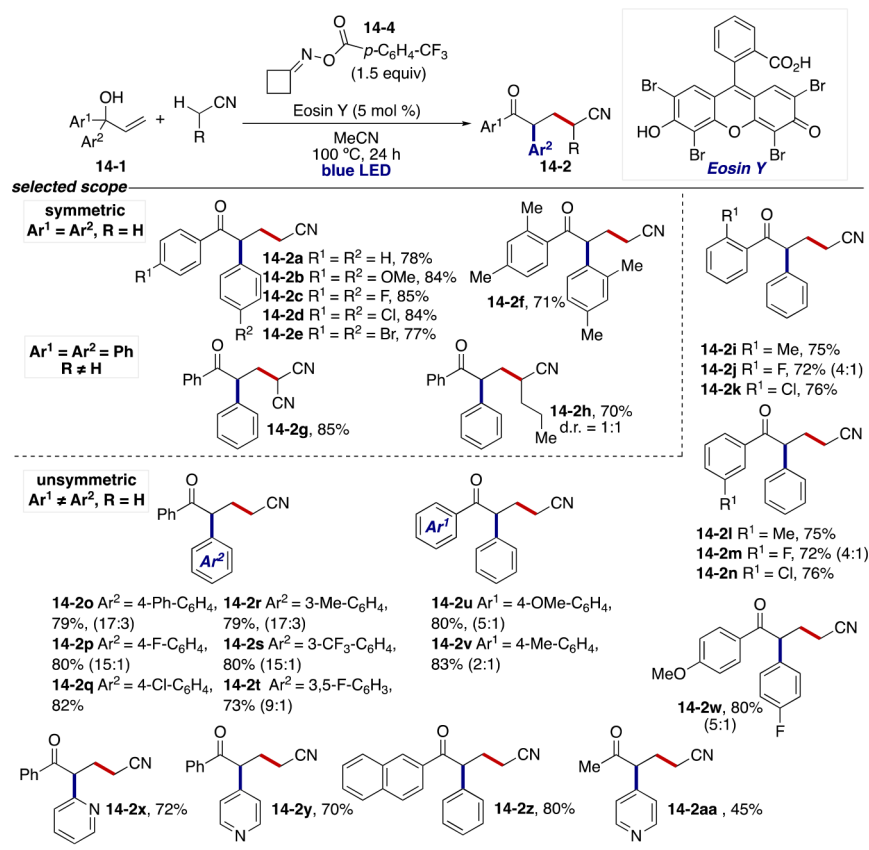


selected examples

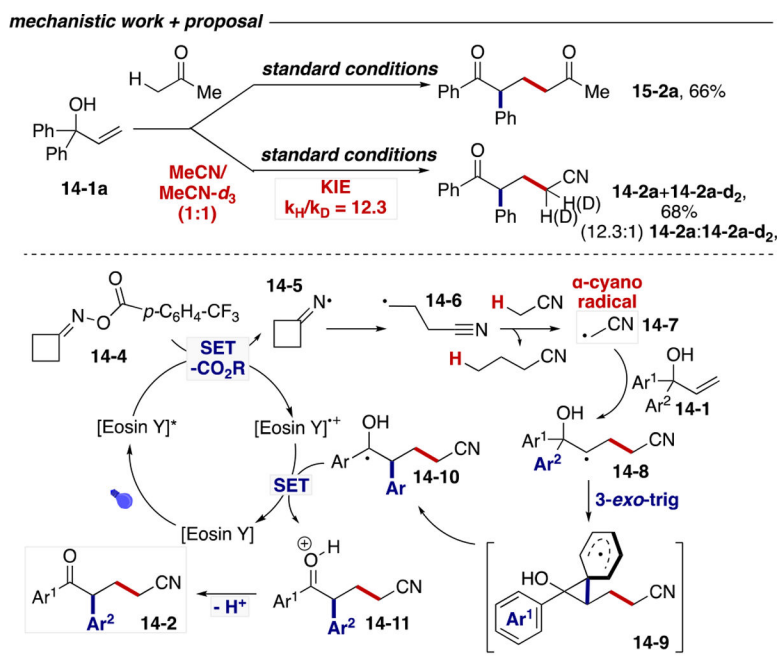


Scheme 12.

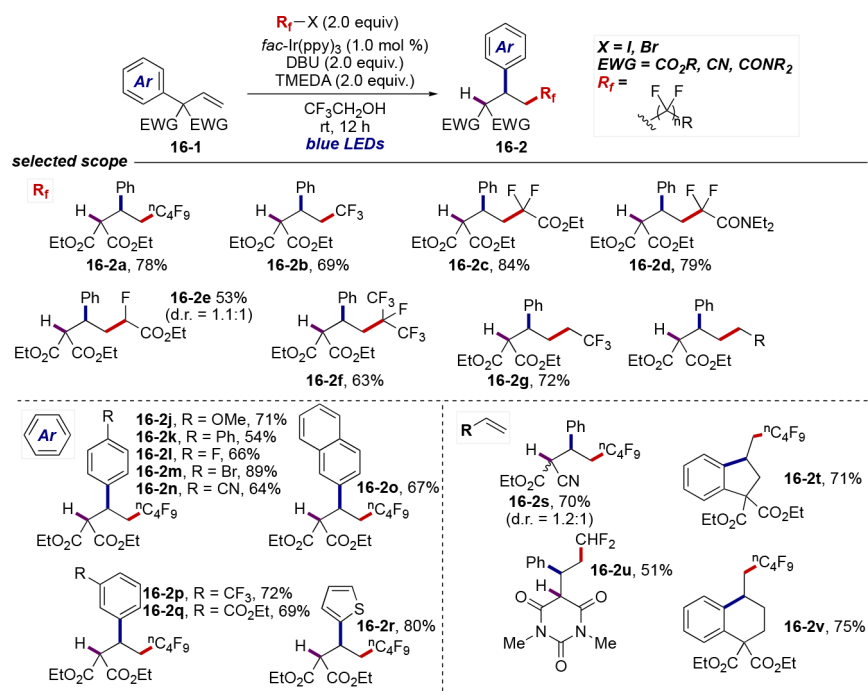
*mechanistic proposal***Scheme 13.**



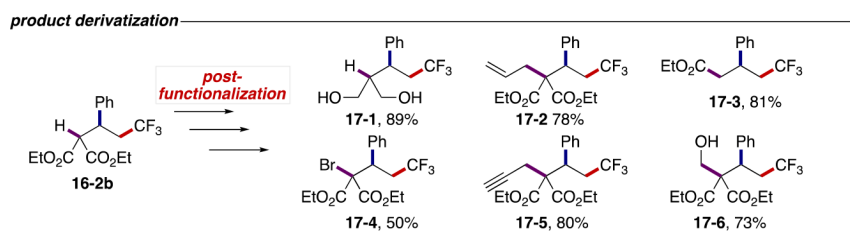
Scheme 14.



Scheme 15.

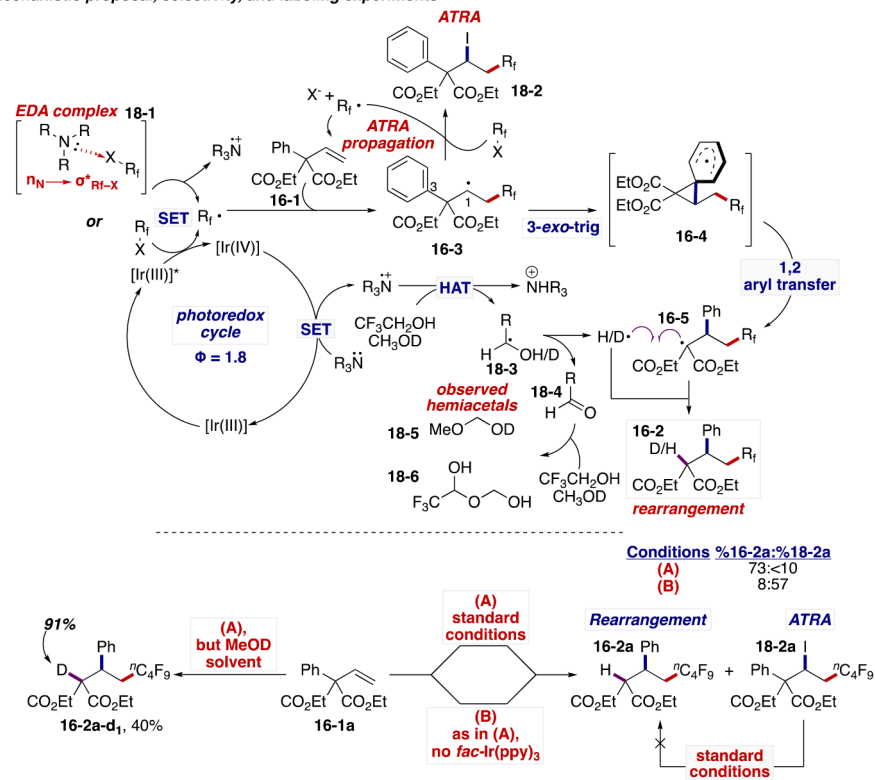


Scheme 16.



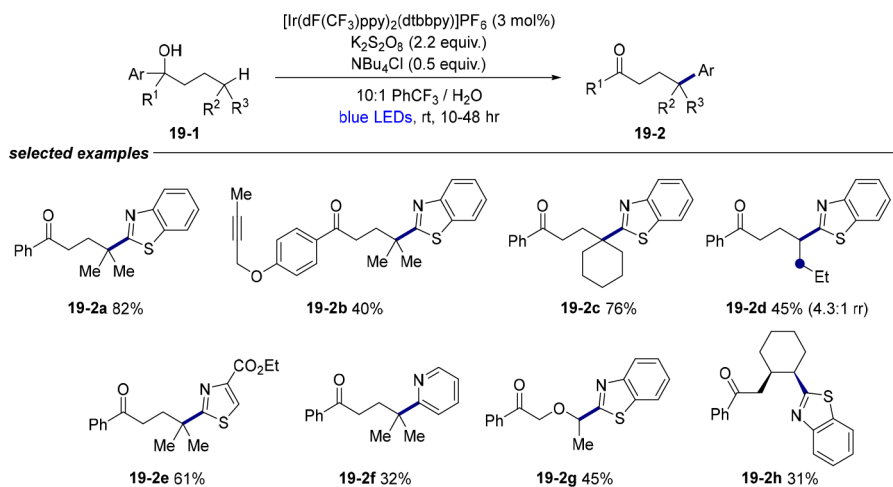
Scheme 17.

## mechanistic proposal, selectivity, and labeling experiments



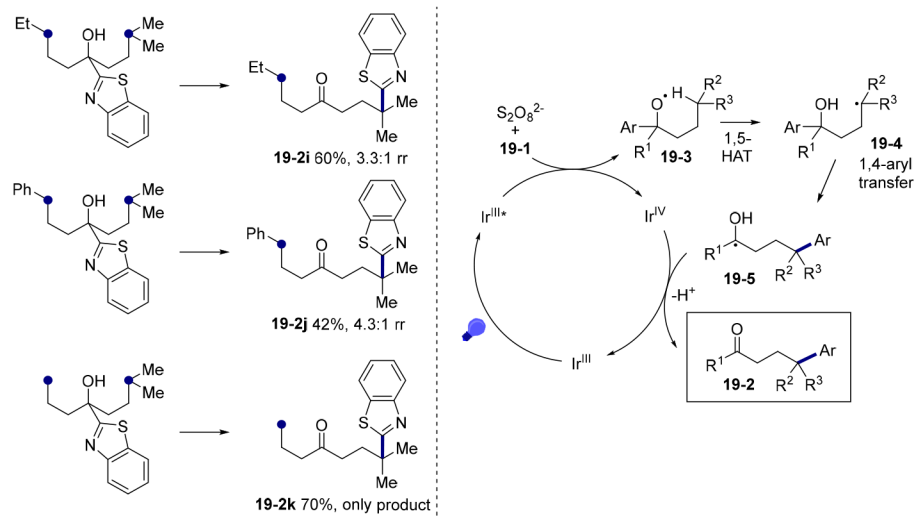
Scheme 18.



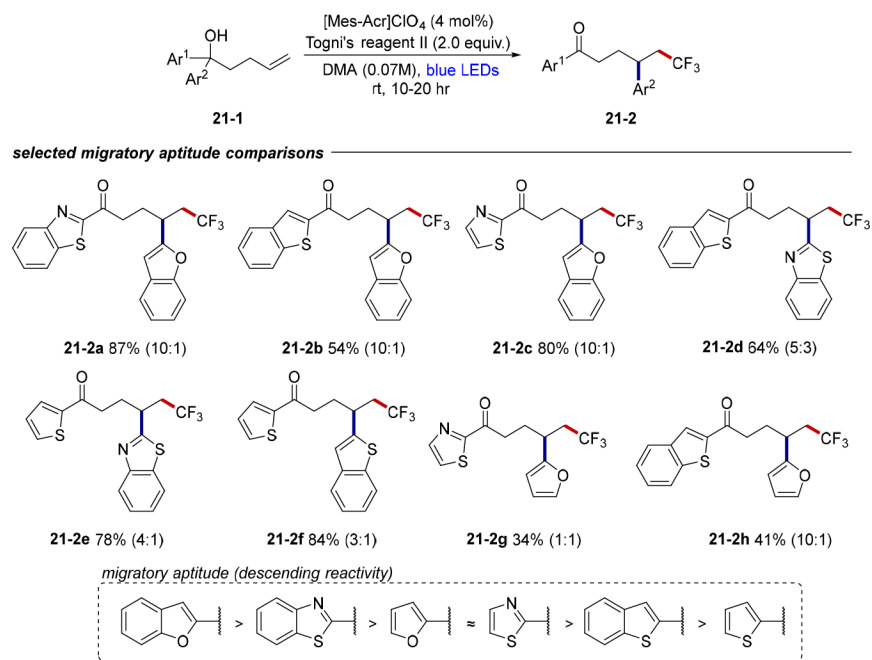


Scheme 19.

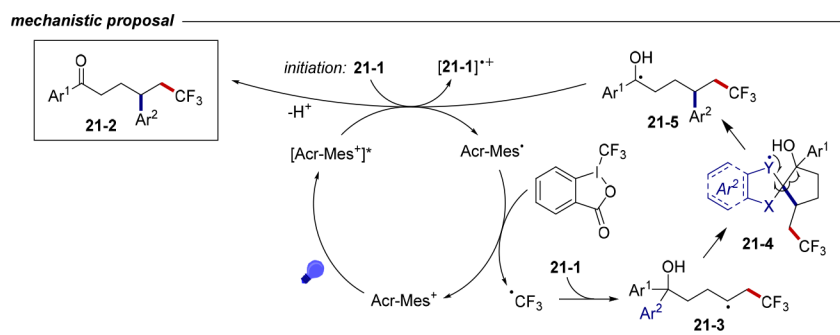
## competition experiments and mechanistic proposal



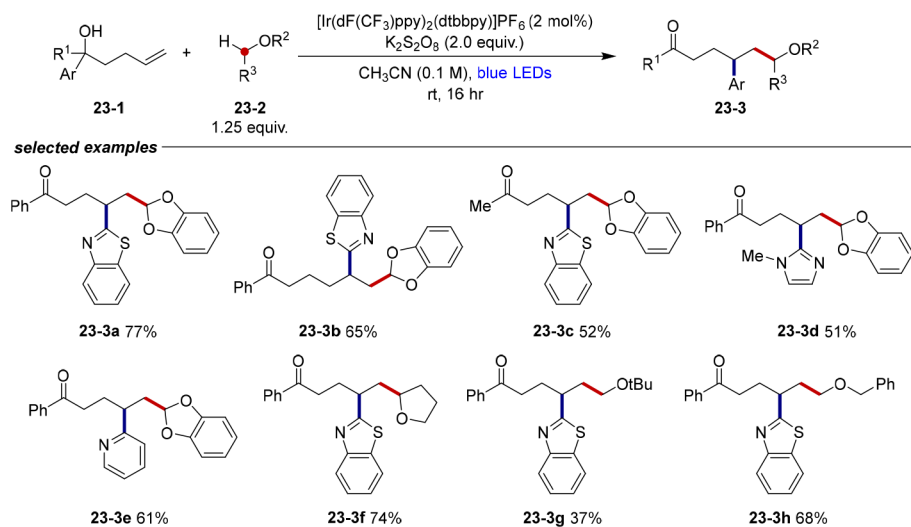
Scheme 20.



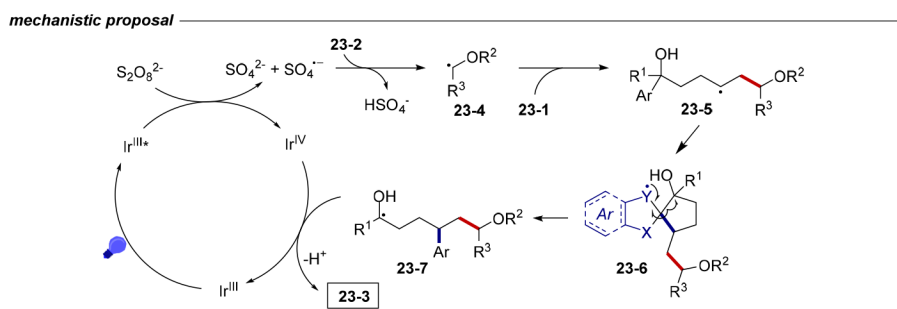
Scheme 21.



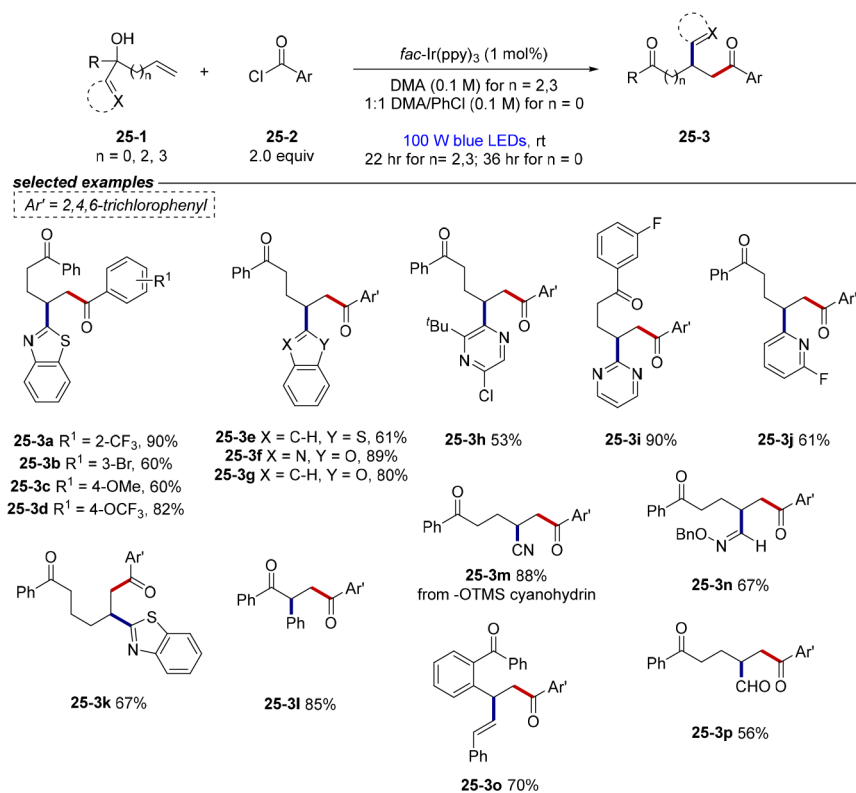
Scheme 22.



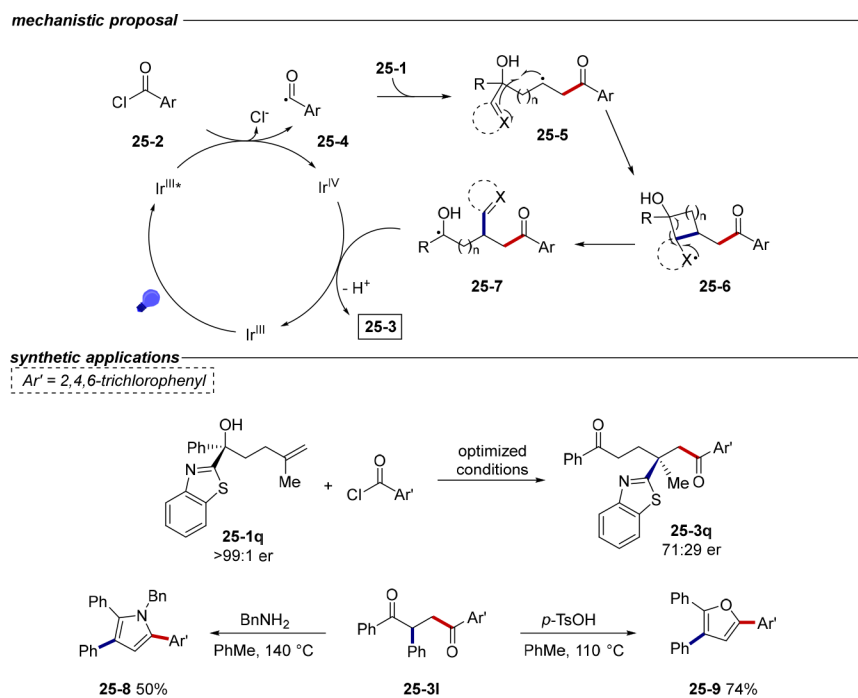
Scheme 23.



Scheme 24.

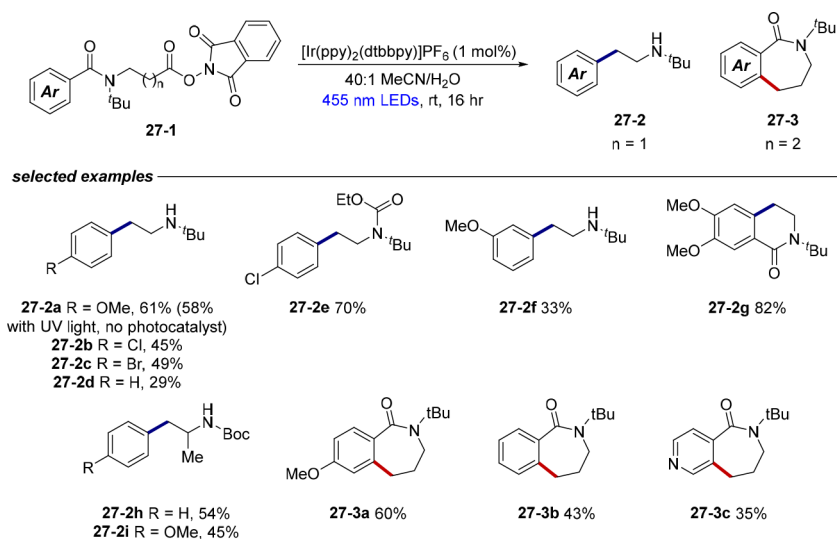


Scheme 25.

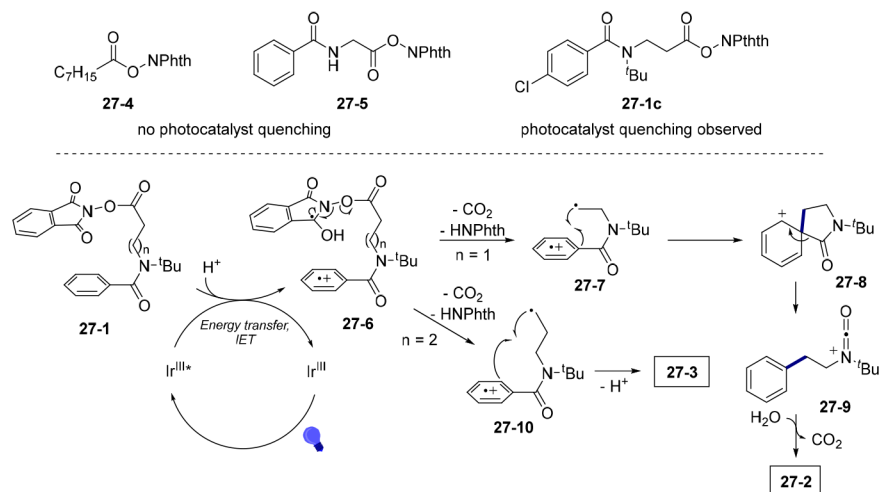
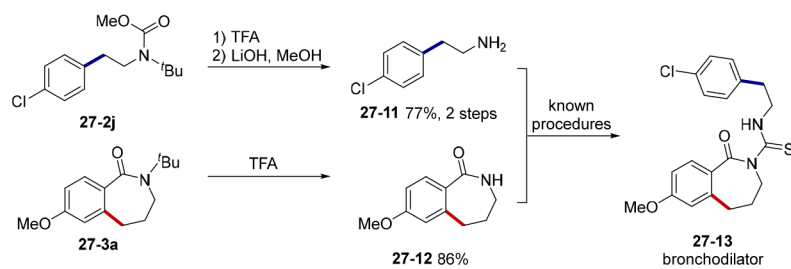


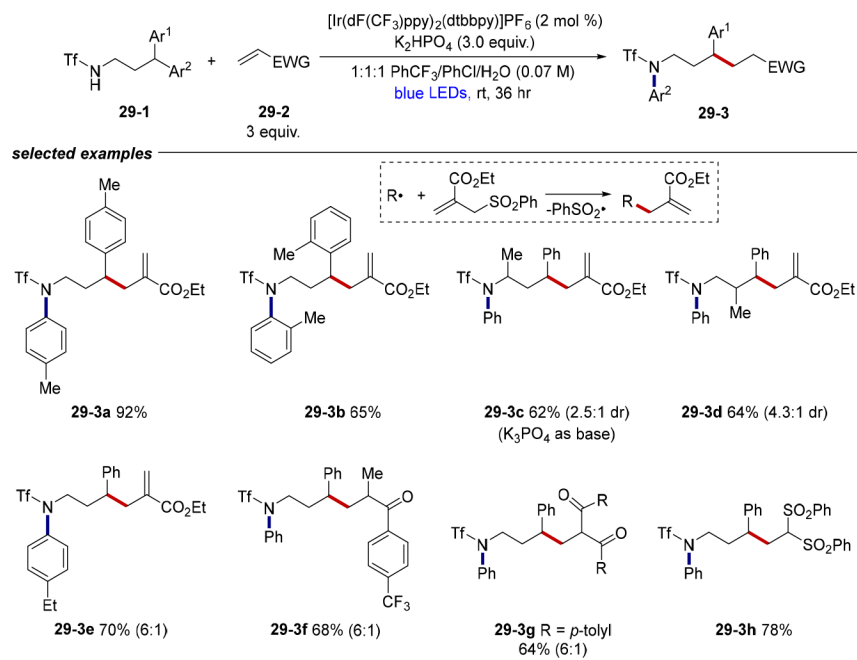
Scheme 26.



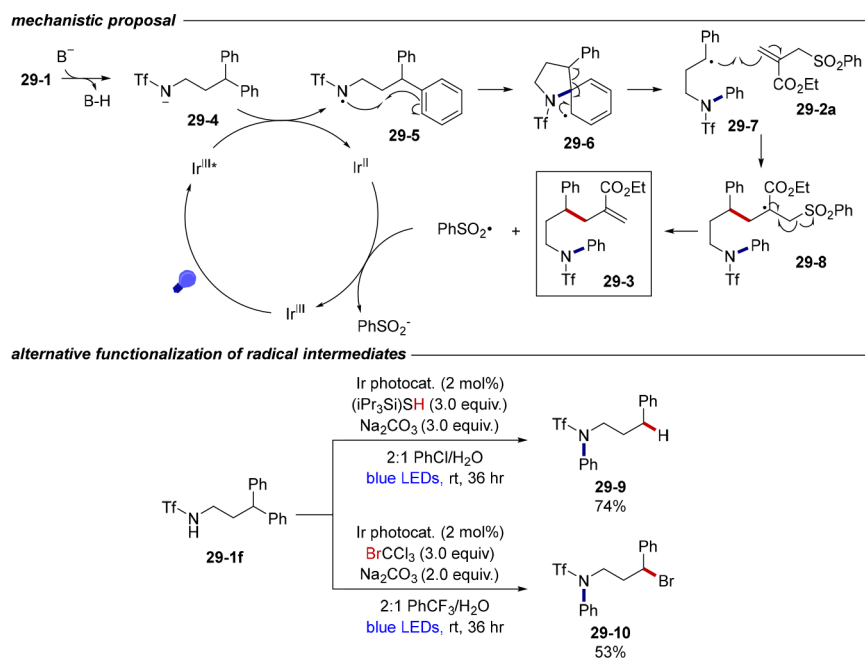


Scheme 27.

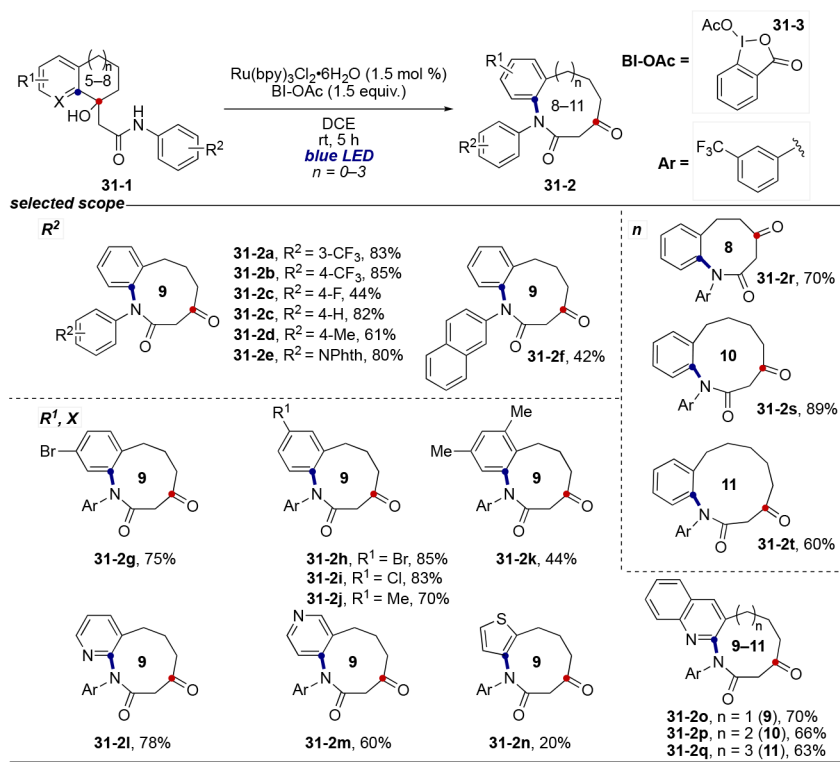
**mechanistic experiments & proposal****synthetic application****Scheme 28.**



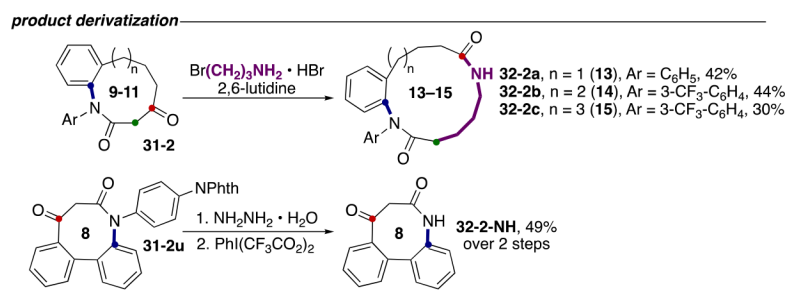
Scheme 29.



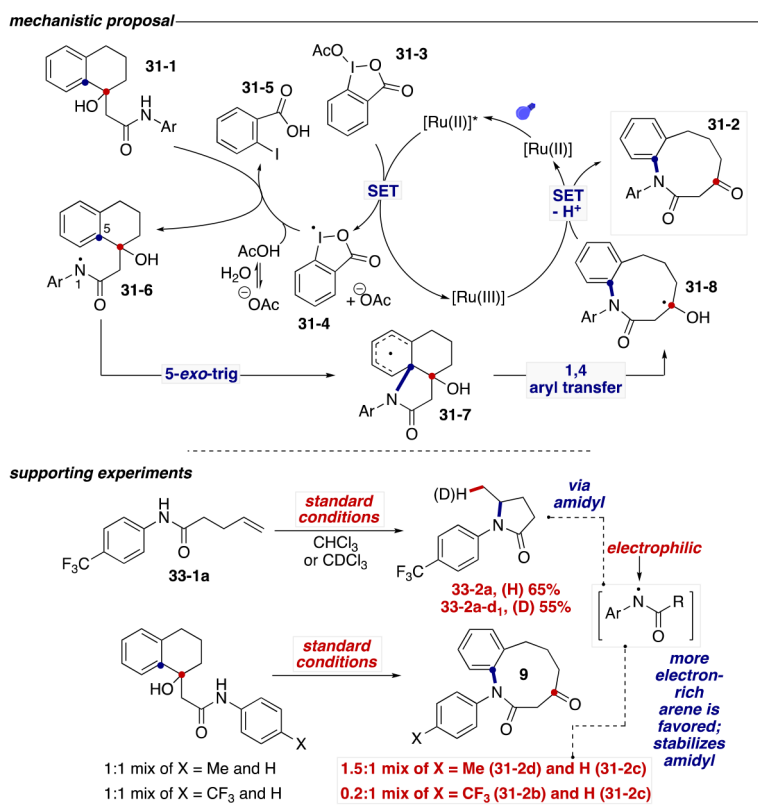
Scheme 30.



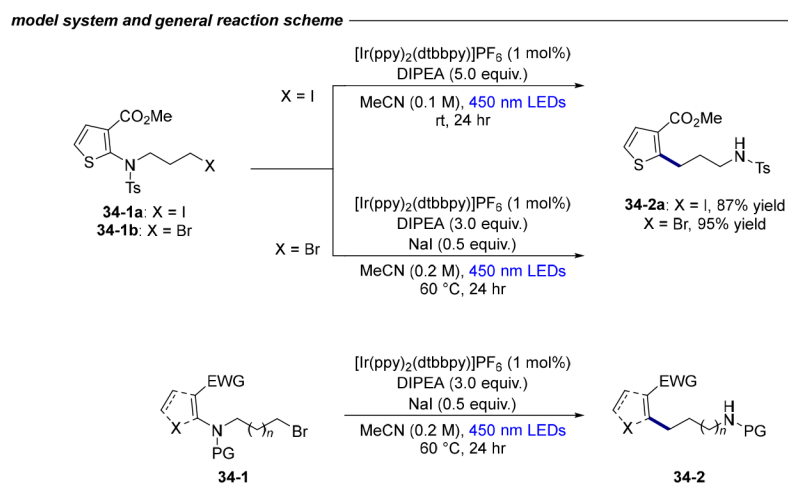
Scheme 31.



Scheme 32.



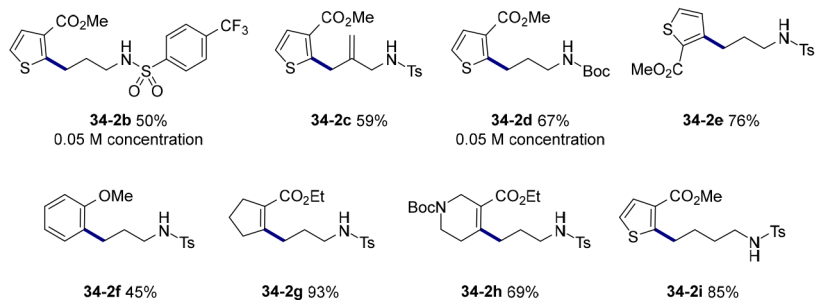
Scheme 33.



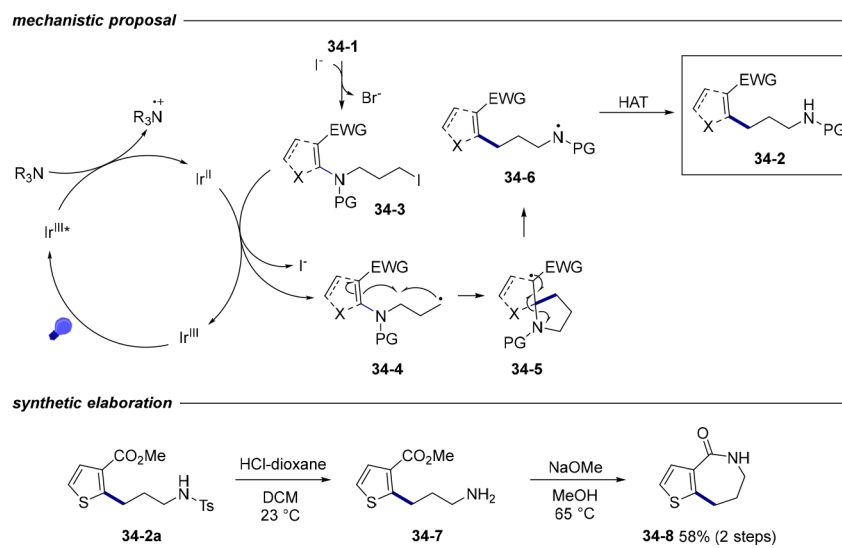
Scheme 34.



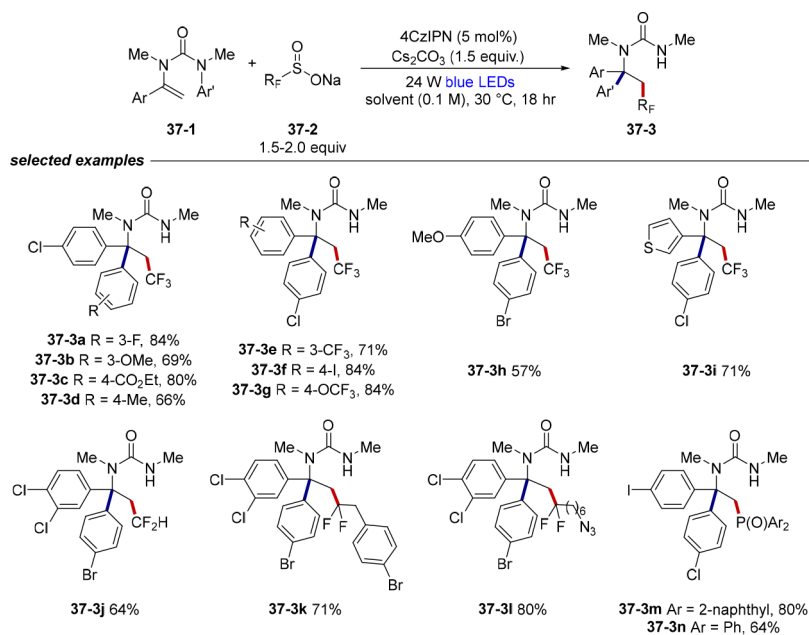
## selected examples



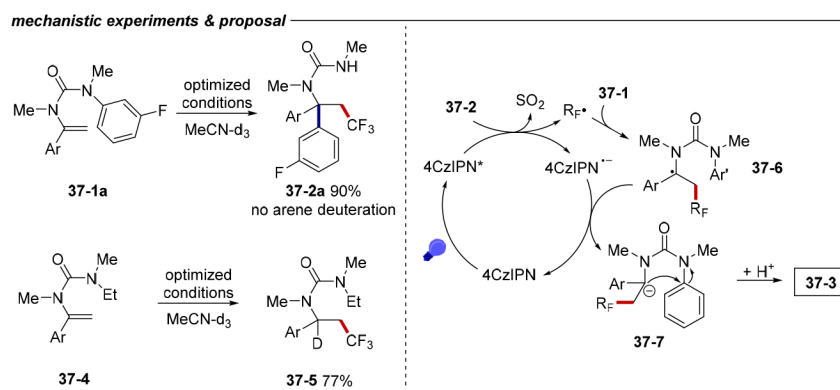
Scheme 35.



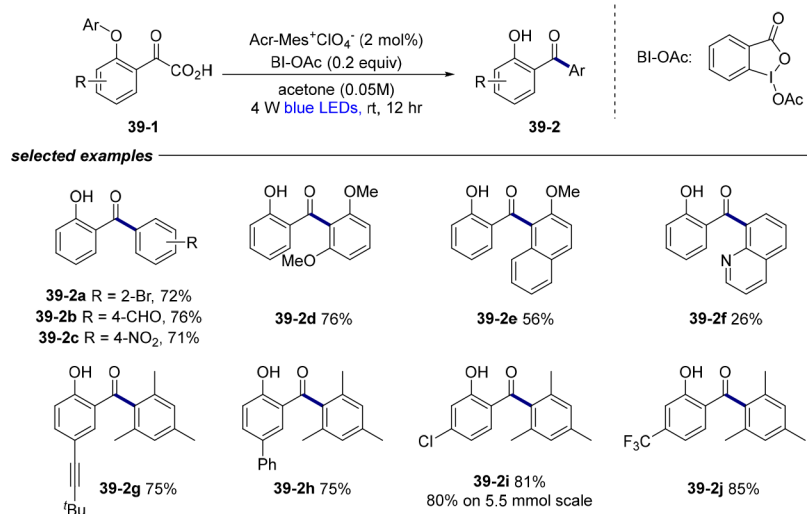
Scheme 36.



Scheme 37.

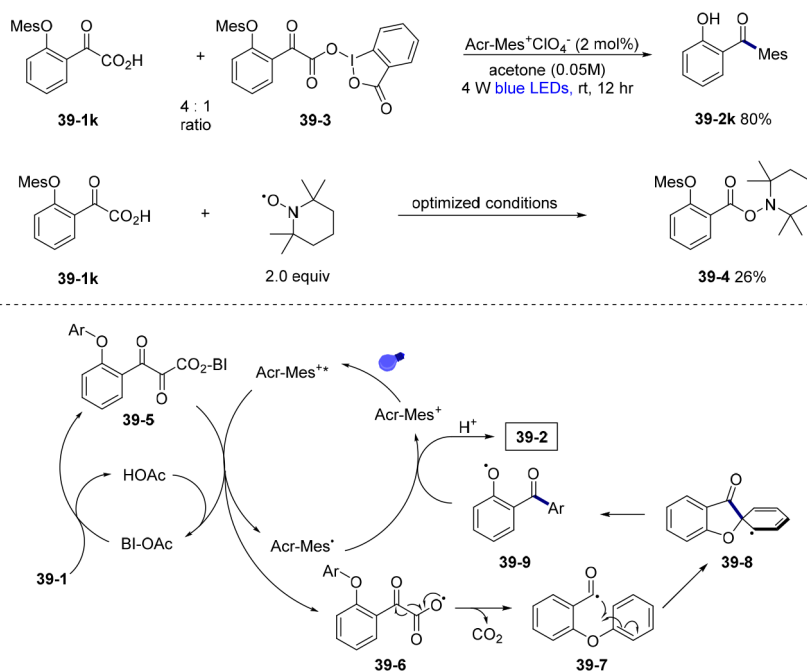


Scheme 38.

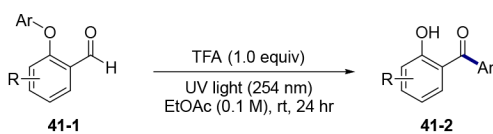


Scheme 39.

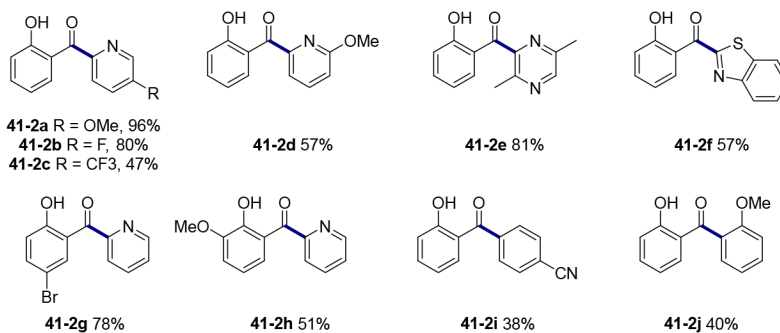
## mechanistic experiments &amp; proposal



Scheme 40.



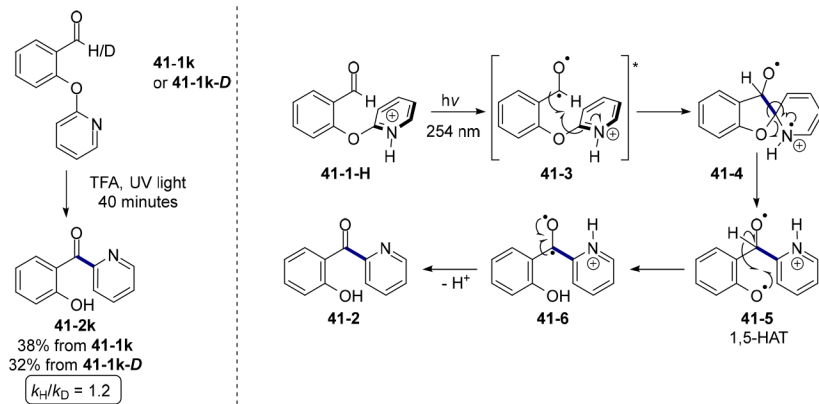
**selected examples**



(\*) = no TFA added

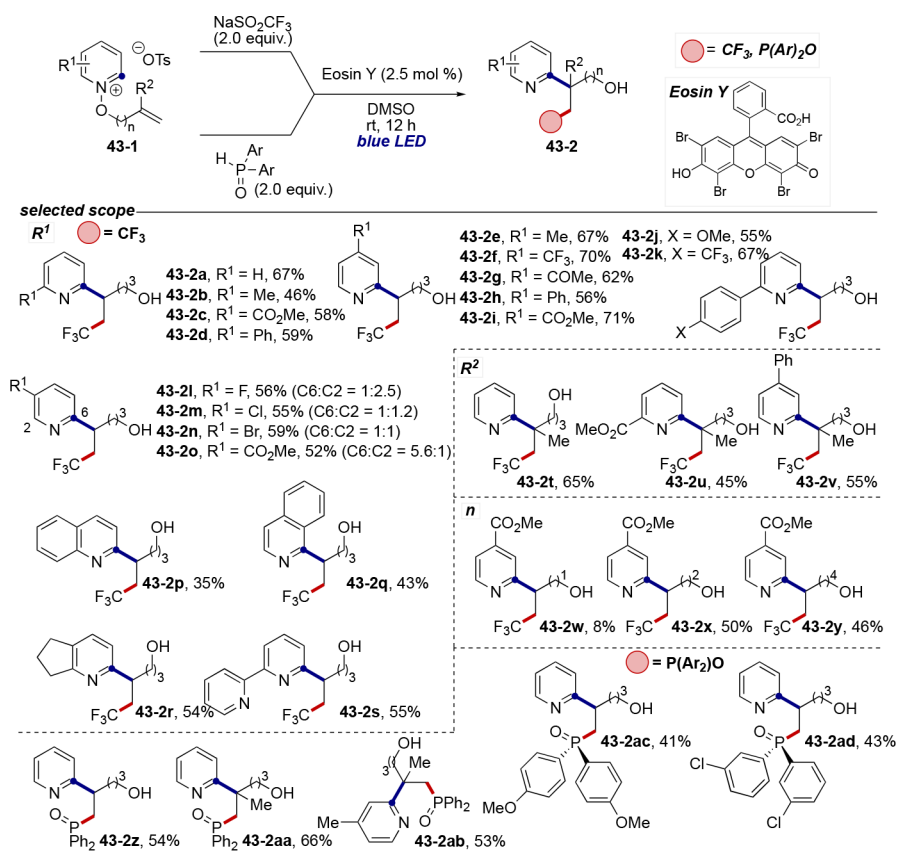
**Scheme 41.**

## mechanistic experiment &amp; proposal



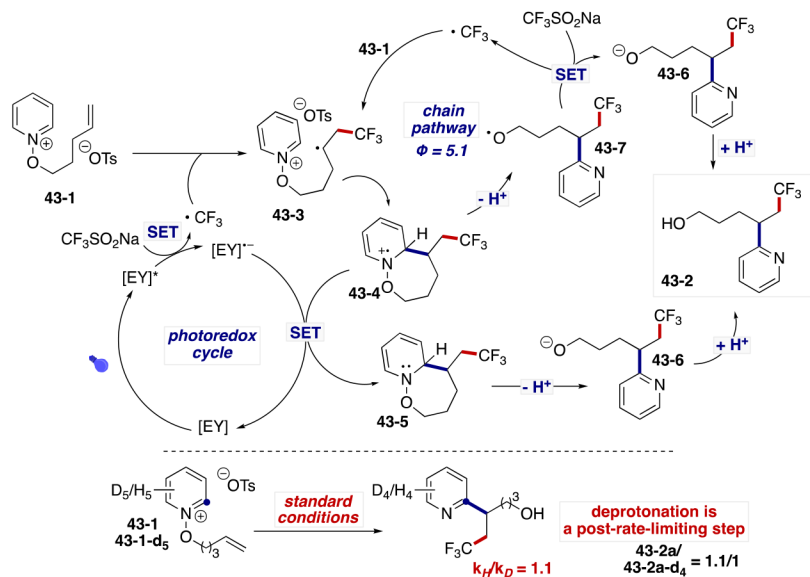
Scheme 42.



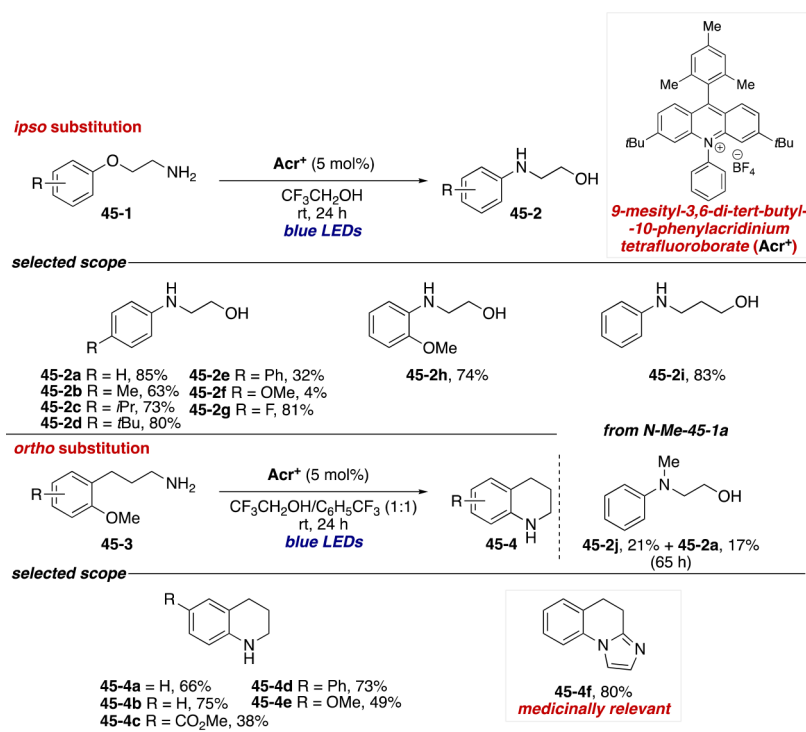


Scheme 43.

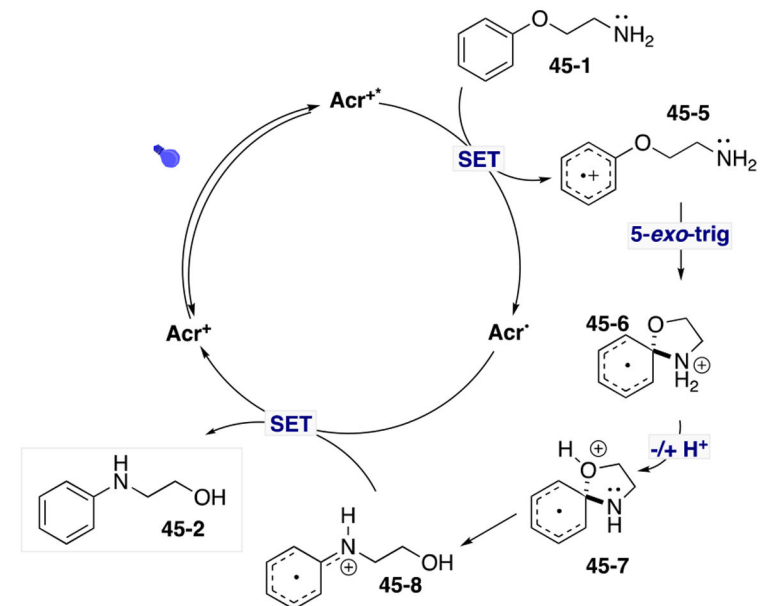
## mechanistic proposal &amp; KIE experiment



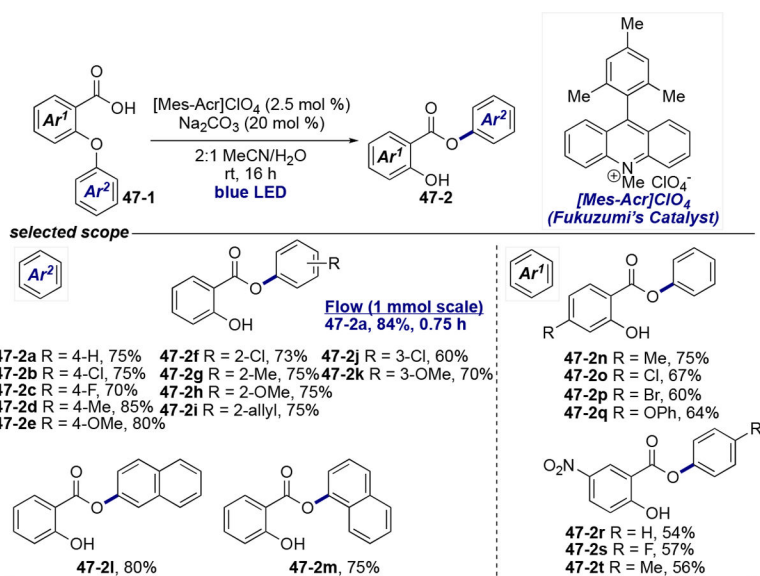
Scheme 44.



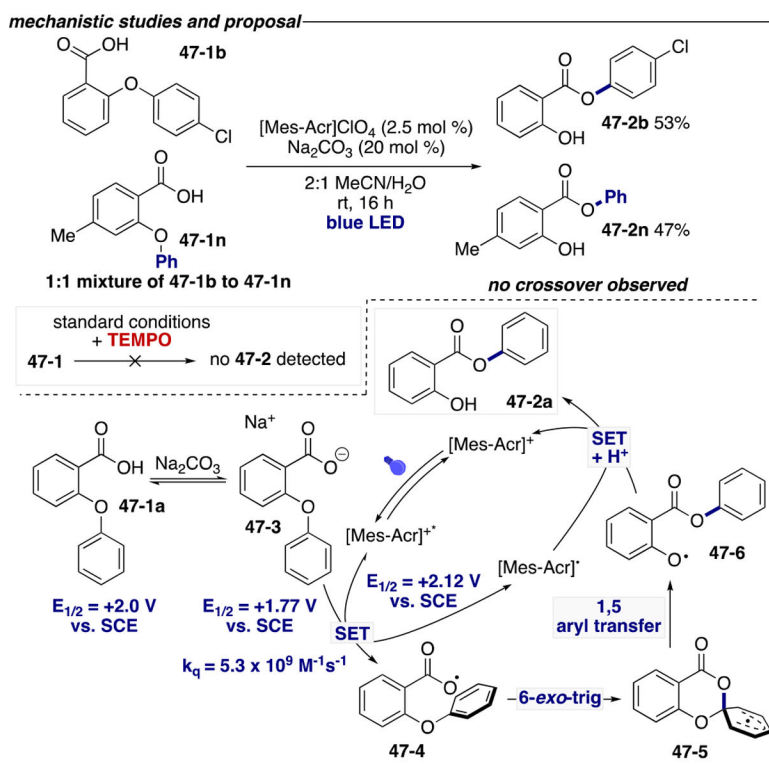
Scheme 45.

*mechanistic proposal*

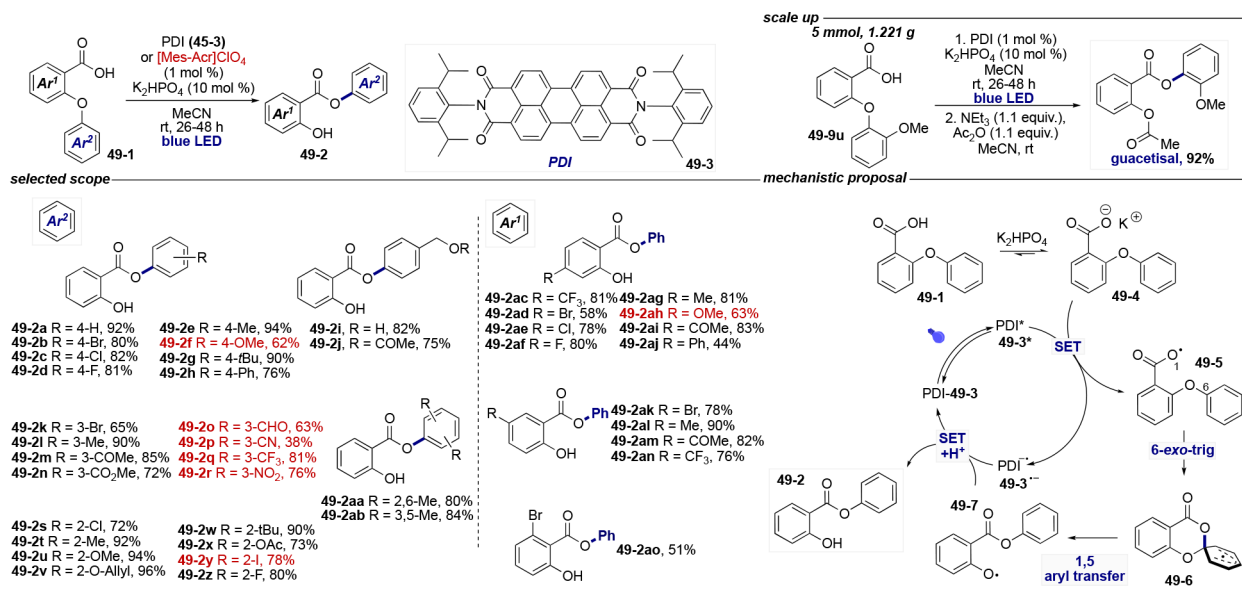
Scheme 46.



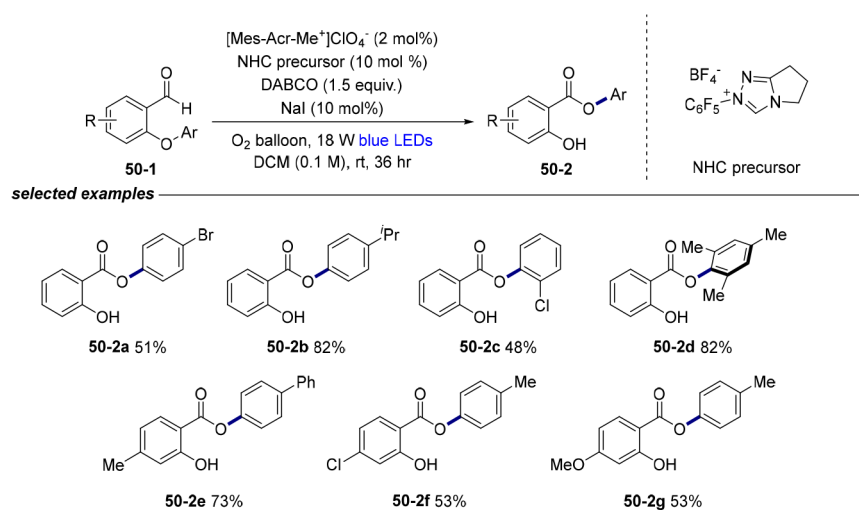
Scheme 47.



Scheme 48.



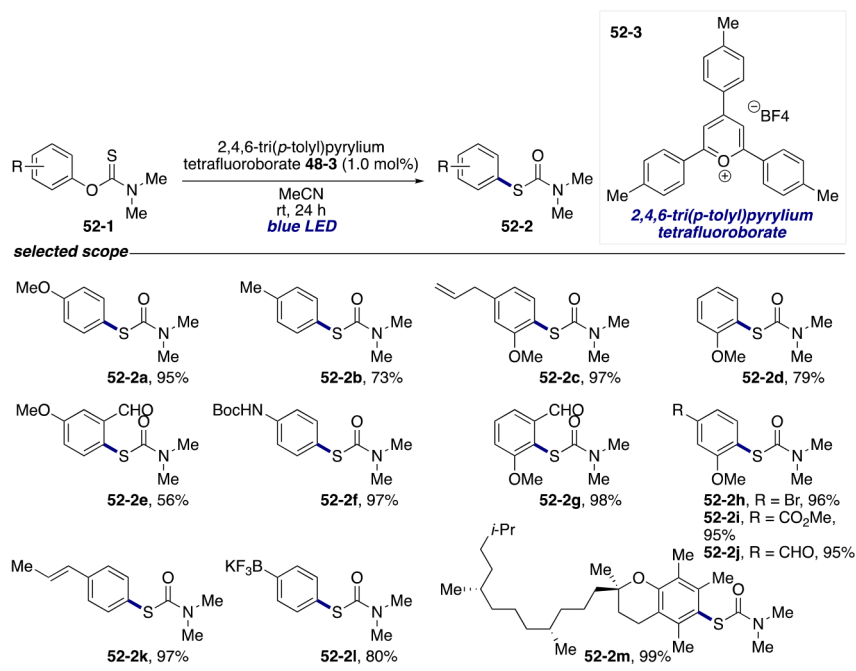
Scheme 49.



Scheme 50.

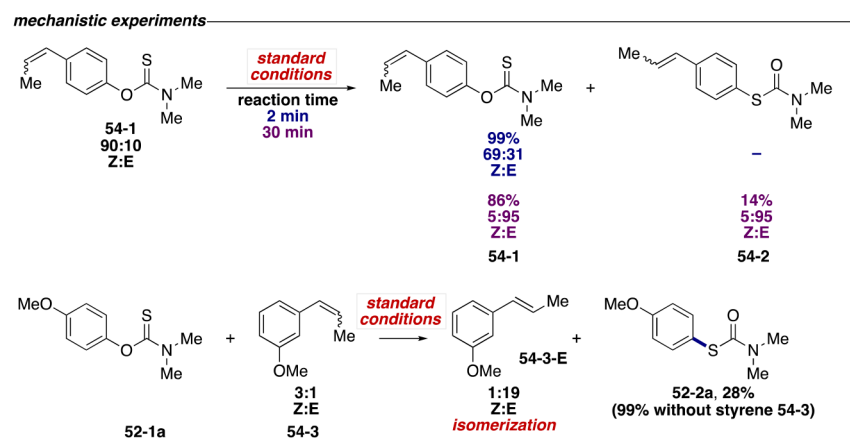




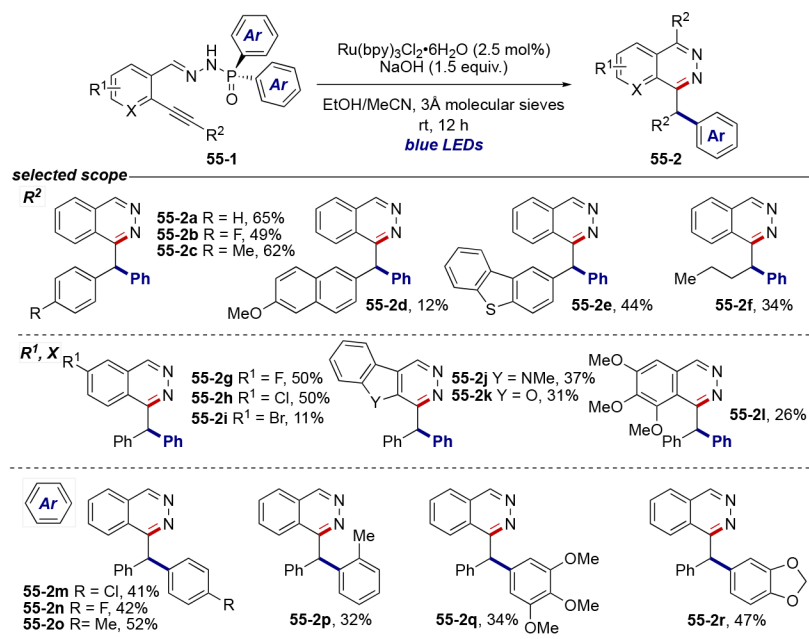


Scheme 52.

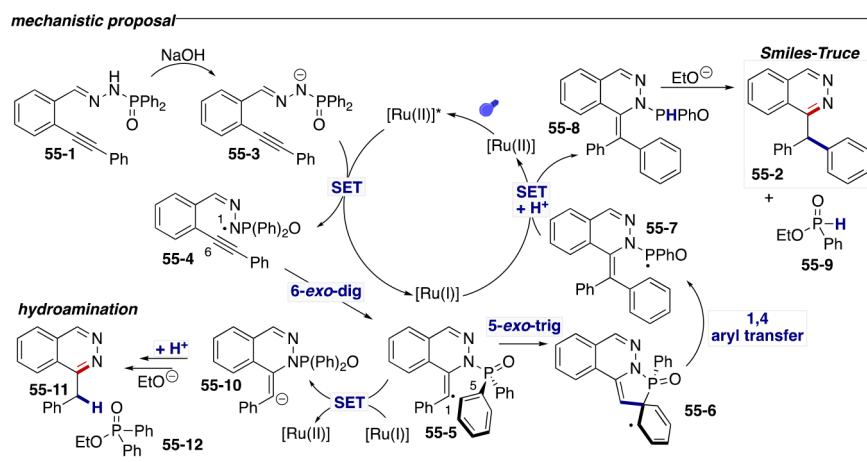




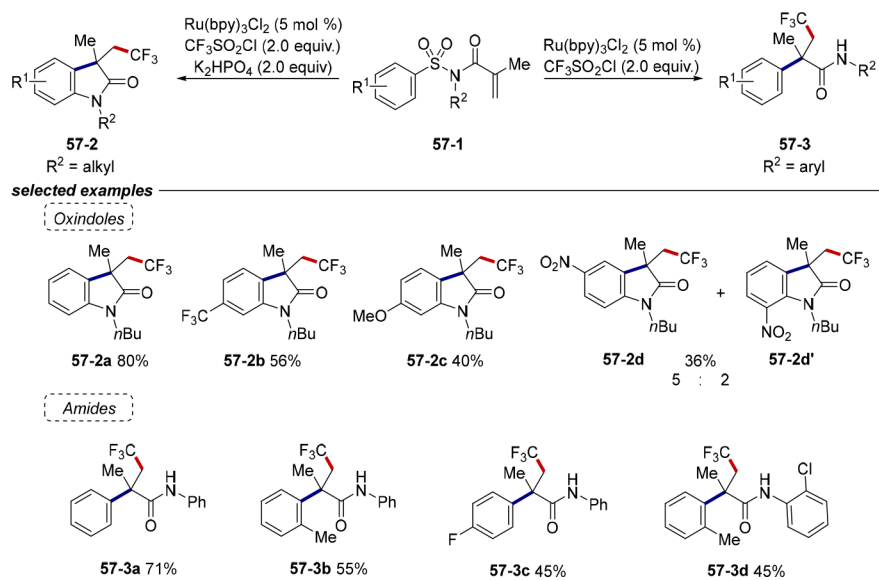
Scheme 54.



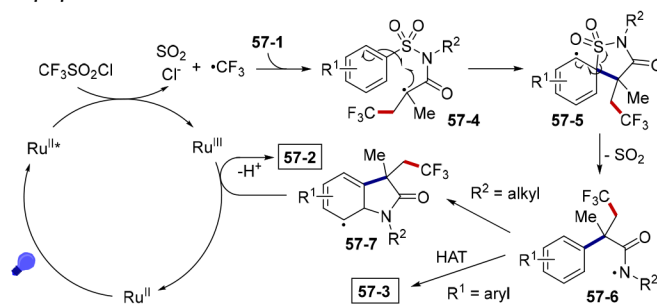
Scheme 55.



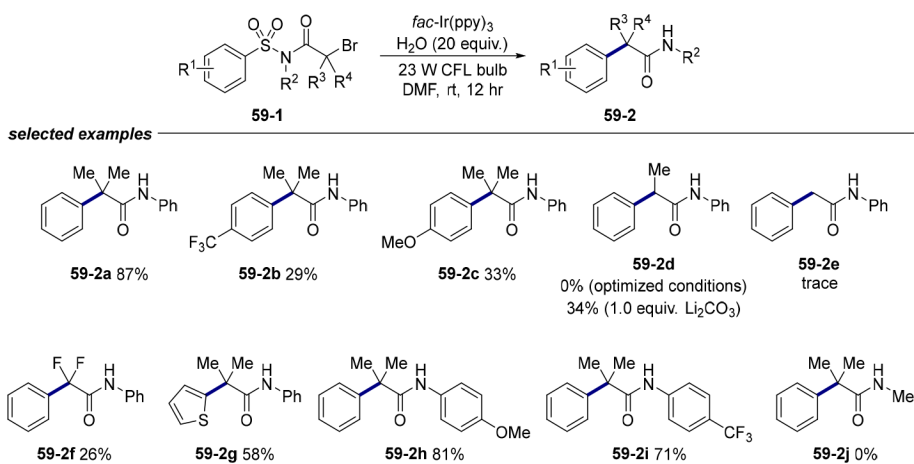
Scheme 56.

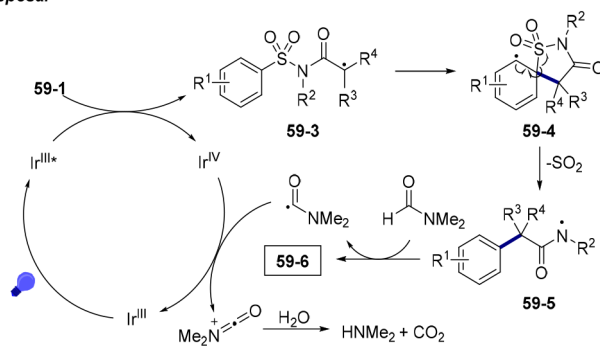


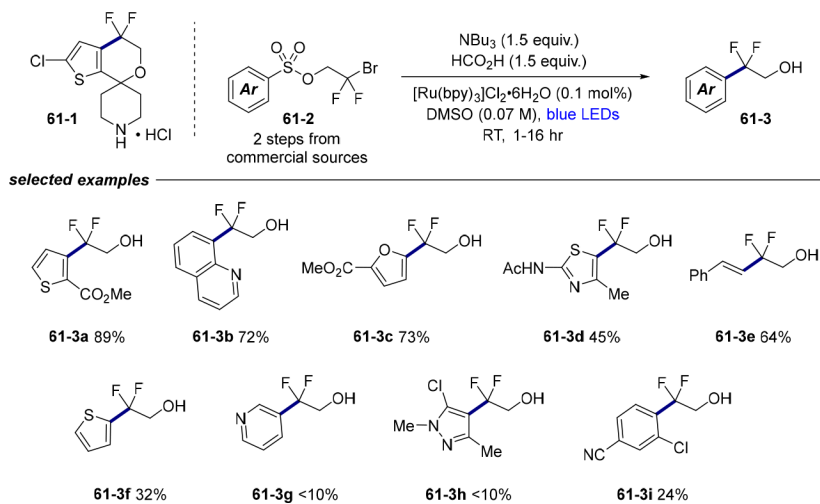
Scheme 57.

*mechanistic proposal***Scheme 58.**

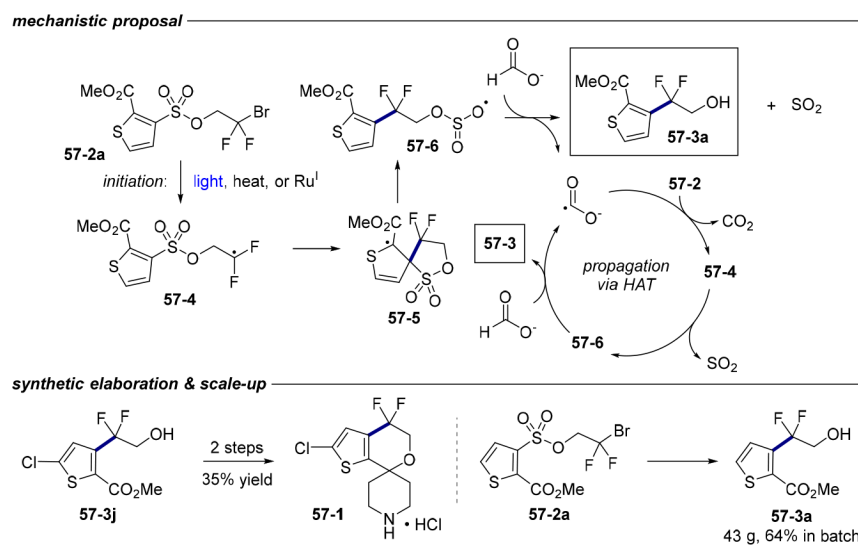


**Scheme 59.**

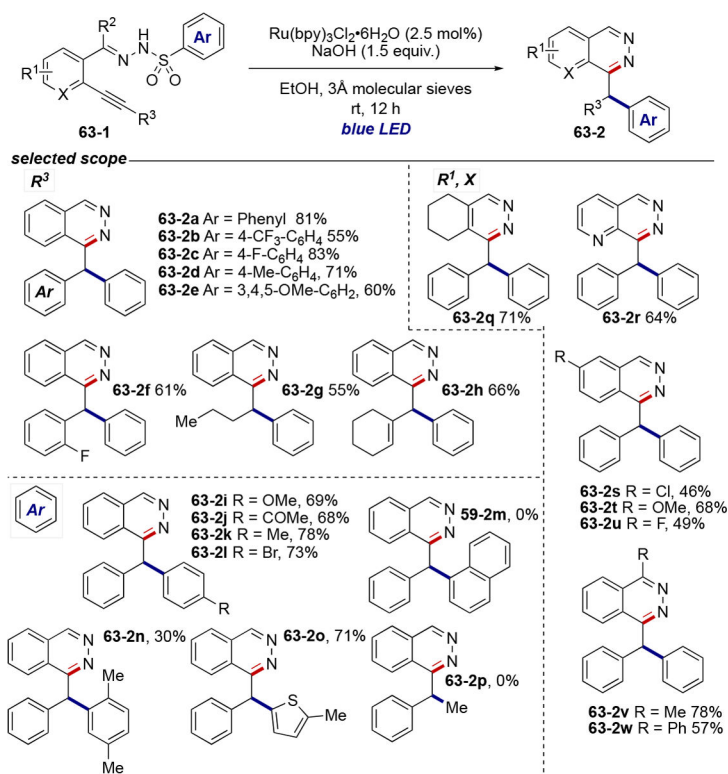
*mechanistic proposal***Scheme 60.**



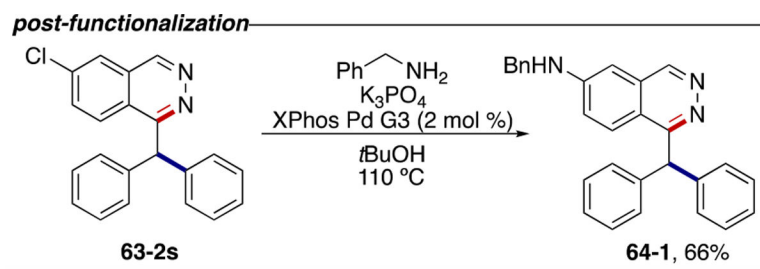
Scheme 61.



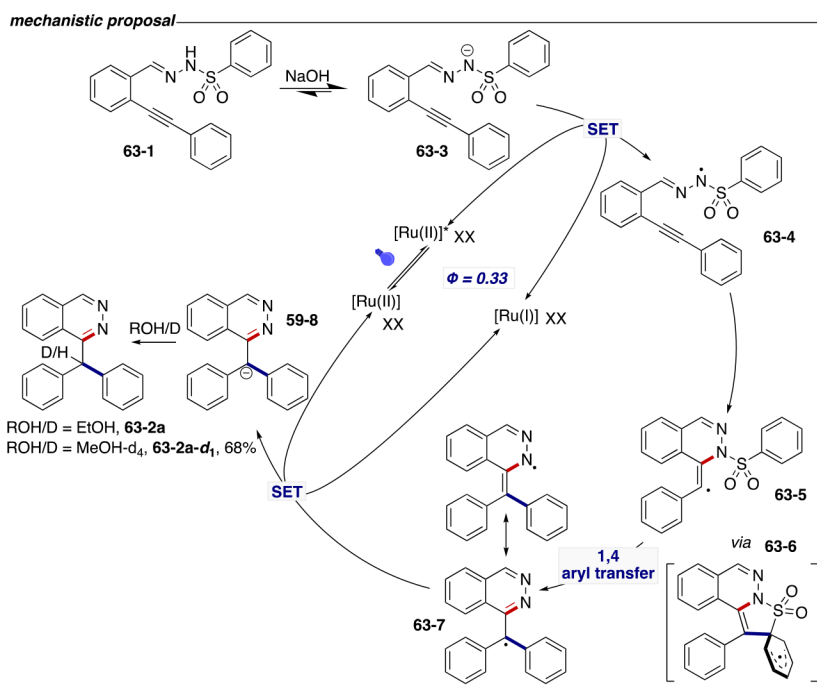
Scheme 62.



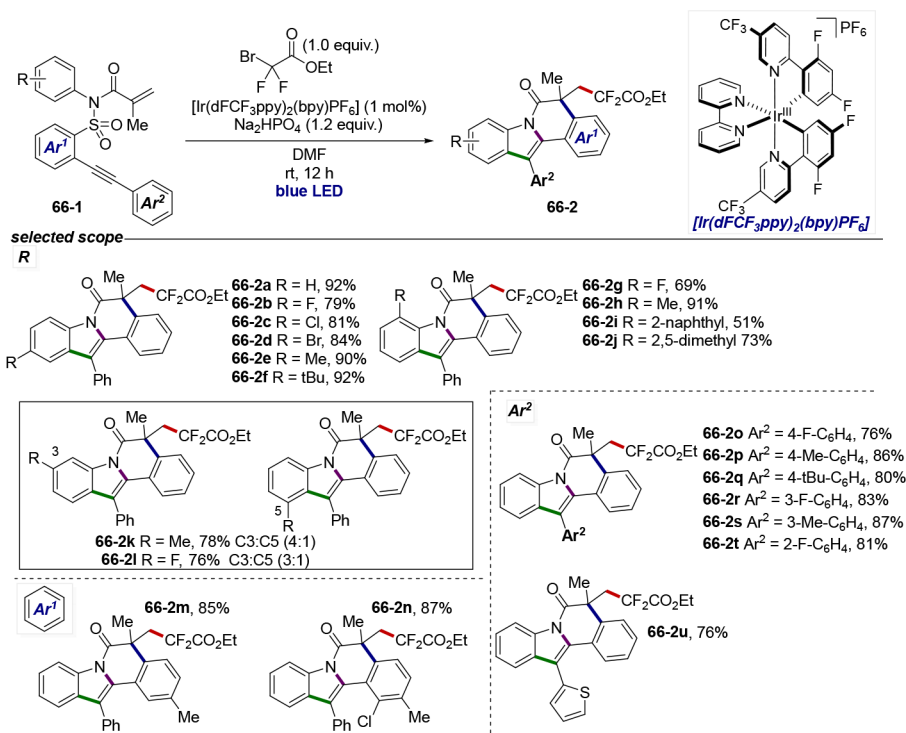
Scheme 63.



Scheme 64.

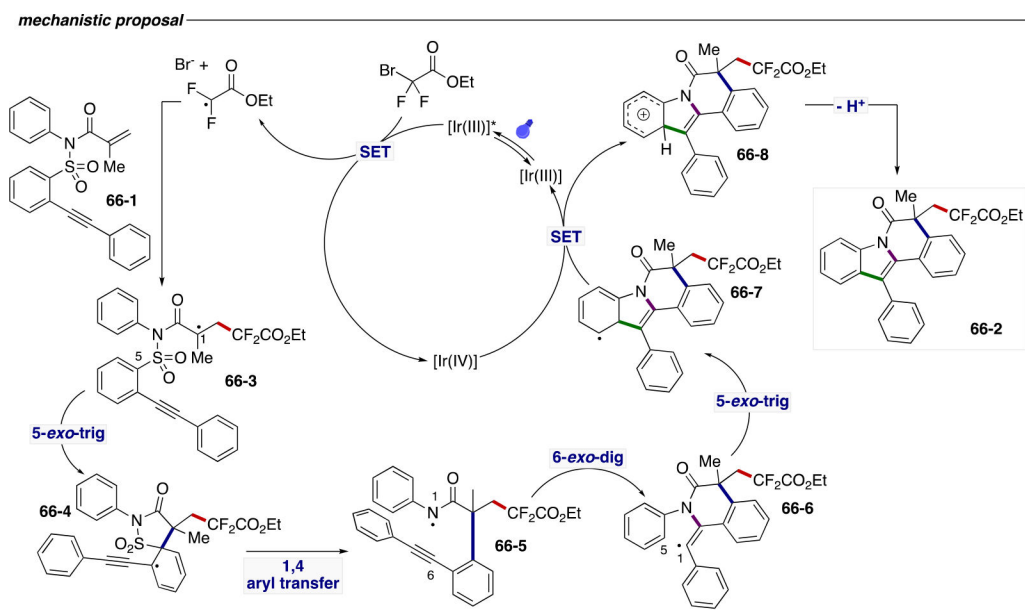


Scheme 65.

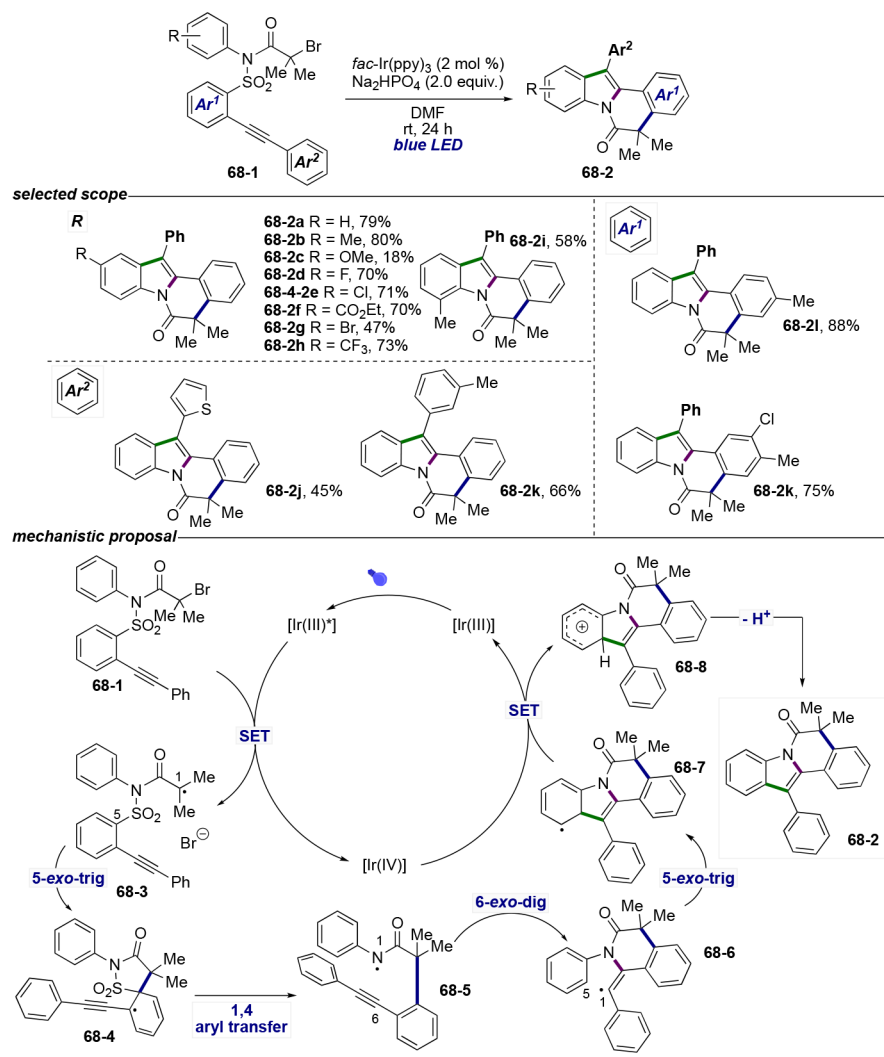


Scheme 66.

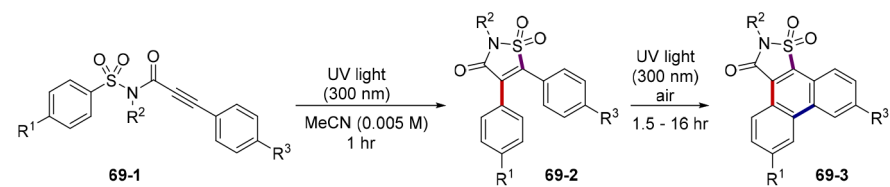




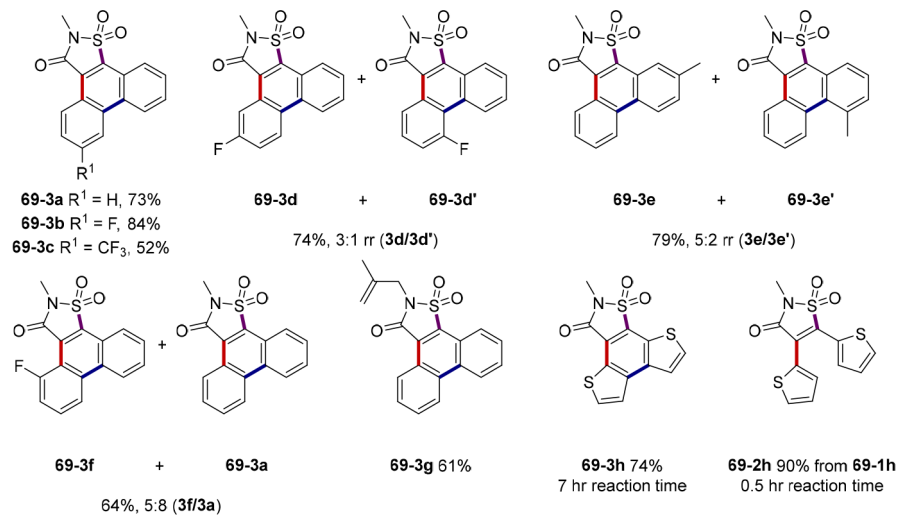
Scheme 67.



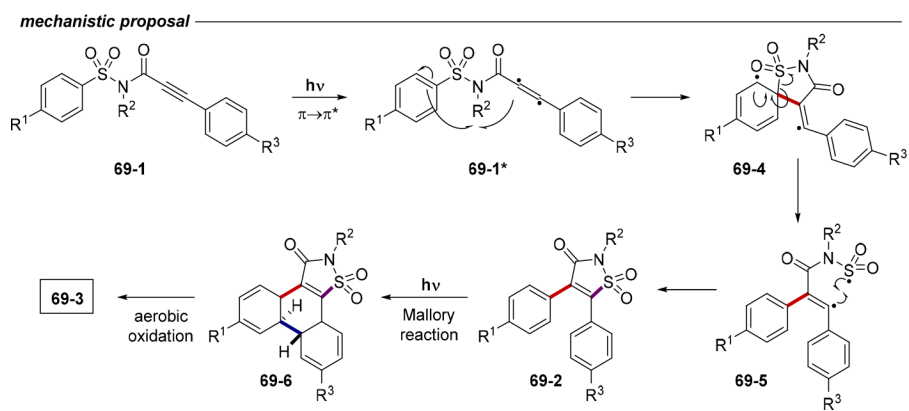
Scheme 68.



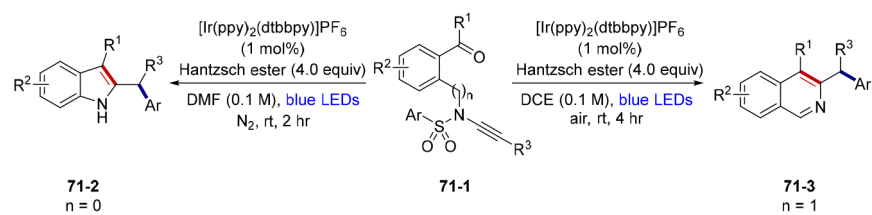
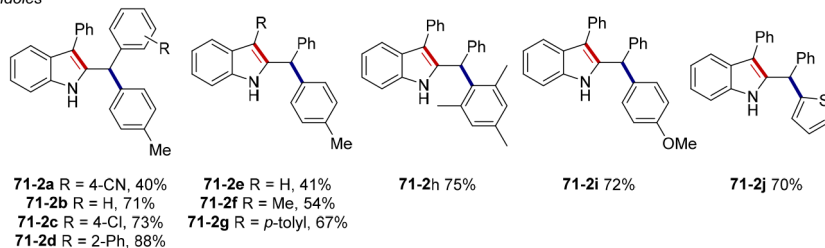
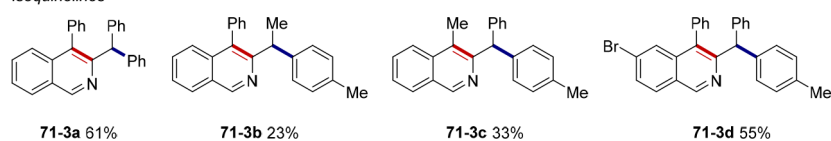
*selected examples*

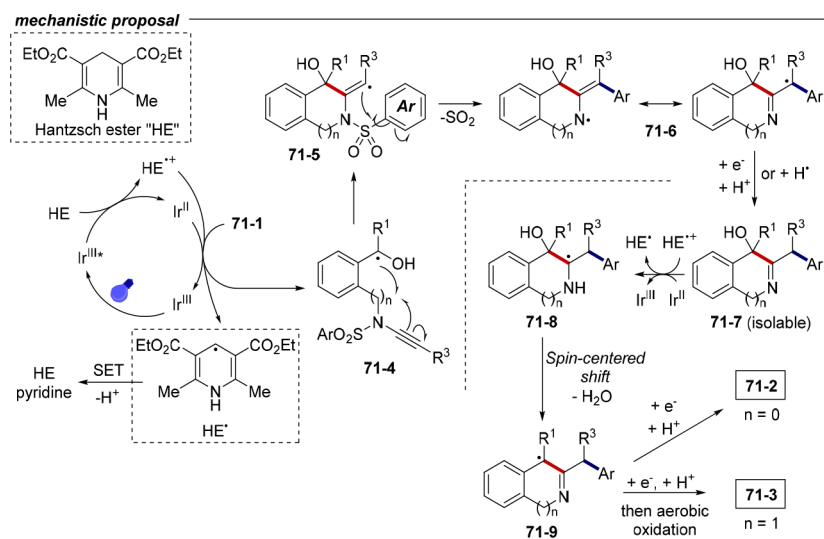


**Scheme 69.**

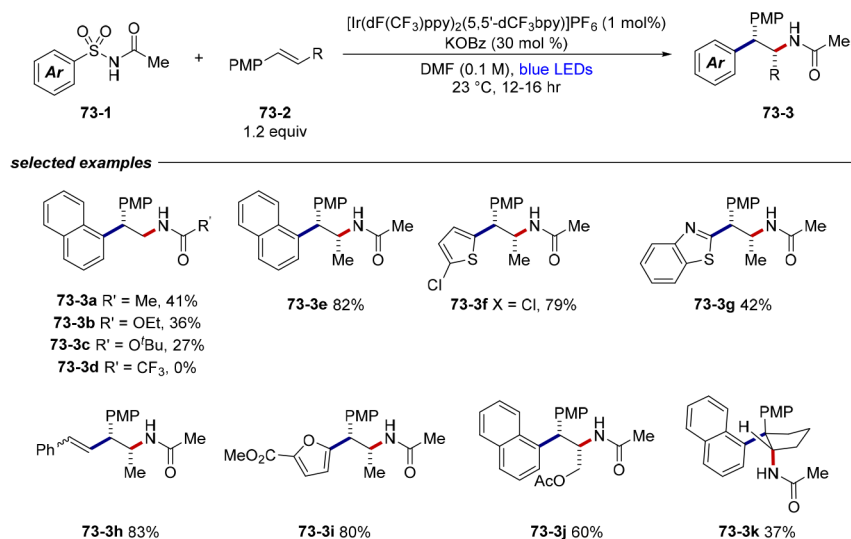


Scheme 70.

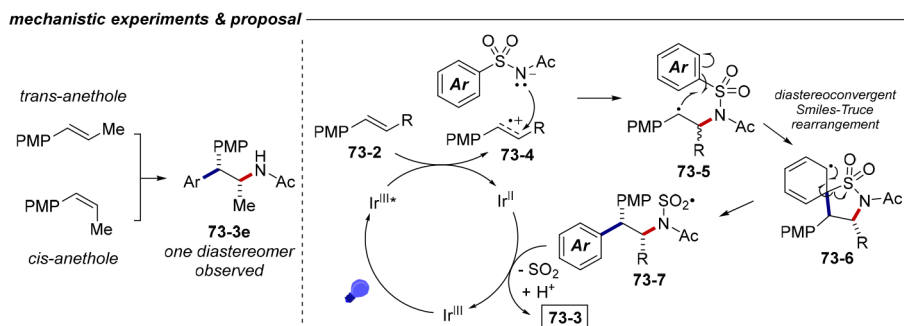
**selected examples***indoles**isoquinolines***Scheme 71.**



Scheme 72.

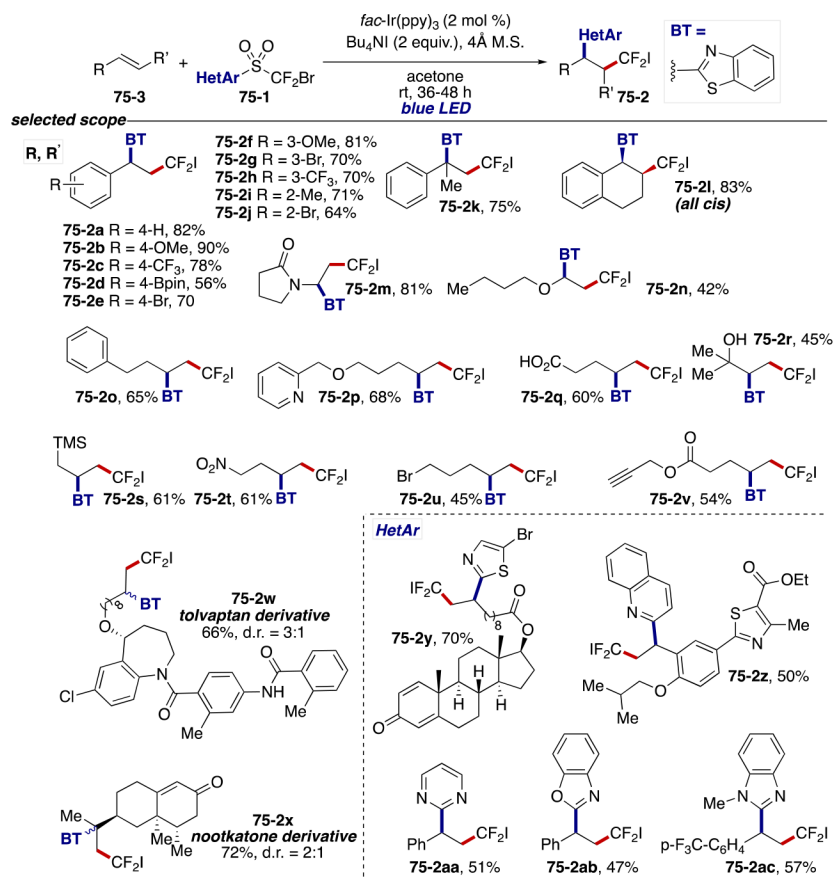


Scheme 73.

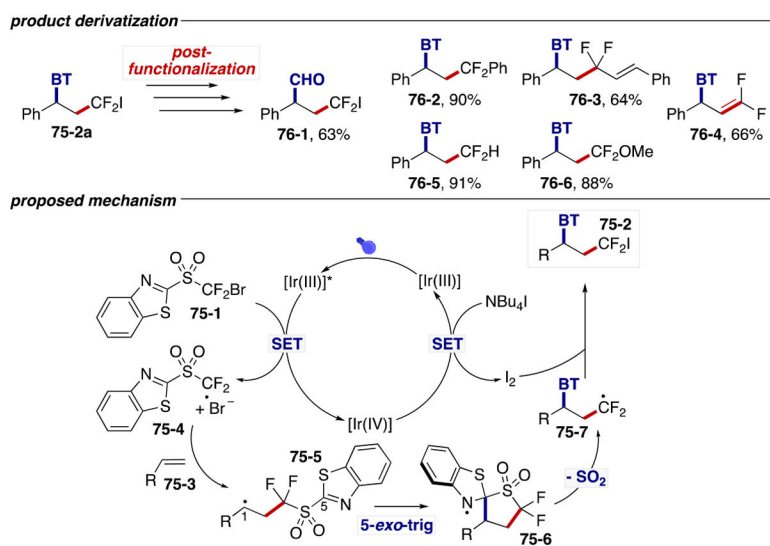


Scheme 74.

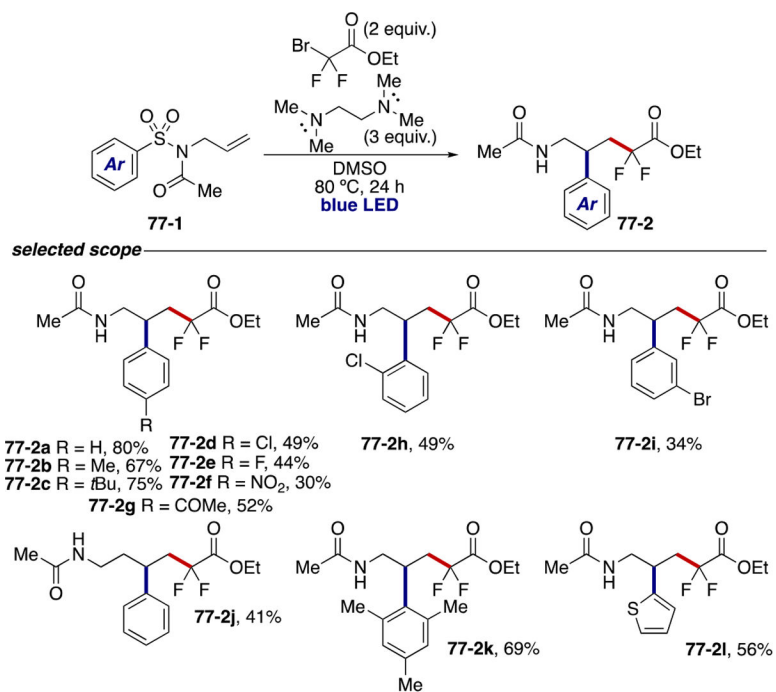




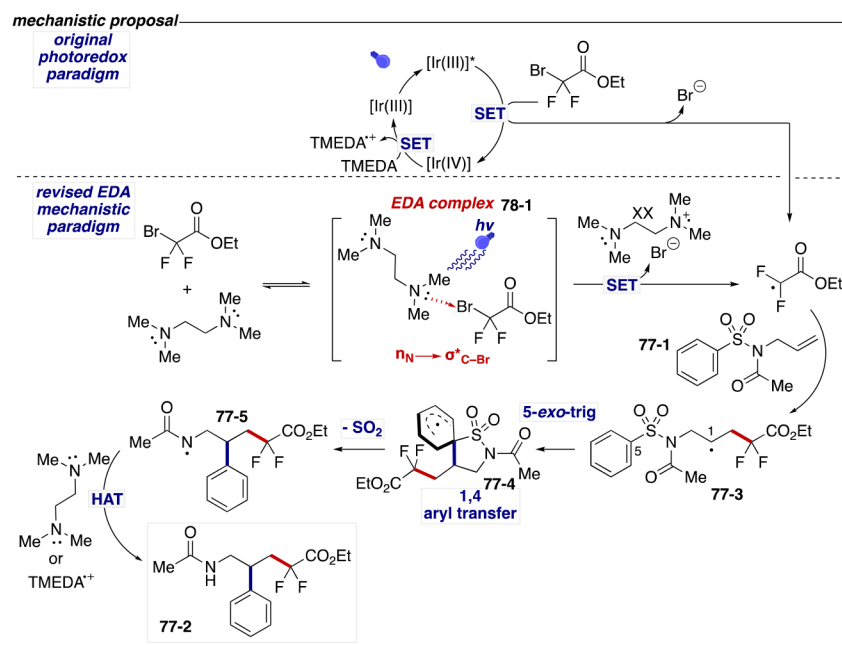
Scheme 75.



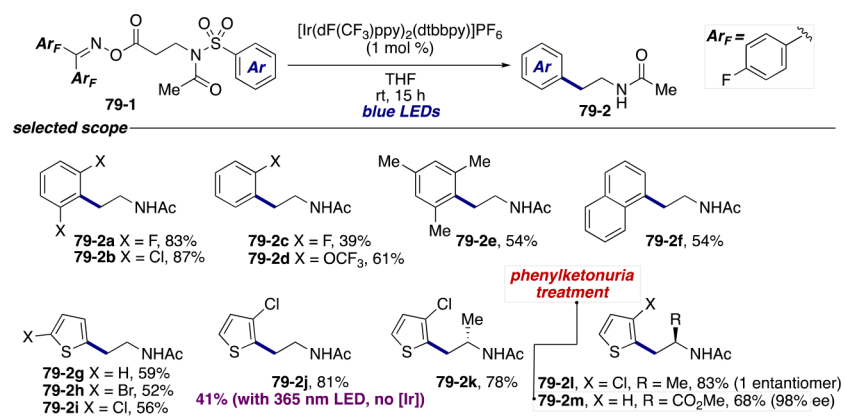
Scheme 76.



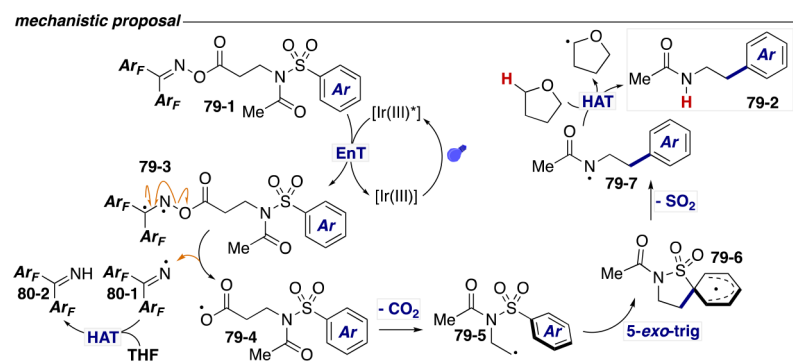
Scheme 77.



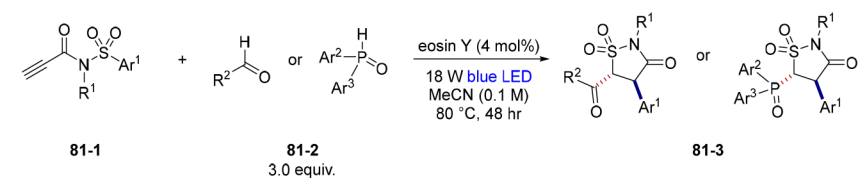
Scheme 78.



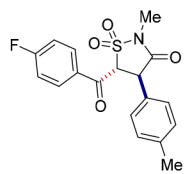
Scheme 79.



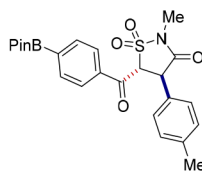
Scheme 80.



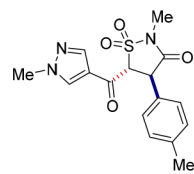
*selected examples*



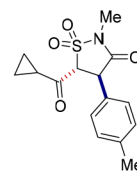
**81-3a** 95%



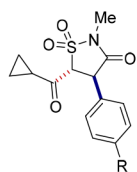
**81-3b** 56%



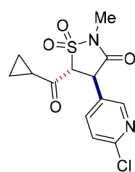
**81-3c** 75%



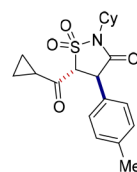
**81-3d** 80%



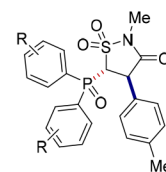
**81-3e** R = OMe, 90%  
**81-3f** R = NHAc, 71%  
**81-3g** R = CF<sub>3</sub>, 75%



**81-3h** 50%

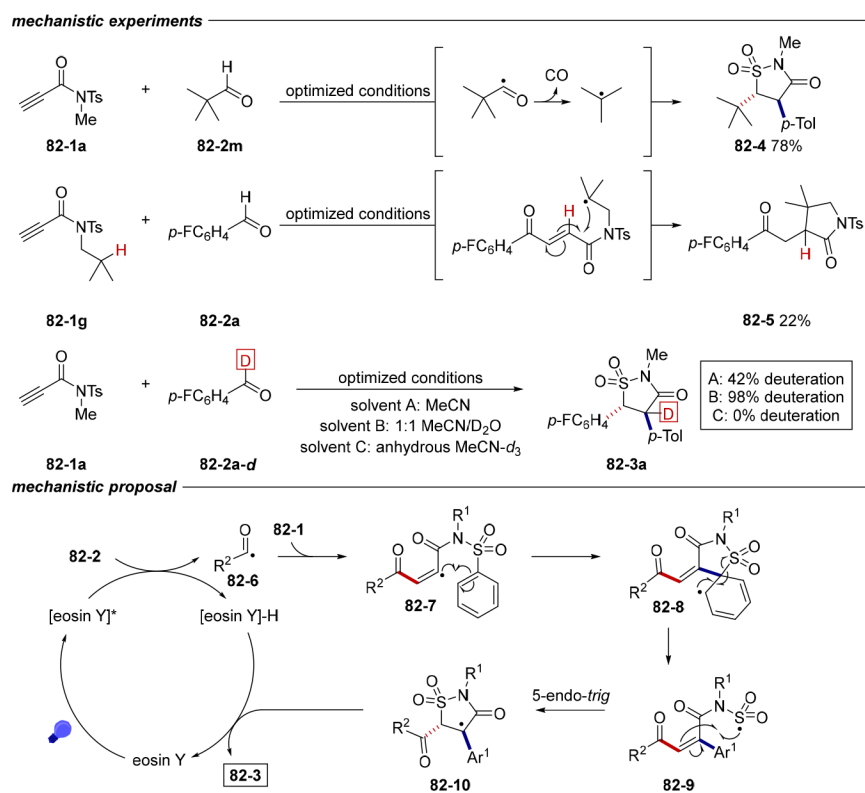


**81-3i** 48%



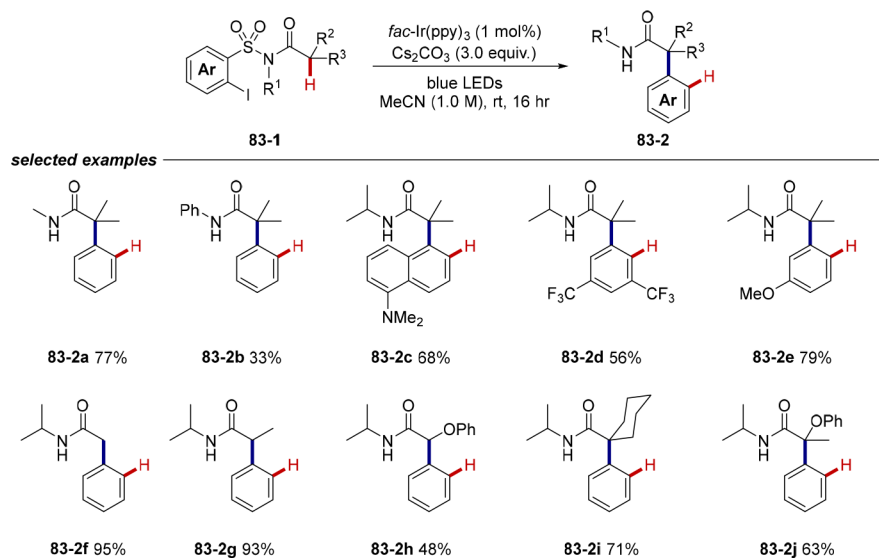
**81-3j** R = 4-OMe, 64%  
**81-3k** R = 2-OMe, 59%  
**81-3l** R = 4-F, 67%

**Scheme 81.**

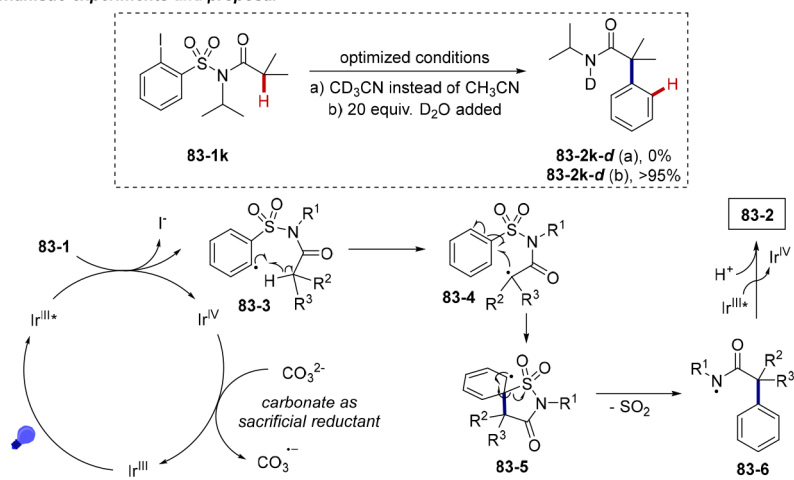


Scheme 82.

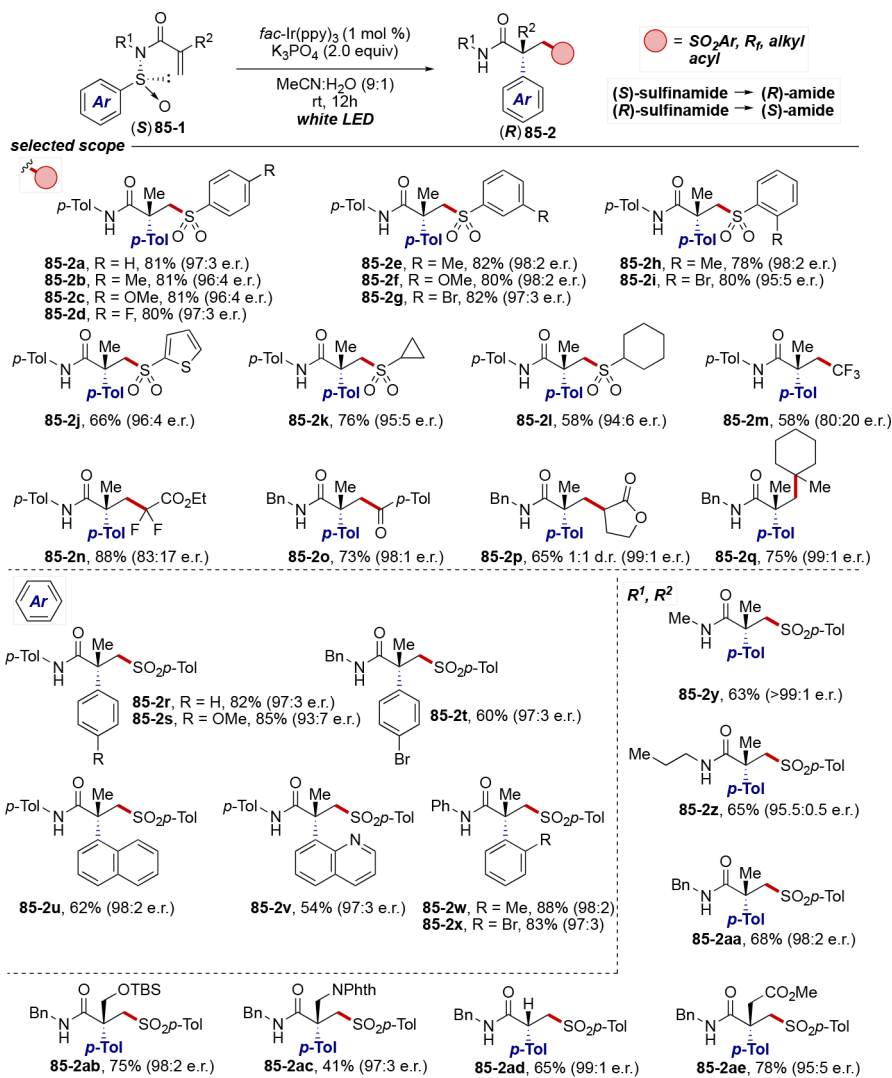


**Scheme 83.**

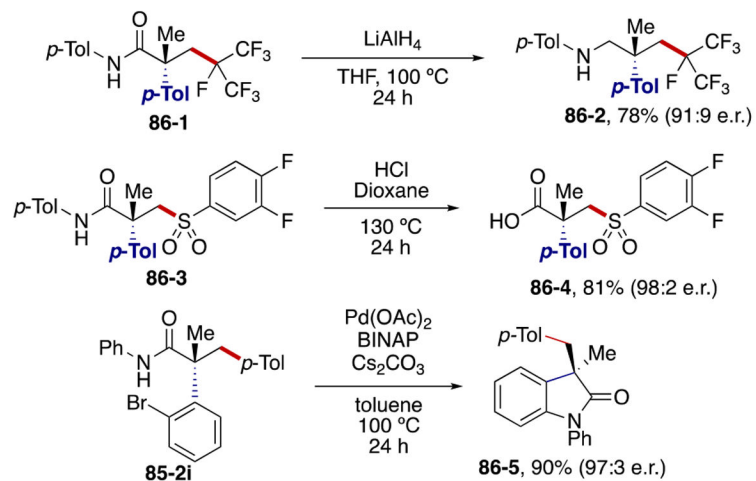
## mechanistic experiments and proposal



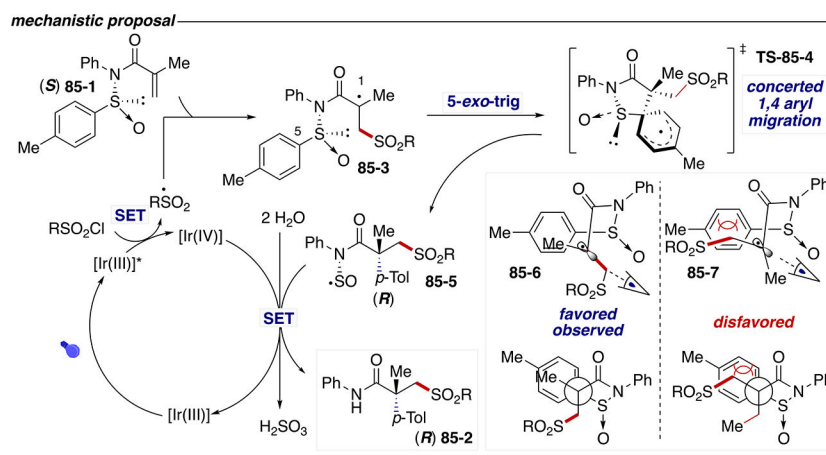
Scheme 84.



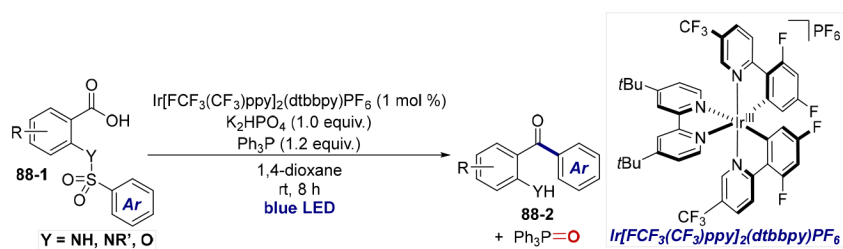
Scheme 85.

**post-functionalization**

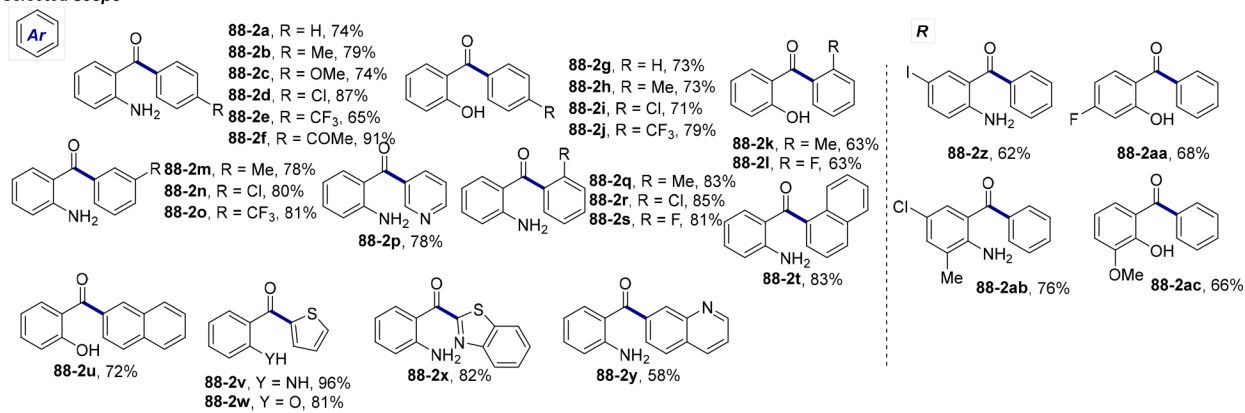
Scheme 86.



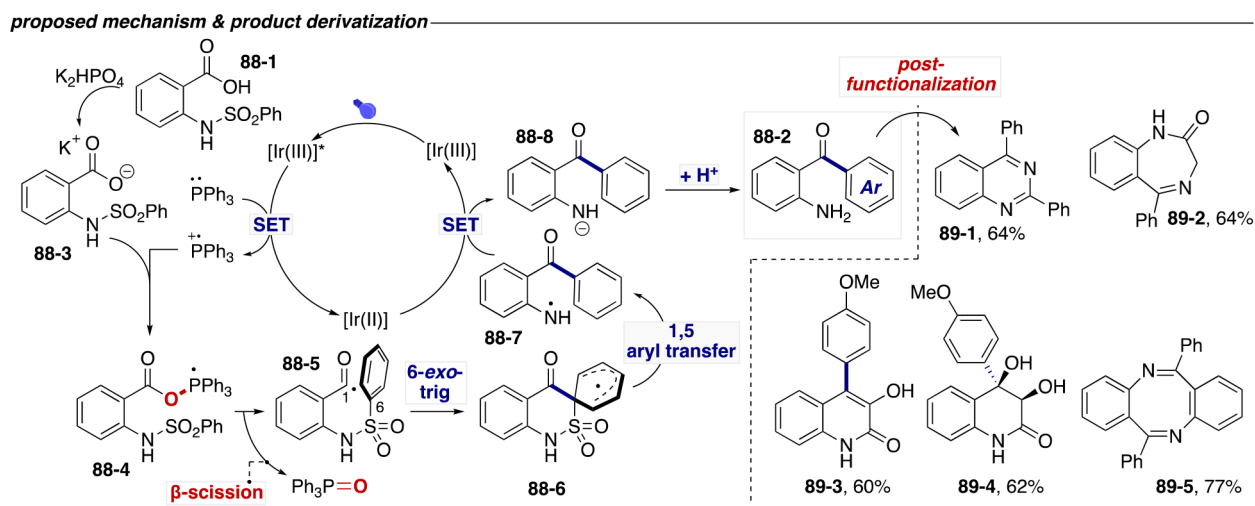
Scheme 87.



selected scope



Scheme 88.



Scheme 89.